TREND

Development Study of Improved models of the Earth's Radiation Environment

(ESTEC/Contract 9011/88/NL/MAC)

FINAL REPORT

(Working paper)

Team Members of TREND

Joseph LEMAIRE	IASB
Michel ROTH	IASB
Jacques WISEMBERG	IASB
Pol DOMANGE	IASB
Dominique FONTEYN	IASB
Gerard LOH	IASB/STI
Georges FERRANTE	MATRA-ESPACE
Christian GARRES	MATRA-ESPACE
Jacques BORDE	MATRA-ESPACE
Susan McKENNA-LAWLOR	STI
Jim VETTE	JIV Assoc.

ESA Technical Manager

Eamonn DALY	ESTEC/WMA

Issued and printed at IASB

4 June 1990

FOREWORD

This Final Report contains the main results obtained and recommendations made by the TREND team during the study "Development of improved models of the Earth's radiation environment". This study has started 1 February 1989 under ESA contract ESTEC/8011/88/NL/MAC.

TREND was initiated and funded by ESA under the ESTEC/CONTRACT 8011/88/NL/MAC. Significant investments have also been made in this project by MATRA-ESPACE (Toulouse), by SPACE TECHNOLOGY IRELAND (STI) (Dublin), by the INSTITUT d'AERONOMIE SPATIALE de BELGIQUE (IASB) (Brussels) and by JIV ASSOCIATES (Virginia) consulted for the whole duration of this study. Invited scientists have participated to TREND's progress meetings in Dublin, in Toulouse, in Noordwijck, and Brussels. The advise obtained from them and support provided by their Laboratory or Organisation is deeply acknowledged by TREND.

The TREND team is formed by

Joseph LEMAIRE from the Institut d'Aeronomie Spatiale de Belgique (IASB), has been the project manager of TREND. He has contributed to the description and evaluation of magnetic field models and transformation to B and L (or other) coordinate systems. He also contributed to the recommendations for future flight requirements and modelling activities.

Michel ROTH (IASB) described and evaluated the different probalistic solar proton event models,and prepared the software design requirements necessary for the implementation of an alternative (new) solar flare proton event model proposed by Feynman et al. . Michel ROTH described and documented the existing methods and software subroutines used in UNIRAD to compute the flux reduction due to 'geomagnetic cut-off'.

Jacques WISEMBERG (IASB) studied physical processes involved in the interaction between the Earth's radiation environment and Earth's atmosphere. He

has also implemented and studied Hassitt's FORTRAN code, which was kindly provided to TREND by Carl McIlwain.

Dominique FONTEYN (IASB) implemented and tested the new models for the external magnetic field by TSYGANENKO (1987, 1989).

Pol DOMANGE (IASB) developed and tested the new software BLXTRA which now permits computation of values of B and L for any combination of internal and external magnetic field models. Local time dependence and Kp dependence of the external magnetic field which have been added.

Georges FERRANTE head of the system division at MATRA-ESPACE, has advised and lead the important data processing and model coding activities

Jacques BORDE from MATRA contributed also to the tasks described in the previous paragraph, but he has been mainly in charge of developing the codes needed to read and process the satellite data used by TREND to improve existing models for the region of geostationary orbit. He compared also the mapping of satellite flux measurements obtained with and without an external magnetic field model. He developed finally a series of new graphical tools

Christian GARRES from MATRA has been involved in the implementations, coding and testing of the new solar flare proton event model of Feynman et al. model; he also integrated this model and BLXTRA into the former TREP software package; he implemented the programs to determine the local time variations and standard deviations of the omnidirectional flux of trapped particles.

Gerard LOH (STI/IASB) supported the data processing tasks at MATRA. In close contact with JIV ASSOCIATES he developed a set of codes to read and process the IUE tapes.

Susan McKENNA-LAWLOR, head of SPACE TECHNOLOGY (Ireland) Ltd (STI) has been responsible for identifying spacecraft missions, instruments, and data sets relevant to this study. Data formats and their availability were identified. Also, future orbital missions of ESA with potential capability for monitoring the Earth's radiation environment were investigated.

Jim VETTE, president of JIV ASSOCIATES, has advised the TREND team during the project. He contributed in so many respects that it would be too long to mention them all. Because of his expertise in the business of modelling the Earth's trapped radiation environment, he contributed basically to the description and evaluation of the trapped particle models in chapter 4 of TREND's TECHNICAL NOTES 1 and 2. He also helped STI and IASB in preparing part of TN 3 and 6. His stimulating advice and action as TREND's 'ambassador' beyond the Atlantic, has been crucial for the project, and is acknowledged by all.

TREND's project started 1 February 1989 for a duration of 15 months. Time and financial limitations necessarily restricted what could be attempted in this project. However, TREND made considerable progress in analysing environment modelling problems, identifying solutions and beginning the data analysis tasks which is a long term effort which needs continuity, motivation and perseverance. Collecting satellite data sets, shipping them over the Atlantic, processing them and analysing them often needs more than 15 months of time. Doing this for more than one data set with totally different tape formats and physical contents made this task of TREND even more difficult and challenging.

During the course of this study a number of interesting extensions of this work have been identified by TREND. For example the improvement of Hassitt's code calculating an atmospheric density averaged over the drift shell of trapped particles would be one of the most useful extension of the present project. But to modernise this fortran code and make it less consuming of CPU time would have needed an additional effort that TREND could not afford under this contract.

TREND was lead to focus its efforts in analysis data covering limited regions of B-L space but nevertheless important ones : i.e. (1) near geostationnary orbit where LANL data offer an excellent coverage, and (2) in the range of intermediate L-values with IUE data which, however, required completely new data processing software. Although TREND identified a number of other satellite data sets (e.g. DMSP data) which would have covered other regions of the B-L space (e.g. the low-altitude region), such additional data processing efforts were, beyond TREND's current resources.

Identification of problems

There are other important contributions of TREND contained in TECHNICAL NOTE 2 : e.g. serious needs for revisiting from a basic and novel point of view the mapping methods of the trapped radiation environment at the low-altitude edge of radiation belts. Indeed, this is the region where future ESA manned spacecraft will orbit, and, where Columbus and the Space Station will operate for a considerable amount of time.

In TECHNICAL NOTE 6 we identified a series of needs for future ESA missions and flight requirements. It results from this analysis that "minimally intrusive" monitors (detectors of energetic particles) should be flown almost routinely, even on non-magnetospheric scientific missions.

The better we will be able to sample and to model the crowded region of space, the better will be the use made of resources of launching rockets and spacecraft. Indeed, the more uncertain the aerospace engineers are, the heavier must be the shielding they will have to lift into orbit to protect man and microelectronic devices. Therefore the relatively minor cost of radiation environment studies can result in substantial project cost-saving and performance improvements.

Outline of this Final Report

After a first chapter containing an over all presentation of the scope, objectives, background and resources of TREND, we describe the evaluation of current models in chapter 2. The software and data requirements & developments are summarized in chapter 3. The data analysis and modelling results form the chapter 4. Chapters 5 and 6 contain respectively future flight requirements and the conclusions of TREND.

Acknowledgments

During this study the ESA study manager, Eammonn DALY has followed TRENDS's model development and data analysis progress. His experience, time and collaboration has been greatly appreciated by TREND's team members. We benefited also from Cecil TRANQUILLE's experience who processed ISEE data.

Carl McILWAIN, Susan GUSSENHOVEN, and Andrei KONRADI participated in the TREND progress meetings where they presented their activities, in the area of Earth's radiation environment modelling and data processing. These contacts have been most useful and future cooperation is envisaged. We are also gratefull to Joe KING, from NSSDC for his support in transferring data to TREND or ESTEC via SPAN or tape. In this respect our tanks are also extended to Howard LECKNER for his interaction with JIV Associates and TREND. R. POST transfered LANL data from MSSDC very quickly and efficiently. Dan BAKER has guided TREND's steps to Tom CAYTON at Los Alamos National Laboratory, who is currently in charge of the processed LANL data. TREND's team is thankful to them all for their cooperation.

Joe KING transmitted the IVE data available at NSSDC to TREND via Jim VETTE. Without this important input much less would have been archieved. Both an hearthy thanked for their collaboration to the TREND project.

Andrei KONRADI, Susan GUSSENHOVEN and Carl McILWAIN participated actively to trend's progress meetings. Their advice and contributions have enlighten and strenghten the work of TREND. We expect to continue cooperation and coordinate future activities with them in the future.

We acknowledge also the Director of Institut d'Aeronomie Spatiale de Belgique, Dr. Marcel ACKERMAN, who gave full support to this study and its realisation. Dr. J.M.LESCEUX, J. BARTHELEMY, A.SIMON, L. FEDULLO and the administrative staff at IASB have provided a most efficient help to the project manager of TREND. They are all deeply acknowledged for their cooperation.

The scientific, technical and administrative staff of IASB, MATRA-ESPACE, and of SPACE TECHNOLOGY IRELAND Ltd have also contributed to make this project a sucessful and most rewarding one.

TABLE OF CONTENT

CHAPTER 1

GENERAL OVERVIEW AND BACKGROUND FOR TREND

Introduction

Radiation damage in outer space is one of the problems confronting any mission in orbit above the protective shield formed by the Earth's atmosphere. The radiation environment above is quite complex, varying by orders of magnitudes both with altitude and time. It effects sensible microelectronic devices and the operation requirements for manned missions.

In this study it is proposed
- to evaluate existing models of the Earth's radiation environment,
- to identify their limitations, and to outline requirements for future generation of environmental models;
- to identify the relevant particle measurements which are available to improve existing Earth's radiation environment models,
- to analyse some of these data and contribute a new step to long term modelling efforts which started at NSSDC/WDC-A-R&S in the 60's after the discovery of the Van Allen Radiation Belts;
- to make recommendation for future flight measurements and monitoring of the Earth's radiation environment.

Radiation effects and hazards

Space missions are heavily impacted by the trapped energetic particles and solar energetic particles in a number of ways. Electric charging of spacecraft surfaces occurs as a result of hot plasma with energies of the order of 20 eV. Such a plasma injected from the geomagnetic tail during moderate and large magnetic storms, can produce surface discharges that result in spurious operation or damage to a high altitude spacecraft.

Relativistic electrons with energies larger than 500 keV embedded within dielectrics, produce electric potentials in excess of the breakdown potential of the material. This results in discharges that act as spurious signals or can damage sensitive components like solar cells, electronic systems. The radiation dose effects which are observed at all altitudes limit the operational life of these components.

At a nuisance level, energetic protons and electrons produce spurious signals in detection sensors. Particle induced backgrounds present complications in the form of increased dead time and requirements for increased signal processing. Energetic particles, through the deposition of energy in matter, can produce spurious signals in any sensors : Cerenkov radiation in optical sensors, photocathode noise in photomultipliers, direct energy deposits in solid-state detectors, e.g. CCD, HgCdTe Infrared sensors...

In some orbits, the transient heat additional input due to enhanced energetic particle population can exceed 5 W/m^2. For ultra-low-temperature IR sensors, such as on the Infra-Red Astronomy Satellite IRAS, this additional heat load must be considered in the design of the spacecraft and in the management of this mission.

The effect of the radiation environment on man in space is another important reason to study and model as carefully as feasible the distribution of energetic particles beyond 150 km altitude, at all latitudes and at all longitudes. The biological hazards are a strong inducement to invest in continous monitoring of the Earth's radiation environment, and modelling of its short term evolution like during geomagnetic storms and solar flare events, as well as over long term periods, like the solar activity cycle.

The feasibility of conducting extended manned space missions is based on an adequate understanding of the biological risks and on providing the adequate protection to reduce the risks to acceptable levels. This implies proper software tools to predict the proton and electron fluxes, and, by consequence the expected radiation doses for the future ESA's manned space missions.

The requirement of shielding the astronauts from the earth radiation environment impact heavily on the weight, cost and operation of manned missions. Therefore, a correct evaluation of this environment is essential to reduce both their costs and risks.

Because the cost of a radiation-hardened microelectronic device is much greater than its non-hardened equivalent, a good estimate of the expected radiation environment is required in order to insure that radiation-hardened devices are used when and where needed and not elsewhere. Thus, space system designers require long-range predictions of the energetic particle environment.

Background of TREND's study

TREND stands for TRAPPED RADIATION ENVIRONMENT DEVELOPMENTS. But TREND has also been concerned with the re-evaluation of the non-trapped solar flare particles penetrating the Earth's magnetosphere and atmosphere during Solar Proton Events. In order to determine the radiation doses that a satellite will experience during its future mission a series of software programs are needed.

Tools available and their links

The tools which were available to TREND when this study was started 1 February 1989, are part of the software package ESABASE containing UNIRAD. The VMS-FORTRAN codes of all main programmes and subroutines used in UNIRAD were provided to TREND by ESTEC/WMA (de Kruyf,1988).

Software used at NSSDC for transformation of geographic or geodetic coordinate systems into geomagnetic B and L coordinates were also provide by

E.J. Daly (ESTEC/WM). Additional software tools were also provided to this study team by C.E.McIlwain (UCSD/CASS, La Jolla) and N. Tsyganenko (Univ. of Leningrad).

On top of the experience of the TREND team members and consultants the large number of scientific papers, reviews and books which have been consulted should be considered as the main tools available. Some of these bibliographical references are quoted in this FINAL REPORT, but a more comprehensive list can be found in the series of six TECHNICAL NOTES prepared by TREND.

The ESABASE/UNIRAD architecture is shown in fig.1-1. The UNIRAD software tools available can be divided into several interlinked packages:

- the SAPRE package generates a given number geodetic coordinates of points along the orbit of a spacecraft whose orbital elements are given as input in a NAMELIST file. These geodetic positions are stored in an interface file for use as inputs to the SHELLG chain of programs.

- SHELLG computes the magnetic coordinates for each of these points. To do so a magnetic field model needs to be choosen. This choice is determined by giving in the NAMELIST file an identification number corresponding to the harmonic expansion adopted to describe the magnetic field distribution. Note that because of the secular variation of the geomagnetic field an epoch (BLTIME) must also be given as an additional input. In UNIRAD only internal magnetic field models were implemented sofar, and some of the key internal magnetic field (e.g. IGRF-85 or J&C-60) were missing. The outputs of SHELLG are the values of B and L for all points along the orbit. These outputs are then stored in the interface file which includes the inputs for the next chain of programs: TREP.

- The third chain is TREP which calculates the expected omnidirectional flux of electrons and protons for each orbital point determined by the B and L values. These fluxes are calculated for a series of energy intervals fixed in the NAMELIST file. In addition to the differential flux, TREP computes also the integral flux above a fixed energy threshold. Furthermore, TREP integrates also these differential energy and integral energy fluxes over the whole duration of the space mission, in order to obtain the fluences. All these outputs are then stored in another interface file which is then used for instance by the SHIELDOSE

programme designed to compute radiation doses predicted behind a shield of given thickness, shape, and composition.(see fig. 1.1.)

TREP uses empirical models for the trapped particles. The latest NASA models are generally used i.e.AE8 and AP8 models. These models are stored as data in matrix form as function of B, L and Energies. Furthermore, the probabilistic model of King is used in TREP to predict the expected number of solar flares and their contribution to the total fluences for the total length of a space mission. Since the expected annual number of ordinary and anomalously large solar flares proton events is larger during solar active years than near the sunspot minimum, there is an additional input parameter that needs to be given to TREP: it is the number of years a space mission will spend during the active period of a solar cycle.

It can be seen that the UNIRAD is already a complex package of software of many different subroutines codes, which unfortunately were not (or sometimes only partially) documented. The lack of documentation of the existing UNIRAD programmes made the updating work of TREND unexpectedly difficult and constrained.

Problems arising in radiation dose predictions

Secular variations of the geomagnetic field

A well publicized problem arising in radiation flux prediction was pointed out by McCormack (1986) and discussed by Konradi, Hardy and Atwrell (1987). As a consequence of secular evolution of the internal components of the geomagnetic field the low-altitude trapped radiation fluxes predicted for the year 2000, increases dramatically when calculated using currently developed methods which are implemented in UNIRAD. This is clearly illustrated in Fig.1-2 taken from Daly (1989). This figure shows the orbit-averaged radiation doses predicted over 13 circular orbits at 300 km altitude and inclination of 28.5° . This orbit passes through the South Atlantic Anomaly (SAA). It can be seen that the predicted doses depend greatly of the epoch of the geomagnetic field model which is used to determine the B and L coordinates along the orbit. The predicted doses and fluxes increase unrealistically when this IGRF epoch is changed from 1960 to 2000.

Note that the AE8 and AP8 trapped radiation models used in these calculations are based on measurements made in the 60's and organized into B and L coordinates with the Jensen and Cain (1962) magnetic field model corresponding to epoch 1960. The upper curve in fig.1-2 shows the secular variation of the doses associated with the secular variation of the geomagnetic field when L is computed using the standard method proposed by McIlwain (1961). In this method McIlwain uses a fixed standard value (0.311653 gaus R_E^3) for M, the magnetic moment of the Earth's magnetic field. But the value of the Earth dipole decreases as a function of the epoch as illustrared in fig 1-3. Therefore it was felt by Vette (1986, personal communication), by Konradi Hardi and Atwrell (1987) and the whole community in general, that the actual magnetic moment M should be used in McIlwain's numerical algorithm to obtain the 'correct' value of L. But even when this change was made in UNIRAD before this project had started, the unrealistic secular variations of the doses shown in fig. 1-2 did not completely disappear, although it was significantly reduced as shown by the lower curve in fig. 1-2. In other words when the standard value of M was replaced in UNIRAD by the actual value of the magnetic moment corresponding to the actual epoch, the spurious secular variation did not vanish as expected by the scientific space community when this problem arose in 1986.

The resolution of this problem was found in the course of TREND's study. It is explained in TREND's TECHNICAL NOTE 1 as due to the secular variations of the quatrupole and octupole terms in the geomagnetic field. Indeed there is not only a secular decrease for the dipole moment (dipole terms in the field expansion), but the center of the eccentric dipole moves secularly away from the geocenter. As a consequence, all magnetic mirror points of particles (for fixed B-L values) are pulled deeper into the atmosphere, at a given location corresponding to the South Atlantic Anomaly. This scientific contribution of TREND will be discussed in somewhat more details in chapter 2 of this FINAL REPORT.

Comparisons of dose measurements and model predictions.

A second series of problems arose from recent comparisons of actual dose measurements and the predicted dose values based on AE8 and AP8 empirical models. Gussenhoven et al.(1987) report short term dose measurements made at low altitudes with the Defense Meteorological Satellite Proram (DMSP) F7

satellite which carried dosimeters (840 km; LEO orbit). Inner radiation belt protons, outer radiation belt electrons and solar flares observations were presented for the period 1984 to 1985. These measurements were compared to predictions of the NASA models AE8 and AP8. The NASA model values for proton dose in the South Atlantic Anomaly (SAA) are approximately 50 % higher than the DMSP average values for a thickness of 0.55 gm/cm^2 Aluminium shielding. Furthermore, the NASA outer zone electron model prediction values are found too high by an average factor of 6.Their reliability for short term predictions was also questionned by the AFGL group.

Pruett (1980) measured radiation dose in the DMSP/F1 orbit for one year: April 1977 to April 1978, a period following solar minimum. His dose measurements showed that near solar minimum the NASA models values were also too high i.e. too conservative.

On the other hand Baker et al.(1986) and Vampola (1988) add the concern that the NASA models understate the very energetic electron flux (E > 2 MeV) in the outer zone. This may especially be the case during the current solar cycle which is a 'robust' one. Indeed, AE8 includes solar-cycle effects based on nominal solar activity observed in the 60's.

Local time and dynamic effects

Another major concern is that observations at high altitude indicate that the radiation belts respond to geomagnetic activity; but current models give average onmidirectional flux values. Although, comprehensive dynamical models are still beyond grasp, complementary models providing the standard deviation of the observed flux values would be a significant improvment, already.

It was also felt that ignoring average local time variations and shell splitting at geosynchroneous was a limitation of currently used AE8 and AP8 models (Daly,1989).

This is the list of major problems which arose in the recent years concerning the radiation dose models. Although, the issues mentioned above are not the only ones, they certainly contributed to stimulate the Development Study of Improved Models of the Earth's Radiation Environment which is described in this FINAL REPORT and in the six TECHNICAL NOTES issued by TREND.

Current and future related activities

The initial momentum imparted to the study of the Van Allen belt particles trapped into the magnetosphere lasted almost a decade from 1961 to 1970. For various reasons this effort has gradually declined until recently, in favor of investigations concerning particles with energies lower than 100 keV. Indeed, it is these softer particle populations that contribute mostly to determine the dynamics of the magnetosphere.

However, a renewed interest for the harder corpuscular radiation environment is now under way, both in the US and within ESA which supports the present TREND study. The reasons for this have been outlined above.

CRRES - The Combined Release and Radiation Effects Satellite (CRRES) is in line with this renewed efforts going on in the US. This satellite mission will perform chemical releases and will measure the Earth's radiation environment, including its effects on spacecraft components. It is a joint US Air force/NASA program. The CRRES program supports, among other experiments, the AFGL Space Radiation Effects Program (SPACERAD). The SPACERAD program is a comprehensive space and ground-test program to:
- measure radiation-induced single event upsets (SEU) and total dose degradation of state-of-the-art microelectronic devices in a known space environment;
- update the static models of the radiation belts and develop the first dynamic models of the high energy particle populations in near-Eath environment, among many other component related laboratory studies.

During the SPACERAD portion of the misson, the CRRES satellite will have a low inclination , highly elliptical (400 km to 36 000 km) orbit that will traverse the most radiation intense regions of the inner and outer radiation belts. The satellite three-year mission goal is to attain a statistically significant data set for the empirical analyses. It will be launched in June 1990.

It is expected that following the launch of CRRES, a large analysis and modelling effort will begin. ESA should remain "in-touch" with this new trend.

NSSDC/WDC-A-R&S - Although the modelling effort of the radiation environment has been slowed down until the CRRES mission, there is still a continuing interest at NSSDC; the SPAN network system which is managed at NSSDC is important for all current and future modelling activities. NSSDC (Joe King, D.M. Sawyer, and D.Bilitza)indicated that they will be becoming more active soon in the area of Earth radiation environment modelling.

GSFC (Greenbelt, Md) - D.S. Stern designs new empirical models for the external magnetic field of the Earth as well as alternative transformation methods to be useful in mapping the contribution of the external magnetic field (see Stern, 1985, 1987, 1990).

JSC (Houston-Texas) - At NASA/Johnson Space Center (JSC) A. Konradi and colleagues specialize in several areas in which further work on models needs to be done.

- Conversion of omnidirectional fluxes stored in current empirical models to time averaged pitch angle distributions.
- Introduction of the east-west asymmetry.
- Development of a scheme for treating secular decay of the Earth's magnetic dipole.
- Development of a method to account for the altitude dependence of the particle fluxes as a function of the phase and magnitude of the solar cycle including the delay times involving the depletion and re-population of low altitude energetic inner belt protons.
- PHIDE detector - protons and heavy ion detector experiment for shuttle and space station.

AFGL - At Air Force Geophysical Laboratory there has been in the recent years a strong emphasis to investigate the distribution of energetic trapped and non-trapped (solar flare) protons and electrons, using the data collected over many years with the DMSP satellite at low altitude (840 km) and on a high inclination orbit. Several important papers based on these data have been published by M.S.Gussenhoven et al.(1985, 1987, 1988), Mullen et al. (1987).

The study of solar proton events is also a standing interest of Smart and Shea at AFGL who published recently a comprehensive review on this topic (Smart and Shea, 1989).

NOAA - Space environment Laboratory (Boulder), Ron Zwickhl, H. Sauer and W. Wagner are responsible for GOES and NOAA satellite data and processing them. They have plans for data products in this area.

NGDC - (Boulder) is the place when NOAA and GOES data are currently archived.

Aerospace Corporation (Los Angeles) - A long standing and continued interest for the earth radiation environment has been maintained since the early 60's. Pruett (1980) from Aerospace Corporation compared DMSP and NTS-2 dosimeter measurements with AE8 and AP8 model predictions. Blake, Paulikas, Schulz, and Vampola contributed importantly to the study of the earth radiation environment during the last three decades. In this respect, see the recent paper by Vampola (1989).

LANL - The Los Alamos National Laboratory has contributed in the recent years a series of papers on relativistic electrons observed in the outer zone, and on their possible jovian origin (Baker et al., 1979, 1987, 1989).The energetic particle measurements made with the LANL satellites contributed tremendously to the area, and provided a unique set of observations to TREND.

JPL - At Jet Propusion Lab. (Pasadena), J.Feynman and colleagues became interested in the statistical distribution of solar proton events over the three last solar cycles. They proposed recently a new probalistic model to replace the earlier NASA model of King (1974).

CASS (UCSD- La Jolla) - At the Center for Astrophysics and Space Science, Carl McIlwain responsible for the B-L coordinate system maintains interest in coordinate systems more suitable for mapping the low altitude distribution of the radiation fluxes.

SFC - John Watts and co-workers are concerned with the East-West asymmetry problem on Space Sation Freedom (SSF). John Watt is also chairman of the SSF Ionizing Radiation Working Group. The group has also studied radiation environment measured on shuttle and performed Cosmic Ray Studies by balloon.

MCD (Huntington Beach) – At McDonnell Douglas Corporation K.A. Pfitzer is also working in an area closely related to the Earth's radiation

environment. He pointed out that as solar activity changes the upper atmosphere heats and cools, and the density at a fixed altitude varies by large factors. The radiation dose in low altitude (300 km to 500 km) orbit is therefore a function of atmospheric density. He showed recently that the atmospheric density is a viable parameter for interpolating the trapped radiation dose at times other than solar maximum or solar minimum when standard NASA models are available (MIN and MAX models).

ESA - Spacecraft designers in Europe rely fully on the NASA environmental models for predictions of the radiation risks of future mission. In this respect Europeans have been consumers of AE8 and AP8 trapped radiation models, more than developers of new or updated models of their own. Although still rather limited in Europe and within ESA, the interest for Earth's radiation environment model development is growing especially at the Mathematics and Software Division of ESTEC. This is confirmed by the present TREND study.

Furthermore, a survey of medium energy electrons at high altitude based on ISEE-1 satellite data has been undertaken and presented by Daly and Tranquille (1989). This analysis provides an overview of the electron geomagnetic coordinates and local time for electrons in the energy range 22-1200 keV for observations collected between November 1977 and September 1979. These observations also show significant differences with the AE8 model, confirming the need for updating the existing Earth's radiation environment models.

OBSERVATOIRE DE PARIS - MEUDON. - Solar activity and solar proton events have been studied here for several decades.

MSSL - At Mullard Space Science Laboratory there is a current interest for the Earth's radiation environment. Meteosat data have been analyzed in this respect at MSSL.

USSR - Beside the very important external magnetic field model development carried out at by N.A.Tsyganenko at the University of Leningrad, we are not well informed of other research, modelling or monitoring activities taking place currently in the USSR.

This list of places where activities related to Earth's radiation environment modelling or monitoring activities are currently underway may not be exhaustive. It summarises, however, informations we were aware of at the time this FINAL

REPORT was prepared (May 1990). We apologize if some other groups active in this area have been overlooked. It would be nice if these groups could react, and inform TREND of their current activities in this field of application.

The scope & objectives of this study

The objectives of this contract are:

- to provide reliable information on the validity or ortherwise of current Earth's radiation environment models;

- to define the recent terrestrial radiation environment and investigate discrepencies between models and measurements;

- to identify and develop computer-based methods for modelling the Earth's energetic particle environment for ESA's radiation environment analyses;

- to provide updated computer-based models and associated software tools which can be applied in these analyses;

- to identify requirements for future modelling and data acquisition.

Models of both magnetospheric trapped energetic particle flux and solar flare energetic particle fluxes have been considered at all stages in this study.

These objectives have been met by TREND as far as resources allowed. The results of this study have been reported in TREND's TECHNICAL NOTE 1 to 6. The main achievements are summarized in this FINAL REPORT. The workload has been divided into seven WORK PACKAGES whose description is given below.

Work Package 1: Evaluation of Current Models

The current models of trapped particle (AE8,AP8) and solar flare particle fluxes ('King model') has been criticaly evaluated. This includes evaluation of model functional descriptions, physical assumptions, effects of secular variations in the geomagnetic field and correlations with available flight data, especially over

the last solar cycle. Items considered include dependence on energy,B,L, pitch-angle, local time and geomagnetic and solar activity. Reasons for discrepancies between models and measurements have been given. Future requirements for models, considering ESA's space programs, have been identified.Technical note 1 has been produced on this work.

Work Package 2: Model Formalism

Existing modelling methods have been evaluated with regard to the physical processes included and excluded, implicitly or explicitly. Potential alternative model formalisms, have been identified and defined. Recommendations of better methods have been made.Technical note 2 has been produced on this work.

Work Package 3: Identification and Acquisition of Useable Satellite Data

Sources of existing radiation environment data which are potentially useable in establishing environment models of the type identified in work package 2, along with data availability and data access methods have been identified. The data have been characterized with respect to species, energy, spatial, directional and temporal coverage. Technical note 3 has been produced on this work. It provides detailed descriptions of the data and instrumentations.

Work Package 4: Data Analysis

Taking into account the results of packages 1,2 and 3, the data analysis requirements have been proposed. Satellite data have been processed to remove unnecessary data and produce appropriate averages. Plots and summary data files have been produced.

The most appropriate data analysis algorithms and data organisations schemes have been defined and implemented. Consideration has been given to temporal, spatial, directional and spectral features of the data and to the characteristics of the instrumentation used in their acquisition. Averaging, binning and fitting have been performed, yielding plots and further reduced summaries. Other analyses and data presentation have been produced where these were found to be useful. Technical note 4 has been produced on this work. The software

developed during execution of this work package will be delivered to ESTEC at the end of this contract.

Work Package 5: Production of New Models and Tools

Taking into account the results of packages 1,2,3 and 4, the most appropriate method of incorporating the reduced satellite data into new models have been defined and proposed.

New tables of the Earth's radiation environment near geostationary orbit have been obtained. The associated tools for model and processed-data access have been developed.Technical note 5 has been produced on this work. The software developed during execution of this work package will be delivered to ESTEC at the term of this study.

Work Package 6: Definition of Flight Measurement Requirements

On the basis of the preceding work, data coverage inadequacies in species, energy, spatial, directional or temporal terms, have been identified and where necessary, recommendations have been made for remedying the situation made. Technical note 6 has been produced on this work.

Work Package 7: Conclusions and Recommendations

Conclusions have been drawn from the work, summarizing the work performed and results produced, and identifying problem areas. Recommentations have been made for tackling the problems and for future work in this area. These conclusions and recommendations form part of this final report which is a synthesis of the principal results of the contract.

CHAPTER 2

EVALUATION OF CURRENT AND NEW MODELS

Brief description of the radiation environment under concern in this study with reference to contributions presented in TREND's TECHNICAL NOTES

What is this environment formed of, and, what are the sources of the main components of the damaging corpuscular radiation under concern in this study. Chapter 4 in TN1 contains a detailed description of this environment. See also Chapter 3 in TN6 as well as the comprehensive review by Vampola (1989), Smarst and Shea (1989). Only a brief outline is given here.

There are energetic particles coming from the Sun, and, there are charged particles trapped into the geomagnetic field; some of the latter ones are a consequence of local diffusion and acceleration processes of magnetospheric particles, but the more energetic ones are 'debris' of Cosmic Ray Albedo Neutron Decay.

Fig.1-1 shows typical energy integral fluxes of these different populations of charged particles which are observed in the magnetosphere.

Particles coming from the Sun

The Sun emits continously charged particles forming the solar wind supersonic flow. But in addition to this relatively low energy (10-200 eV) and dense plasma(5-10 cm^{-3}), the Sun emits from time to time, at the occasion of large

solar flare eruptions, robust showers of protons and relativistic electrons travelling between the Sun and Earth at almost the speed of light. These particles which have energies larger than 0.5 MeV, penetrate most easily the Earth's upper atmosphere above the polar caps, where the geomagnetic field line distribution allows easier access into the magnetosphere.

Geomagnetic cut-off

The Earth's dipole magnetic field filters charged particles according to their 'magnetic rigidity' (: momentum/charge). For each point along the orbit of a spacecraft, and, for each direction from that point, there exists a magnetic rigidity below which protons cannot arrive from outside the magnetosphere. This 'cut-off geomagnetic rigidity' increases as when the latitude decreases. It is maximun at the geomagnetic equator. The resulting gradual reduction of flux of these solar particles at lower geomagnetic latitudes is called the called 'geomagnetic cut-off'. More details about the geomagnetic cut-off and the method used in UNIRAD to compute the resulting flux reduction are given in Chapter 6 of TREND's TECHNICAL NOTES 1. The code used in UNIRAD to calculate the reduction factor due to geomagnetic cut-off has not been changed by TREND.

Effects of solar flare protons

Solar proton events produce dramatic geophysical effects in the high latitude ionosphere, e.g. Polar Cap Absorption (PCA) of high-frequency radio waves. The precipitation of solar protons in the polar cap ionosphere enhances the ionization density and changes the electromagnetic propagation characteristics of the medium. Useless to mention that these unpredictable showers of solar cosmic-ray particles can be rather detrimentral for scientific instrumentation, electronic components flown in earth's polar orbit.

Flux and fluence

Figure 2-2 shows the flux of protons observed by GOES-7 at geostationary orbit (36 000 km altitude) during the solar proton event of 29 september 1989, respectively for energies larger than 10 MeV, 30 MeV, 60 MeV and 100 MeV. The flux per square centimeter integrated over the time duration of the event (3 days) is called 'fluence' of the solar proton event. For this particular event the

fluences have been $415x10^7$, $175x10^7$, $38x10^7$ and $12x10^7$ protons/cm2, respectively for energies above 10 MeV, 30 MeV, 60 MeV and 100 MeV. More important and therefore more dangerous solar proton events have been observed last year. One of the largest event ever observed was that of August 1972; its fluence was twice as large as that of 29 september 1989. This event is often taken as reference. It is one of the few 'anomalously large' (AL) solar proton events recorded since 33 years.

Probability of occurence

The probability of occurence of solar events with a fluence exceeding a given threshold (e.g. 10^9 protons/cm^2) for the whole duration of a space mission is of course of key importance for the safety of the orbiting instrumentation. The small number of solar proton events during the 33 years of observations severely limits statistical analyses and hardly can satisfy spacecraft engineers requiring a reliability with 90% confidence level factors. The practice of dividing the available data into solar cycle groups further limits the stastitics, and the results are open to a variety of interpretations (Smart and Shea, 1989).

King's probabilistic model

Based on observations for the 20th solar cycle (which contained 24 ordinary (OR) solar flare events and only one AL event), King (1974) developped the first probablistic model which is still in use today. This model has become a standard against which other work is currently compared. This model, also called the 1975 NASA model, predicts the probabilty of exceeding a given fluence for a given mission scenario.(Stassinopoulos, 1975). It is this model which is currently implemented in ESABASE software package. In the past years this model has been criticised as being too limited and not truly representative of the current cycle 22 which look to be rather similar in amplitude to cycle 19 (Chenette, and Dietrich, 1984; Feynman et al., 1988).

Feynman et al.'s model

A new statistical model has recently been proposed by Feynman et al. (1988); see also Feynman and Gabriel (1989). Based on larger sample of solar proton events spread over solar cycles 19, 20 and 21, they conlude that there is no

need for separating statistics for AL events and OR events. Indeed, all fluence data combine to form a continous log-normal distribution. Furthermore, most of these events cluster within a period of 7 years around the date of maximum sunspot number. Note however that this new distribution of solar proton events differs sharply from that reported by Goswani et al. (1988). There is not yet general consensus on what is the most realistic interpretation. Definitely more data need to be collected to settle this important debate.

Although not definitive, the alternative probabilistic model of Feynman et al. (1988), appears to be an interesting alternative and a valuable one. It has been described and evaluated more thoroughly in Chapter 5 of TREND's TECHNICAL NOTE 1. Its implementation by TREND in the UNIRAD software as an alternative to the earlier model has been described in TN 2 and 4. There will be more about this issue, the numerical methods and the FORTRAN codes developped by TREND, in Chapters 2, 4 and 5 of this FINAL REPORT.

Particles trapped in the geomagnetic field

Sources

In addition to the solar energetic component (sometimes called solar cosmic rays events,or Ground-Level-Events: GLE), the magnetosphere is filled with trapped charged particles of all energies. The origin of the most energetic ones isnot yet fully understood, although it is established that part of them are the result of the CRAND process. The CRAND or Cosmic Ray Albedo Neutron Decay is the main source of protons above 10 MeV and electrons above 1-2 MeV in the inner zone. Magnetospheric acceleration and diffusion are producing the more abundant protons in the range 0.5-5 MeV, as well as for the electrons of the outer zone. Baker et al. (1981,1989) considered that part of the relativistic electrons flux observed at geostationary altitude could be of jovian origin.

Charged Particle motion in the geomagnetic field.

As a result of the Lorentz force a charged particle with a velocity perpendicular to a uniform magnetic field describes a circle whose radius (gyro-radius) is proportional to the momentum (mass x velocity: m v) and inversely proportional to Ze, the electric charge of the particle. Its cyclotron rotation period

(gyro-period, or cyclotron period) is inversely proportional to the magnetic field intensity, B.

In a non-uniform magnetic field like the geomagnetic field, a charged particle has a helicoidal trajectory like that illustrated in fig 2-3. It is then a combination of a gyration and a drift-motion along magnetic field lines as illustrated in this figure.

When the charged particle spirals towards a region of higher field intensity a point is eventually reached at which all the parallel kinetic energy has been converted into transverse energy. This point is called a 'mirror point'. There the particle reverses its parallel motion and spirals backwards in opposite direction. In the geomagnetic field, a charged particle bounces back and forth between two conjugate mirror points located on both sides of the geomagnetic equator. At an equatorial distance of 4 R_E a proton of 10 MeV has a gyro-period of .1 second and a latitudinal bounce period of about 1 second.

The fact that the field is not uniform and that geomagnetic field lines are curved causes the particle to drift in longitude around the Earth; electrons drift eastward and protons drift westwards as indicated in fig 2-3. At an equatorial distance of 4 R_E the guiding center of a proton of 10 MeV turns around Earth with a period of 50 seconds.

Adiabatic invariants can be associted with the three different types of particle motions described above. It has been shown in Chapter 2 of TREND's TECHNICAL NOTE 1 how the conservation of these adiabatic invariants is useful in determining a new coordinate system of basic importance for mapping the fluxes of trapped particles in the geomagnetic field.

Drift shells

As a result, of the combination of their azimuthal drift motion and latitudinal bounce motion the guiding centers of trapped particles move indefinitely along a surface which is called 'drift shell'. This surface along which a particle guiding center drifts is also often called a 'B-L shell' for reasons which are explained in TREND's TECHNICAL NOTE 1 and briefly recalled in Chapter 2 of this FINAL REPORT.

Van Allen Radiation Belts models

Energetic charged particles can remain trapped in the geomagnetic field along their B-L drift shell for a considerable amount of time, forming what is called the Van Allen radiation belts.This has been demonstrated by the observations of the energetic particles injected by the Starfish nuclear detonation of July 9,1962.

The Earth's radiation belts, consisting of natural energetic electrons and ions trapped in the geomagnetic field, were discovered more than thirty years ago (Van Allen, et al., 1958; Vernov, et al., 1959). Fig. 2.4 is a meridional cross-section of the Van Allen radiation belts showing iso-intensity contours for the flux of electrons with energies above 40 keV (on the left), and of protons above 100 MeV. For more than a decade after this major discovery, the energetic charged particle environment has been intensively studied and modelled.

The series of NASA radiation environmental models are the result of this long term modelling effort. The latest version of these models are AE8 and AP8 for trapped electrons and protons, respectively. A historical review of the trapped radiation models developed in the USA has been presented in Chapter 4 of TN1 (sect 4.4). It is interesting to note that no similar efforts to model the Earth's radiation environment have ever developed in Europe until today.

Geomagnetic coordinates

To map the flux of trapped particles in outer space geographical coordinates are not very convenient. Since, charged particles tend to move along magnetic field lines and since their guiding centers drift along given geomagnetic shells, the omnidirectional flux of trapped protons and electrons are satisfactorily organised in terms of a coordinate system characterising the drift shells for particles mirroring at the point of measurement. This is why the geomagnetic coordinate system B-L introduced by McIlwain (1961) became so popular.

In TREND's TECHNICAL NOTE 2 it has been argued that the classic B-L should be used in the future to map the omnidirectional flux of trapped particles at high altitudes. However, it has been emphasized there that because of the field deformation due to distant magnetospheric currents, an appropriate external magnetic field model must be taken into account in the subroutines for transformation of coordinates.

Magnetic field models

The magnetic field models necssary to determine geomagnetic coordinates B and L, has been described in details in section 2.4 of TREND's TECHNICAL NOTE 1. From this evaluation it results that an external magnetic field model is mandatory in addition to the internal geomagnetic field to determine correctly the geomagnetic coordinates of a point at an altitude above 4 R_E where magnetospheric current systems perturb significantly the geomagnetic field. Different external magnetic field models have been considered and discussed in section 2.6 of TN 1. The external magnetic field model of Tsyganenko (1989) which is among those reviewed, has been adopted by TREND.

The existing software currently used in the UNIRAD package of ESABASE has been described and evaluated in sections 1.2 and 1.3 of TN 2. From this analysis and the conclusion of TN 1, a new software (BLXTRA) has been produced to transform geodetic coordinates into geomagnetic coordinates. Different versions of the external magnetic field models of Tyganenko (1987, 1989) have been implemented in the new chain of UNIRAD software programmes. Additional internal magnetic field models with their associated secular variations (e.g. IGRF 85) have also been added, as described in TN 2 & 4. These aspects will also be developped further in chapter 2 and 4 of this FINAL REPORT.

Atmospheric cut-off

At low altitudes where the atmosphere plays a dominant role as a sink for trapped particles, the traditional B-L geomagnetic coordinates cease to be appropriate to map the trapped radiation fluxes as it is the case at higher altitudes. This effect is called the 'atmospheric cut-off'.

Pfitzer (1990) has confirmed recently that at low altitude the flux of trapped particles depends in a rather systematic manner on local atmospheric density. Based on these experimental results and on early ideas of Hassitt(1964), TREND has identified a new coordinate system to replace the classical B-L system. It requires however a comprehensive empirical model for the upper atmosphere of the Earth. Although TREND recomends the implementation of this atmospheric effect into future version of UNIRAD, this substantial task was beyond the ressourses of TREND.

Trapped radiation model requirements

The existing series of trapped radiation models built at NSSDC/WDC-A-R&S have been described in chapter 4 of TN 1. (See section 4.4). The usefullness and the limitations of the most recent and most comprehensive models AE8 and AE8 for trapped electrons and trapped protons has also been given in TN 1 (see section 4.5). The need for a local time distribution has been identified. Empirical models for the mean fluxes and for their standard variations have also been identified as new requirements for the future models. These requirements for future trapped radiation models have been presented in chapter 4 of TN 2. The software descriptions of these new software tools are given in TN 4 and will also be recalled in chapter 3 and 4 of this FINAL REPORT.

Outline of TRENDS contributions to model evolutions.

In the previous sections a brief description of the radiation environment and of its origin has been presented in order 'to set the stage'. A series of definitions and concepts in this area have been introduced with reference to the chapters and paragraphs in TREND's TECHNICAL NOTES where more details are given.

In this second part of Chapter 2 we wish to summarize the main contributions and new ideas proposed by TREND during this study in the area of Earth's radiation modelling. Critiques of existing models are also recalled in a constructive manner. Alternative solutions have been identified and evaluated. The software requirements and developments of these new and alternative ideas will then be presented in Chapter 3.

TREND has suggested new solutions and answered several critical questions and issues: e.g.

- What is the precise definition of McIlwain L-parameter? Indeed, the very meaning of L is often misunderstood and misused outside the specialized modelling community!

- Is there a simpler algorithm to compute McIlwain L-parameter?

- What is the meaning and usefulness of alternative generalized L^*-parameters

(i.e. 'truly invariant' field line coordinates and Euler's constants)

- Can B-L coordinates still be used at high altitudes where drift shell splitting becomes important i.e. at and beyond geostationnary orbit? How to accomodate for local time variations in trapped radiation at high altitudes?

- Should an external magnetic field model be added to determine B and L at high altitude? Which model to suggest? What are the limitations of such an improvement in modelling the geomagnetic field and in determining the associated B-L coordinates?

- How to cope with atmospheric cut-off? What kind of coordinate should be used instead of B and/or L at low altitude where atmospheric effects are important?

- What are the reasons of the spurious secular increase of the low altitude fluxes of trapped particles, when the epoch of geomagnetic field models is extended to the year 2000? How to resolve this issue, which was first emphasized by McCormack (1986)?

- How to cope with the short term but large amplitude variability of outer zone relatistic electrons fluxes? What are the standard deviations of fluxes observed at and below geosynchronous orbit?

- What are the alternative models for prediction of solar flare events? Which model(s) should be implemented in future UNIRAD software?

- What are future requirements for future generations of trapped radiation models?

Let us now consider these different questions one by one and summarize the answers proposed by TREND.

What is the precise definition of McIlwain L-parameter? How is it calculated?

It is not unusual to see in magnetospheric plasma physics paper : "...let consider the geomagnetic field line characterized by McIlwain's parameter L = 6 or L'...". This is, however, an incorrect statement since according to its original

definition McIlwain's parameter L does not identify a geomagnetic fiels line, but a 'drift shell'.

As explained in the previous sections, a drift shell is the surface along which the guiding center of a charged particle drifts forever provided the magnetic field distribution is time independent and that there are no collisions to change its mirror point altitude. Fig. 2-5 shows a 3-D representation of the drift shell of a particle whose mirror point is located at S. This is the place where the pitch angle α of the particle becomes equal to 90°. At this point the magnetic field intensity is equal to B_m. The value B_m is either measured in-situ by a magnetometer, or it is determined from the geodetic coordinates of S using a geomagnetic field model. The geomagnetic field line passing at S and at the conjugate point S' is drawn in the figure. Only the segment SS' of this magnetic field line is part of the drift shell.

To characterize uniquely this drift shell a second quantity is needed. McIlwain (1961) suggested to use the field-aligned integral defined by

$$I = \int_S^{S'} (1 - B(s)/B_m)^{\frac{1}{2}} ds = J/2p \qquad (2.1)$$

where J is the second adiabatic invariant associated with the latitudinal bounce motion of the particle and the p is its momentum. This line integral is calculated numerically along the actual magnetic field line between the conjuguate mirror points S and S'. A model magnetic field distribution is again needed for this purpose. The IGRF-65 or 75 model is often used.

In a time independent magnetic field distribution the total energy and the momentum p of a particle is conserved. Furthermore, the adiabatic invariant J is also nearly constant. Therefore the geometric field invariant I can be used to characterize the segment of geomagnetic field line SS' along which a particle spirals. Therefore, the pair of values B and I can be used to characterize the geomagnetic field line segment SS' as well as the drift shell resulting from the azimuthal drift of the particle guiding center.

But instead of using this B and I to characterize the drift shell or the segment of geomagnetic field line SS', McIlwain (1961) felt that it would be more practical and user-friendly to introduce an alternative length L, instead of I. This alternative parameter L coincides with the equatorial distance of the magnetic

field line if the field would be a dipole. In this ideal case there is a functional relation between the value of and L R_E, the equatorial distance of the magnetic field line. This is formally written as

$$\frac{L^3 B_m}{B_E} = F\left(\frac{I^3 B_m}{B_E R_E^3}\right) \qquad (2.3)$$

Even in the case of a simple dipole the function F(X) is not an analytic one. McIlwain (1961) determined the values of F (i.e.the value of L^3B_m/B_E) as a function of X defined by

$$X = \ln(I^3 B_m / B_E R_E^3) \qquad (2.4)$$

The function Y

$$Y = \ln(L^3 B_m / B_E - 1) \simeq \sum_{n=0}^{9} a_n X^n \qquad (2.5)$$

is then used to calculate F or L^3B_m/B_E. The constant a_n are given in Tables which are given in McIlwain's (1961) article. (seed also TN1). In other words to determine L from a pair of values (I, Bm) one must first calculate X; depending on the value of X one uses, the values of an given in these Tables and the series (2.5) is used to compute the value of Y and finally the value of L.

Conversely, the coefficients b_n also given in McIlwain Tables , can be used to calculate the value of X from any known value of Y (i.e. the value of I, knowing the value of L and B_m) by using the following series:

$$X = \sum_{n=0}^{9} b_n Y^n \qquad (2.6)$$

Non-dipole field geometries would yield a different functional relationship between I and Bm along a given field line. Furthermore, in an asymetric field the relation between I and B_m along a field line will be longitude dependent for a given drift shell.

It is, however, always possible, even for a non-dipole magnetic field model to compute the value of B_m corresponding to any geographical point, P, in space; similarly it is also possible to compute the corresponding value of I, by numerically integrating (2.1) along the non-dipole magnetic field line, between the two conjugate mirror points. This pair of I and Bm coordinates are to some extent equivalent to the geodetic coordinates of point P, or of the ring of mirror points passing through P.

The pair of coordinates I and Bm can be used to characterize (i.e. to label) a drift shell formed by the segments of the non-dipole magnetic field lines located between the two conjugate rings of 'mirror points', like that which is illustrated in Fig.2.5. McIlwain labels these non-dipole drift shells with the parameter L, which is determined from I and B_m by using the function F corresponding to a pure dipole, i.e. the formal mathematical expression (2.3).

It may be pointed out here, that in McIlwain's original derivation of F, the value B_E was assigned the value of 0.311653 Gauss; this value corresponds to the magnetic dipole moment M at Epoch 1960 in the GSFC interim magnetic field model of Jensen and Cain (1962).

To conclude this section, we wish to emphasize that it is essential to realize that L does not correspond to the actual equatorial distance of the geomagnetic field line SS', as it is sometimes assumed, although it is in general not very much different from this value. It is only for a pure dipole that L is equal to this equatorial distance and may be used to characterize a whole magnetic field line. However, for a non-dipole field the whole magnetic field line cannot easily be characterized by a single L-parameter. Indeed, each point along any non-dipole field line is characterized by a different pair of B_m and I values i.e. a different pair of B_m and L values. However, it has been shown by McIlwain (1961) that the variation of L for points along geomagnetic lines computed from a standard IGRF field model is less than 1 % in the inner magnetosphere. This implies then that it is

not correct to say : "...let us consider the geomagnetic field line characterized by McIlwain's parameter L = 6 or L'...".

Is Hilton's algorithm simpler to compute McIlwain's L-parameter?

Hilton (1971) has found a simpler empirical relationship for L^3B_m/B_E for the case of a pure dipole:

$$\frac{L^3B_m}{B_E} \simeq 1 + 1.350474\, g^{1/3} + 0.465380\, g^{2/3} + 0.047546\, g \qquad (2.7)$$

with $$g = I^3B_m/R_E{}^3B_E \qquad (2.8)$$

For a given pair of I and B_m the value of g can be calculated by (2.8); the value of L is then easy to compute from (2.7).

This procedure formulated by Hilton is therefore more straightforward than that based on the eqs.(2.4) to (2.6). The error obtained by using Hilton's approximation (2.7) to determine McIlwain's L-parameter is less than 0.01%.

Notice that Hilton's approximation (2.7) represents the relation between I and Bm along a dipole field line (or dipole drift shell). Non-dipole field geometries would yield a different functional relationship between I and Bm along a given field line.

It is shown in TN 1 that the algorithm proposed by Hilton (1971) 'does the same job' as that proposed almost 10 years before by McIlwain (1961), except that the former is simpler to use and to code in FORTRAN. This is the only reason why TREND has recommended to change the method of calculation of L in UNIRAD and to implement Hilton's formula given by eq.(2.7), instead of McIlwain's former algorithm.

Should the magnetic moment be changed in the programs for transforming geodetic coordinates to B-L?

It has been argued that it might be more reasonable to compute McIlwain's L-parameter using the value of B_E from the best available field model for the

corresponding Epoch of the measurements (Schulz and Lanzerotti, 1974, p 24). The reason for such a claim was to take into account the secular decrease in the Earth's dipole magnetic moment, M. Not only did B_E decrease but the equatorial radii of all particle drift shells decrease also slightly as a consequence of the welknown betatron effect. Many theoreticians have become sensitive to this issue, and have searched for 'truly invariant' shell parameters like the generalized L* parameter introduced by Roederer (1970). For more details see TN1, sections 2.2.5 , 2.3.2. and 2.4.2.

The alternative procedure to compute L with BE changing from one Epoch to another, instead of being fixed to 0.311653 Gauss, appears to have more practical disadvantages than it has advantages. In fact, McIlwain (1989,personal communication) has shown that an overestimation of B_E or M by a factor 1-e would result in a relative underestimation of e/3 for L. At Epoch 1985 the value of the B_E was 0.30438 Gauss while the value of 0.311653 Gauss is used in eqs.(2.7) and (2.8); this implies that e = (0.311653-0.30438)/0.311653 = 0.023337 = 2.3%. Consequently the values of L calculated with the true value of B_E differs by less than 0.8% from that calculated with McIlwain's standard value. This is a quite small difference compared to other uncertainties associated to any choice of a particular B-field model or associated to the errors of flux measurements themselve.

Therefore, we share the opinion that changing constantly the value of B_E in eqs.(2.7) and (2.8) from one set of measurements to the other would lead to more confusion than it would resolve problems. Changing B_E would be alike to constantly change the unit of length of a ruler to measure distances at different Epochs! This can certainly be done as long as each PI explicitely informs the community as to which value of B_E he has used to compute the B,L coordinates corresponding to his flux measurements; but since an L-parameter should only be regarded as a 'LABEL' (or a coordinate) to identify a geographical point or a drift shell, it seems reasonable to keep using the same value of B_E (i.e. the unit of length) all the time. This is a recommendation of TREND.

What is the meaning and use of an alternative generalized L^*-parameter?

It can be shown that in the case of a pure dipole magnetic field, the third adiabatic invariant (i.e. the magnetic flux encompased by a drift shell) is related to

the value of McIlwain's L-paramater by

$$\Phi = \frac{2\,p\,R_E^2 B_E}{L} \qquad (2.9)$$

The inverse relation has been used by Roederer (1970) to assign to each trapped particle a 'truely' invariant L^*-parameter, which characterizes not only a drift shell but the magnetic field lines forming this shell. While McIlwain's L determines (with B) a segment of a magnetic field line, the L^*-parameter can be used to identify the magnetic field line as a whole. In other words L^* is the same for each point along a given geomagnetic field line, while this is not the case for McIlwain's L-parameter.

This generalized invariant L^*-parameter, looks more satisfactory and appealing to some theoreticians, indeed it is derived from the third adiabatic invariant U. When the geomagnetic field moment, or B_E experience slow secular changes it is expected that the drift shell shrinks or expands accordingly, and, that L^* varies in phase, such that the flux invariant Φ is conserved.

This would be correct provided that all the geomagnetic field variations have characteristic time constants which are much longer than the time period required for the trapped particles to drift around the Earth (i.e. 1500 seconds for a 1 MeV proton or electron). It is not often the case that the geomagnetic field is inactive -unperturbed- for time exceeding 25 minutes, and that this adiabaticity condition is really met. It is therefore illusory to except than Φ remains constant over times comparable to those corresponding to the secular variations of the geomagnetic field i.e. 2000 years (Schulz and Paulikas, 1972). Of course, this limits terribly the usefulness of a 'truely invariant L^*-parameter'.

Furthermore, the actual lifetime of trapped protons and electrons is limited by collisions and wave-particle interaction which is much lower than 2000 years. This has been demonstrated by the decay time of the energetic electrons injected in the region between L = 1.75 and 2 by the Starfish nuclear explosion.

Although an expression of L^* can easily be obtained for a pure dipole or for a uniformly compressed dipole magnetic field (see Roederer, 1970), however for more realistic geomagnetic field models (e.g., the IGRF or Tsyganenko's external magnetic field model) the calculation of a generalized L^*-parameter is currently

beyond grasp. Therefore, it appears that the usage of such a generalized L^*-parameter is not likely to supersede that of McIlwain's L-parameter, although the latter is not strictly constant along non-dipole magnetic field lines.

The same remarks apply of course also to the Euler potentials, which are also interesting theoretical concepts. Northrop (1963) and Stern (1976) have introduced Eulers potentials (α and β) as alternative magnetic coordinates. They use α and β as parameters (or coordinates) to label magnetic field lines. These parameters are of course constant all along a magnetic field. This is what makes their conceptual interest and appeal. Furthermore, from the point of view of classical mechanics the (α, β) coordinates are canonical. Finally, Stern (1987) has shown how 'streched transformations' can be applied to Euler potentials to describe distorted dipole magnetic field lines.

But since these Euler potentials are difficult and cumbersome to calculate in the case of non-dipole magnetic field distributions, these curvilinear coordinates have never been used in practice to represent geomagnetic field lines corresponding to a multipole harmonic expansion like that given by the IGRF, nor for any complex external magnetic field like that of Tsyganenko (1989).

Based on these pragmatic considerations TREND recommends to continue using McIlwain's L-parameter instead of any generalized L^*-parameter, or Euler's potentials for the multipolar geomagnetic field description.

What are the reasons for the spurious secular increases of low altitude fluxes of trapped particles, when the epoch of the geomagnetic field model is extended to the year 2000? How to resolve this issue which was first highlighted by McCormack (1986)?

This question has already been briefly addressed in Chapter 1 of this FINAL REPORT, as well as in TREND's TECHNICAL NOTE 1. Fig. 1-2 in this report shows how the orbit-avaraged dose (and omnidirectional flux) at low altitude increases when the epoch of the geomagnetic field model changes between the 1960 and the year 2000. The AE8 and AP8 models based on observations made in the 60's are used in all cases. These models are organized as functions of B and L. As a consequence of the secular evolution of the geomagnetic field is characterized by a time constant of about 2000 year. The dipole moment of the International Geomagnetic Reference Model (IGRF) was equal to 0.311653 Gauss

R_E^3 in 1960; its value changes by 23 nT/year which corresponds to 8 % in 100 years. But there are also secular variations of the higher order terms in the harmonic expansion i.e. the multipole components. The effect of these different multipole terms and of their secular evolution has been discussed in detail in section 2.4 of TN 1.

As a consequence of the slow decrease of Earth's magnetic moment, M, (illustrated in fig. 1-3), it results that the geodetic positions corresponding to a pair of B and L values, decreases with epoch. The consequence is that ,at a fixed low altitude, the omnidirectional flux calculated with AE8 and AP8 increases with epoch as illustrated by the upper curve of fig. 1-2. When the secular evolution of the dipole moment is canceled, and the tilt angle of the Earth's dipole is held fixed also, one obtains the results illustrated by the lower curve of fig. 1-2. This indicated that the unexpected secular variation of the predicted radiation doses could not be explained solely by the gradual decrease of M nor by an associated betatron effect as argued in the modellers milieu after 1986.

The solution to this problem was found by TREND and is documented in TN 1. Indeed, it was found that the residual secular variation shown by the lower curve of fig. 1-2 is a consequence of the change of the higher order multipoles as a function of epoch. It is TREND who draw the attention on the fact that not only the dipole terms (i.e. the value of M) should be considered, but also the higher order terms and their secular variations.

In this respect the quadrupole terms correspond to an eccentric displacement of the main dipole from the center of the Earth which is currently of the order of 500 km (see fig. 2-8). This distance increases at a rate of 2-3 km/year, or 60-90 km in 30 years of time. This implies that the drift shells are shifting deeper into the atmosphere in the region of the South Atlantic Anomaly. This secular eccentric displacement of the magnetic dipole center with respect to the atmosphere by more than one density scale height in 30 years contributes a significant fraction of the residual dose variation illustrated by the second curve in fig 1-2. This has been shown by TREND. Indeed, when the secular variation of the quadrupole terms are also cancelled the predicted secular variation of the dose is reduced again; a.s.o. with the octopole and higher order terms.

It should be pointed out the magnetic dipole center experiences also a westward drift. This westward drift, combined with the change of the magnetic

dipole tilt angle, explains the observed westward drift of the South Atlantic Magnetic Anomaly (SAMA or SAA).

This exercise has lead TREND to the following conclusions and practical recommendations concerning the utilisation of geomagnetic field models at different epoch. The epoch for the geomagnetic field given by BLTIME in the UNIRAD input-file should be set equal to the epoch of the geomagnetic field model used to build the trapped radiation model; e.g. Jenssen and Cain's geomagnetic field model corresponding to the epoch 1960 has consistently been used to build AE8 and AP8 flux models. Consequently, dose calculations for any future period of time should be based on the Jenssen and Cain's magnetic field model with BLTIME = 1960, when the NASA flux models AE8 and AP8 are employed for the prediction.

On the other hand when the UNIRAD software routines are employed to organize new flux measurements in B-L space with the aim to build a new flux model, the obvious choice for BLTIME will be the actual epoch when the flux observations have been taken in the magnetosphere, let us say: 1986 for LANL data.

If this new environmental model produced with IGRF-85 and BLTIME = 1986, should later on be employed for predicting the radiation doses expected for a mission to be flown in the year 2000, the BLTIME variable which determines the epoch in the geomagnetic field model in SHELLG, or now in BLXTRA, should not be taken equal to 2000 (as done before, and, as for instance done to obtain the results illustrated in fig. 1-2); but BLTIME = 1986 is then the right setting in this simulation with BLXTRA.

This results illustrated in fig.1-2 clearly indicate also that it would be useless to replace the standard value (0.311563) of the magnetic moment M in McIlwain's or Hilton's procedure by the actual value which is epoch dependent.

How to accomodate for local time variations at high altitudes?

When a directional detector measures a particle flux at right angle with respect to the local magnetic field direction, it measures particles which mirror at the location where this measurement is made. The drift shell of these particles is uniquely determined by the values of B and L provided that the magnetic field

model used to compute B and L is 'appropriate'. According to the conservation of the first and second adiabatic invariants, and, as a result of Liouville's theorem, this same detector would measure the same flux at other longitudes and/or local time provided that B and L are identical, and that the pitch angle is also equal to 90 °.

But to be 'appropriate' a magnetic field model must properly describe the local time variation of this field which is very significant at large radial distances due to all magnetospheric current systems.
If the model magnetic field comprises only the internal geomagnetic field components (IGRF-65 as in UNIRAD software package), it is obvious that the calculated values of B and L will not correspond to the actual drift shell of these mirroring particles. As a consequence of the actual local time dependence of the magnetic field (not taken into account in IGRF models), the particle flux measurements will be local time dependent, when they are mapped with this uncorrect B-L coordinate system. To remove this undesirable local time dependence from these flux measurements, there is no better solution than to include a proper model taking into account the local time dependence of the external magnetic field component.

The inclusion of such an external magnetic field in the UNIRAD software package was therefore recommended by TREND. It was not only recommended in TREND's TECHNICAL NOTE 1, but it has been implemented in the BLXTRA software program replacing the former then SHELLG. The software requirements and description of BLXTRA have been presented in TN 2 and 5. They will be recalled in Chapter 3 of this FINAL REPORT.

Which 'appropiate' model can be recommended to describe the external magnetic field component due to magnetospheric currents?

In TREND's TECHNICAL NOTE 1 we have reviewed most current empirical models which have been developped at various places to describe the field perturbations produced by the ring current, by the Chapman-Ferraro currents at the magnetopause, by the magnetotail current systems... There are many of such models on the shelf. All have advantages and limitations.

MEAD-FAIRFIELD (1975) model is one of the oldest and easiest to implement. It has been used very often and is based on a large amount of

measurements scattered between 4 and 17 R_E for the period of 1966-72. The tilt angle of the magnetic dipole can be changed and there are different versions depending on the level of geomagnetic activity. TREND recommended to implement this model as a first alternative in BLXTRA.

The 1987 and 1989 versions of TSYGANENKO's models are based on an even broader set of observations more evenly distributed in the magnetosphere ranging down to 2 R_E and up far into the magnetotail. The different current systems depend also on the tilt angle of the Earth's dipole with respect to the Sun-Earth direction. In Tsyganenko's 1989 version there are 6 different models corresponding to 6 different ranges of Kp, Bartels geomagnetic index. This model is not only one of the most sophisticated one now available, but it simulates rather well the observed local time variations of the equatorial magnetic field distribution near geostationnary orbit.

Because of the poor coverage in the ring current region, it seems, however, to be less reliable in the inner magnetosphere. But at these smaller radial distances the components of the internal magnetic field dominate anyway over the small external field contribution. This makes the errors of Tsyganenko's external field relatively modest in the inner magnetosphere were some have disclaimed it.

Therefore, despite these limitations TREND recommended to implement TSYGANENKO's external magnetic field models as an alternative (default) option to the Mead-Fairfield model. Both the 1987 version and the 1989 version have been implemented by TREND as explained in the next chapter, and, in TREND's TECHNICAL NOTE 5.

Can B and L coordinates still be used at high altitudes where drift shell splitting becomes an important factor to cope with?

First of all what is shell splitting?

Let us assume a particle that starts at a given longitude φ, circling around a given field line and mirroring at $B=B_m$. The integral computed along the field line between the two mirror points has a value I. This means that when drifting through any other longitude, for example 180° away, this particle will bounce along a field line that passes through the intersection of the corresponding I = const and B_m = const surfaces (see Fig.2-6). Now take a particle which starts on the same initial field line but mirrors at a lower value $B_m' < B_m$. Its integral I' will also be

smaller, I' < I. After a 180° longitudinal drift, this second particle will be travelling along a field line that passes through the intersection of the surfaces I' = const and B_m' = const. Only in the case of perfect azimuthal symmetry (as in the pure dipole case) will these surfaces intersect exactly on the same field line. This is called shell degeneracy. In the general case, particles starting on the same field line at a given longitude will populate different shells, depending on their equatorial pitch angles. This effect is called shell splitting.

Fig.2-7 shows how particles, starting on a common line in the noon meridian, do indeed drift on different shells which intersect the midnight meridian along different field lines. The dots represent the particle' mirror points. Curves giving the position of mirror points for constant equatorial pitch angles are traced for comparison. Notice the change (decrease) in equatorial pitch angle for the same particle when it drifts from noon to midnight.

Notice that, as equatorial pitch angles increase, shell splitting is directed radially inward for particles starting on a common field line at noon, and radially outward for particles starting on the same field line at midnight.

It should be emphazised that shell spitting does not exists in dipolar magnetic field and in general for any multipole component which is azimuthaly symmetric. But since the contribution of odd multipole terms is small and vanishes rapidly at large radial distances, the main origin of shell splitting in the outer magnetosphere comes from the external magnetic field which is azimuthally asymmetric as a consequence of its local time dependence.

Particles measured at S with pitch angles smaller are larger than 90 ° do not drift on shells characterized by values of B and L corresponding to the point of measurement, but their mirror point is located at a lower altitude along the same magnetic field line. Therefore, when unidirectional flux measurements are available one needs to determine the actual position of the mirror point corresponding to each particular pitch angle α. This is easily done by tracing (by numerical integration) the magnetic field line from the point of measurement S down to the mirror point P' where the magnetic field intensity is equal to

$$B' = \frac{B}{\sin^2 \alpha} \qquad (2.10)$$

Once the geodetic coordinates of the actual mirror point P' are known, it will be easy to follow the normal procedure to determine L' using the BLXTRA program.This is the procedure that TREND has recommended to analyse the directional flux measurements of IUE.

It must be pointed out that in the case of omnidirectional measurements particles with all pitch angles enter the detector. As a matter of consequence particle drifting on a wide range of different drift shells are measured at once. These different drift shells are characterized by L values which are nearly the same (at least in the inner magnetosphere where the magnetic field lines are closely dipolar) and by values of B which are varying over a wide range in any case.

The success of B-L coordinates comes from the fact that they organise very well omnidirectional fluxes in the inner magnetosphere where L has nearly the same value for all points along a given magnetic field line, and, where shell splitting is relatively unimportant. But in the outer magnetosphere, where magnetic field lines become less dipolar like, and where shell splitting takes place, the usefullness of the B and L coordinates has been questioned to map omnidirectional fluxes.

Although TREND recognized this problem, it recommends to continue with B and L, until a better solution will be found. For directional flux measurements with good angular resolution there is not so much of a problem than for omnidirectional flux measurements, as indicated above. Unfortunately, the view angles of directional detectors are often quite large, therefore the pitch angle resolution is rather poor in many cases. Consequently, the range of mirror point altitudes corresponding to the wide range of pitch angles is also rather broad; the corresponding values of B' and L' coordinates of these mirror points are not very well determined. This leads TREND to recommend narrow angle directional detectors instead of wide angle ones in future data surveys.

How to cope with the atmospheric cut-off? What kind of coordinate system should be used instead of B and L at low altitudes where the atmospheric effects are important?

This question has already been introduced in the previous chapter. A full chapter was devoted to this question in TN 1. TREND has pointed out that at low altitude the atmospheric density plays a comparatively more important role than

the geomagnetic field on the distribution of trapped particles at low altitudes in the inner radiation zone. This has also been demonstrated and confirmed by Pfitzer (1990) who suggests to use the local atmospheric density instead of B or B/Bo to map omnidirectional fluxes between 150 km and 1000-2000 km altitude.

But instead of the atmospheric density corresponding to the altitude of the flux measurement, TREND has suggested to introduce a new 'averaged height' parameter. Indeed to account for the global effect of the atmosphere it is necessary to integrate the density over the trajectory of the particle or of its guiding center. The reason is that the altitude of mirror points varies with longitude from 100 km up to 1500 km in certain cases . For comparison it can be pointed out that the density scale height is about 50-70 km in the thermosphere.

A direct numerical integration of the trajectory of particles as C.STORMER did it more than 80 years ago for cosmic ray particle, would be too demanding in CPU time. To avoid such a time consuming calculation of atmospheric averaged over a drift shell, Hassitt (1964) has developed an elaborated and interesting method which is outlined in sect 1.3.3.2 of TREND's TECHNICAL NOTE 2. The FORTRAN code of HASSITT has been unearthed by C.E.McIlwain at UCSD/CASS (La Jolla), where it had been developped more than 25 years ago by one of his post doc. TREND is very thankful to C.E.McIlwain for providing to TREND this software package . This code has been implemented at the IASB (Brussels) were it has been tested, and where it is now waiting for further developments and resources.

This program calculates first a drift shell averaged atmospheric density, then it determines a corresponding 'height' using a simple standard atmospheric model with exponentially decreasing densities.At McIlwain's suggestion TREND has called this: the Hassitt shell height (H_S). The definition of H_S is then: the altitude where the density in the standard (conventional and simple) atmosphere model is equal to the actual average density that the guiding center of a trapped particle sees when it drifts along its B-L-shell. TREND recommends the use of this new coordinate instead of Pfitzer's local atmospheric density, and in any case instead of B or B/Bo.

The original version of the Hassitt code is based on the Jenssen and Cain (1960) 48 terms expansion of the geomagnetic field. This old field model and the primitive atmospheric model used 25 years ago by Hassitt need to be updated. The software needs also to be optimized to reduce the rather long CPU time. The lack

of resources prevented us to develop and optimize this code any further within the framework of this contract. But it is hoped to find new support to carry out this work later on in collaboration with C.E.McIlwain.

What are the latest models for the trapped radiation environment? What are their marks and also their limitations?

A comprehensive description of the distribution of omnidirectional fluxes of trapped protons and electrons, given respectively by the NASA AP8 ad AE8 models, has been presented in Chapter 4 of TREND's TECHNICAL NOTE 1. No one else than Jim Vette, the father of these models, could have presented a better description and overview of the modelling efforts undertaken by NASA at NSSDC/WDC-A-R&S since the 60's. An interesting historical review of the development of the series of NSSDC models has been given in section 4.4 of TN 1. It would be too long to repeat all this within this FINAL REPORT. We will only recall here the main features of the AP8 (for the proton environment) and AE8 (for the electron environment).

The AP8 model

This model was issued in December 1976 (Sawyer and Vette, 1976). It resulted from the analysis of 34 instruments that partially covered the time period from July 1958 to June 1970. It is a static model except for the solar cycle dependence afforded by the incorporation of AZUR data and the work of a number of investigators who studied the processes involved in producing the effect. This solar cycle effect is too small to warrant trying to describe changes on a year basis unless work like that of Blanchard and Hess (1964) or others would be revisited. Otherwise it is a static model.

Time variations that have been observed are pointed out in the document but it was not possible to incorporate these into the model. In that regard an effort should be made in the future to study these effects in more depth. More effort has gone into the time variations of electrons in the past, because of the effect on the models. This is a recommendation made by TREND.

The incorporation of the model into a one large numerical matrix has been convenient from a use standpoint now that computer memories are large enough. However, some of the feel for the data has been removed. Local time effects were

not studied since only the particles below 10 MeV reach the regions beyond 3 R_E, where electrons show local time effects. TREND made the recommendation to study this local time effect in future modelling efforts.

The production of differential forms (in pitch angle and energy)are possible and a matrix for unidirectional flux was made during the production of AP8. The differential forms do not have the same validity as the basic model; the numerical derivatives taken may produce some peculiar bumps, since the models were not built in a way that insures smooth derivatives.

The AE8 model

The AE-8 model was issued in its computer form around 1980. The model is a synthesis of three previously issued models and the incorporation of new data. The new data were incorporated to improve the model in several respects. The energy spectrum in the outer zone above 2 MeV was found to be low relative to the ATS 6 and the Azur data. Using the data from all four experiments, the whole distribution above 2 MeV was changed. The B/Bo dependence of the two models is the same. The B dependence is given by the function G (Singley and Vette, 1972a), which is normalized to 1 at the magnetic equator, where

$$G(B/B_0'L) = (B/B_0)^{-M} \{[B_C/B_0-B/B_0]/[B_C/B_0-1]\}^{M+1/2}$$

Note that B_C (B cutoff) is the value where the omnidirectional flux goes to zero. The atmospheric cutoff for AE-8 models is strictly empirical since there are many effects that result in particles being lost into the atmosphere. AE-4 had a low altitude cutoff that was based on the amosphere and had been conservatively vhosen where B_C occured when h_{max} = 200 km. The parameter h_{max} is the maximum altitude that the particle reaches in drifting around the Earth at a fixed B,L.

Thus for AE-8

$$\underline{B_C}/B_0 = \begin{cases} 0.7000(L/R_e)^{3.4206}; 1.2R_e \leq L \leq 3.0R_e \\ 1.4589(L/R_e)^{3.0495}; L < 3.1R_e \end{cases}$$

The AE-8 model has an inner zone with energies ranging from 0.04-4.0 MeV and an outer zone with electron energies from 0.04-7.0 MeV. If the highly energetic electrons observed by Baker et al.(1986) at the geostationary orbit are probably from Jupiter, they are not trapped and should be treated in a similar fashion to that used for solar protons.

The solar cycle changes are the same as the previous models used to construct AE-8. The L coverage remains 1.2 to 11 R_e. The basic product that is distributed is the matrix of omnidirectional integral flux as a function of energy, B/B_O, and L.

The local time dependence has been averaged out in this matrix form, since most satellites would average out the effect with time in orbit. Adding a new variable to the matrix would increase its dimensions by a factor of 5, which might place a burden on the storage capacities of users, particularly those using personal computers. The model remains quasi-static.

Ill-use of environmental models, errors and inaccurracies

Like any model in geophysics the AP8 and AE8 models have their limitations, but it must be admitted that no other space agency has yet produced any trapped environmental model which is better than those of NSSDC. A number of critiques against these models have been formulated and published in the recent years. These critiques have been summarized in Chapter 1 of this report and will not be repeated here.

Some papers indicate that the fluxes observed at low altitude with recent spacecraft like DMSP are factors of 2 or 6 smaller (i.e. less pessimistic) than those predicted by the NASA models. There can be several reasons for these differences. First, one may argue that the old data sets used to build the models are in error or uncorrect. This blame for systematic errors in the measurements would than go to the community of PI's. In addition to wrong calibrations, instruments failures, there could be contamination of proton flux measurements by high Z particles. This latter effect could have polluted the AP8 model. Other data including the S^3 data from Fritz could be studied to improve this situation.

Systematic errors in the model are not tractible to identify. Those data sets with problems stand out clearly in disagreement with the overall body of data. The

clarification as to the cause of those problems may never be done. The OV1-19 electron data shown in fig 2-9 as well as other measurements and AE-8 model predictions, caused conncern and confusion for several years before a resolution was at hand. But, even if we admit that there are a few data sets wich lack the expected high quality and reliability, it is unlikely that the average fluxes values of the NASA models obtained by averaging many sets of data can be drastically in error because for these particular reasons.

Assuming, therefore that most of the old data sets (as well as the new DMSP, LANL, IUE data sets) are correctly calibrated, and, that they have been analysed in a consistent way by all the different PI's groups, the observed difference between the recent observations and the model predictions can result either

(1) from a true secular or solar cycle change in the population of trapped particles between the 60-70's and the more recent epoch; indeed the 'magnetospheric weather (or climate)' might have changed since the time the first data sets used to build these models were taken; or

(2) from the spurious 'secular variation' effect described above due to an ill-use of the NASA modls and resulting in unrealistic values for the predicted radiation doses; indeed, the over pessimistic predictiond could partly be due to an improper choice of epoch for the IGRF field used when B-L coordinates are determined for the new data sets,(i.e. BLTIME not taken equal to 1960; see discussion above); or

(3) from statistical fluctuations around the average values given in the AE8 and AP8 models.

This latter possibility induces the question of the need for standard deviations of the omnidirectional fluxes not provided with AE8 nor AP8. Although these statistics where given in earlier NASA models like AE4, TREND recommends to provide to the future users of UNIRAD, updated values of the standard deviations for the logarithm of the omnidirectional fluxes at all energy thresholds and at all pairs of B-L values. Not only the average of the logarithm of the omnidirectional flux should be given.

TREND recommends also that future trapped radiations fluxes for the regions close to geosynchronous orbit and beyond be built with a proper magnetic

field model including the external magnetic field components. It is also argued by TREND that the local time coordinate should be stored as an independent variable in the data sets. Although it is expected that with a proper external magnetic field to compute B-L coordinates the local time dependence will disappear, there will generally remain a residual LT effect for several reasons; shell splitting is one mentionned above; another reason is that the external magnetic field model used for B-L the mapping is not necessarily realistic for the data sets analysed. Therefore, in order to identify these residual LT effects the new data and new environmental models should possibly be organized as a function of LT also.

What are the alternative models for prediction of solar flare events? Which model(s) should be implemented in future UNIRAD software?

The question of fluence due to solar proton events has been rised already above as well as in Chapter 6 of TREND's TECHNICAL NOTE 1. There are two alternative models available. The first due to King (1974) is already old and based on one solar cycle worth of data (i.e.cycle 20 which is now known to be less representative of the current one). The second and more recent model is based on data collected during for three solar cycles, and is due to Feynman et al. (1988).

Figs 2-10 and 2-11 show the probability of exceeding a given level of fluence for solar protons whose energies are larger than 30 MeV. The missions lengths are given in months and years. The results shown in figure 2-10 based on King's model were already implemented in UNIRAD. This model is a well referenced standard. Despite its limitations due to the smallness of the data sample, it is likely to remain the standard model that most users may wish to employ. This is the reason TREND recommends to leave this first model as an option in the future UNIRAD software.

The results displayed in fig. 2-11 are obtained from Feynman's probalistic model which is based on the wider sample of observations and on simpler basic assumptions (e.g. the absence of 'Anomalously Large' events; all solar proton events, even the largest one are considered as 'Ordinary' events). This is one of the decisive reasons to incorporate this new model into the new UNIRAD software as the default option. This will then also be the recommendation made by TREND.

This closes the outline of the TREND's evaluations of existing models; the major rcommendations suggested by TREND concerning future models have also been presented here.

We are now ready for chapter 3 where software and data requirements and developments will be explained.

CHAPTER 3

SOFTWARE & DATA REQUIREMENTS & DEVELOPMENT

Based on the model description and evaluation given in TN1 and on model formalism and software requirements outlined in TN2, we present here the new software tools which have been developed to analyse the selected set of satellite data. All available data relevant to this study have been presented and catalogued in TN3 and will first be recalled below. The rationale for selection of the two sets of data (LANL and IUE) which have been analysed by TREND as part of this contract will also be given below as well as the analysis plan.

Data available and selection criteria

Based on Table 3-1 from the 'ESA statement of Work', NSSDC and NGDC catalogues of spacecraft and particle experiments, as well as other compilations more specific to satellite instrument descriptions, a comprehensive listing of energetic electron and proton data have been identified by TREND. Technical Note 3 contains a catalogue characterizing data with rexpect to species, energy range, spatial, directional and temporal coverage.

The presentation of the new catalogue has been made as user friendly as possible. Full details as to why particular formats were adopted are given in TN3.

The satellite instrumentation with respect to reliability and accuracy has also be given for each of the entries given in TN3. The Laboratory address and Name of the PI for these instruments is also provide.

A comprehensive summary table of data available and relevant to test the environmental models is given in Table 3-2. This table contains on the left orbit type information and provides one with an initial indication as to where a particular spacecraft was located i.e. if the orbit was geosynchronous, polar high latitude, low latitude circular, elliptical or whatever. Next we see the spacecraft name and with it an ancronym representing the instrument from which relevant data is available. In the next columns are listed the energy range and detector threshold information for each instrument.

These data show up strengths and weaknesses in the existing coverage of the earth's radiation environment. For example, in the 5-15 MeV range for protons, which are known to produce significant damage to spacecraft borne solar cells, energy coverage is essentially non existent. GMS and STP 78-2 are in the wrong area of space to monitor these particles. CRRES will fill this gap later on. The region from atmospheric cut-off to geosynchronous orbit will be covered by appropriate CRRES monitoring. Meanwhile, although DMSP provide coverage of protons, > 20 MeV these data are truncated in B-L space and there is no coverage of protons with energy >75 MeV.

It is notable that the natural electron population in the inner zone has never been determined well since remenants of the Starfish fission experiment were present up until about 1970 when monitoring instruments were flown. Thus, as noted in Technical Note 2 it would be very interesting to compare DMSP data with inner zone AE8 with a view to investigating the long term behaviour of sources and the processes of atmospheric loss.

At the present time the Geostationary Region is well covered by LANL and TREND has to improved the standard deviation model from AE-8 using these data and the 1989 magnetic field model of Tsyganenko. The role of very energetic electrons in producing deep dielectric charging and system break down is presently not well understood and the behaviour of electrons with energies greater than a few MeV is currently of interest. The SEE instrument on LANL could provide the data necessary to carry out this study.

Almost all of the trapped radiation measurements from 1958 through early 1970 have already been used in producing some 8 proton and 8 electron models. The TN3 catalogue then excludes these measurements. Further, not all the available data accumulated since then, have been included. The Criteria for inclusion are :

Species. In the trapped radiation environment electrons and protons are so dominant that higher Z trapped particles experiments are not included.

Since s/c charging is outside the scope of TREND, plasma data have been excluded. There, working criteria of including only energies > 40-50 KeV for both electrons and protons were used (this eliminates most electrostatic analysers, mass analysers, etc.). There are a number of instruments which span across these thresholds and these are included in the relevant ranges.

Proton detectors which orbited within the trapping region but had energy thresholds too high to measure the ambient particles were also excluded. These are the solar proton monitors.

Having laid the ground rules, the spacecraft with their payload instruments included in the study were broken up into two categories: research or development spacecraft investigations, and, operational spacecraft including the well known GOES, NOAA, LANL series etc.

TREND then set about accumulating information relevant to the individual spacecraft, to the instruments acquiring data within our constraints for acceptance and to existing data set descriptions. In this TREND drew heavily on information in the catalogues of NSSDC and NGDC. However, as a result of activities within TREND, much more detailed information than has been already pusblished concerning many instruments and data sets has become available and this expanded material replaces the data center entries in the catalogue of TN3 summarized in Table 3-2.

The suite of satellites indentified in TN3 occupy four types of orbits: (a) highly elliptical, near equatorial, (b) low-altitude, near polar, (c) high-altitude, nearly geosynchronous, and (d) geostationary.

AMPTE/CCE, AMPTE/IRM, and ISEE 1 & 2 are in class (a), while DMSP 5D-2/F7, N0AA 6 - 10, ISIS 2, and STP P78-1 are the ones in class (b).

Class (c) contains IUE and SCATHA. The largest class, of course, is (d) containing 7 DoD satellites carrying the Los Alamos National Laboratory (LANL) detectors, the 3 GMS series, the 7 GOES series, and Meteosat 3, which is carrying the low-energy electron portion of the LANL instrument.

Description of the data selected for analysis, and selection rationale.

As a result of the limited ressources available to TREND, only two sets of data have been analysed in some details using the new software tools designed and built by TREND. The data analysis and data processing considered in this study have been based on the Los Alamos National Laboratory (LANL) electrons measurements, and secondly on the electron measurements obtained from a "minimally intrusive" particle monitor added to the astronomical payload of the International Ultraviolet Explorer (IUE).

Selection of tasks

There are several criteria which determined TREND to concentrate on satellite data from the high altitude region more than from the low altitude one. First of all as a result of the model evaluation and software requirements in TREND's TECHNICAL NOTE 1 and 2 it was concluded that the traditional B-L coordinates must be replaced by a new coordinate system (like the Hassitt's shell height) to map adequately the trapped radiation fluxes between 150 and 1000-2000 km altitude. Indeed, at these altitudes the atmospheric density determines the flux of the Earth's radiation environment more significantly than the geomagnetic field distribution.

Despite all the interest such a study extension would have offered for future ESA mission in low-altitude orbit (e.g. Columbus, Hermes), TREND decided to focus its data analysis and data processing efforts on LANL and IUE data which are respectively near geostationnary missions and highly altitude missions on a GTO type of orbit. Indeed, these types of mission orbits are often choosen for astronomical satellites, communication and meteorological spacecraft.

There was an additional reason to prefer high altitude data instead of low-altitude ones in the present case: indeed, the new programme BLXTR was build by TREND to accomodate for the local time dependent deformation of the geomagnetic gield by magnetospheric currents. It was obvious that the best test repository for this new software was by using data from the outer part of the magnetosphere, and not from the region closer to the Earth where the effect of magnetospheric currents is negligible.

LANL provides geostationary data, whereas the IUE satellite is on high elliptical orbit with a period of 24 hours. These orbits are appropriate to study B-L space for L between 3 and 8. The instruments on board cover an energy range which is adequate to improve the existing AE-8 model in that region of space. In both cases the data cover a long period of time of many years, allowing to identify possible solar cycle effects, long time averages and reliable standard deviations of the particle fluxes measured. The local time coverage is also complete for these two sets of data. The easy and quick availability of these data from NSSDC was another reason for TREND to select these two data sets instead of any other which needed clearance and heavy preprocessing or reformating. Indeed, the duration of this contract was only 15 months. With the limited resources available, excessive time delays to acquire data had to be avoided.

The ISEE 1 data of Don Williams has been undergoing analysis by E. Daly and C. Tranquille at ESTEC/WMA for more than a year and data from a similar instrument on ISEE 2 will soon be brought into their analysis.

There are other also interesting data sets available, possibly for post-TREND studies : e.g. the DMSP data which are collected on a near polar orbit at low altitude (see TN2 Ch.4)

The SSJ* instrument of DMSP/F7 and B-L coverage has energy ranges which would offer be a valuable complement to the results obtained by TREND with the LANL and IUE data sets. But as indicated in chapter 2, mapping of the radiation environment at low altitudes (150km-2000km) requires a novel approach and a new coordinate system: e.g. the Hassitt shell height, which a parameter determined by the density distribution in the upper atmosphere. Since, this new coordinate system needs serious software developments and optimisation which were not amenable within the time span of this contract, the low altitude DMSP measurements, have been given a lower priority by TREND, despite their great relevance in testing the validity of existing models at low altitudes.

For similar reasons,(i.e. limited resources and the limited validity of B-L coordinates at low altitudes) TREND did not attack the updating of the proton AP-8 model. Indeed, such an undertaking needs much more time and extended efforts to develop additional software tools, to acquire and process additional data sets.

The LANL and IUE data will now be presented in somewhat more details.

Los Alamos National Laboratory (LANL) geostationary charged particle analysers(CPA)

The LANL instruments

This instrument has been flown on seven DoD geostationary satellites and the low energy part on Meteosat P2. The DoD satellites were 1976-059A, 1977-007A, 1979-053A, 1981-025A, 1982-019A, 1984-037A, and 1984-129A (USA 7). Following the third launch, there were two active satellites with the third acting as a backup. Since these satellites were moved in longitude during their lifetime (Baker et al. 1981, 1982 and Cayton et al. 1989) only the expected parking positions are given here. They are 35°, 70°, 135°, 155°, and 290° W.

The CPA consists of separate electron and proton systems. The electron detectors are designated LoE and HiE.LoE consists of a fan of five separate detector-collimator units mounted at 0°, ± 30°, and ± 60° relative to the spacecraft (s/c) equatorial plane. The s/c rotate with a 10-s period about an axis that points toward the center of the Earth. Thus complete (over the unit sphere), continuous pitch-angle measurements of electron distributions are made by LoE every 10 s for essentially all magnetic field orientations. The s/c latitude extent of each LoE field of view is 30° and the geometric factor is 3.6E-03 cm^2-sr and there are six energy channels: 30-300, 45-300, 65-300, 95-300, 140-300, 200-300 keV. The basic CPA sampling rate is 8 ms so that each energy channel of each sensor is sampled 40 times per spin period.

The HiE consists of a single detector-collimator unit that is pointed outward along the Earth-satellite radius vector. The conical collimator has a half-angle cone of 4° giving the system a geometric factor of 1.8E-02 cm^2-sr. There are six energy channels: 0.2-2, 0.3-2,0.4-2, 0.6-2, 0.9-2, 1.4-2 MeV. Only a relatively narrow portion of the unit sphere is sampled as the s/c rotates. However, for

normal (approximately dipolar magnetic orientations) nearly all pitch angles will be sampled. For tail-like magnetic configurations HiE samples a very small range of pitch angles.

This data set consists of hourly averages of the energy channels of all the CPA instruments as well as the daily averages; these daily averages are based on estimators and so constitute some type of a model. This averaging then converts the fluxes into isotropic directional fluxes so that the pitch angle information is lost.

The data set starts in January 1979. Their Synoptic Data Set covers the period July 1976 to January 1979. Dr. Thomas E. Cayton is the LANL contact now that Dr. Paul Higbie, the original PI, is no longer associated with the activity. Based on discussions with Tom Cayton the data sets through 1983 are available for TREND and NSSDC was given access to these five files (one for each of the LANL satellites, 1976-059A, 1977-007A, 1981-025A, 1982-019A, and 1984-037A) for transfer over SPAN. A VAX standard "backup" tape was produced. The tape also contains a FORTRAN routine to read and print any portion of the files. The routine identifies each field in the logical record and gives the representation and the physical units of them.

The LANL data sets

From this data set TREND needs the 12 electron channels, which are available as hourly averages in 24 local time (LT) bins. Except for the identification of the appropriate bins for performing longer term averages. The LT is the useful variable both for binning and for graphical display. To prepare for the analysis, i.e., construct the production software, the following processing was done. The electron data as received represents isotropic directional flux. Thus the inputs must be multiplied by 4π to be a more physically meaningful quantity, the omnidirectional flux, denoted by $J(E_i - E_{ui}, LT, \phi)$ with units of electrons/cm^2-s within the energy band $E_i - E_{ui}$, where

$$E_{ui} = 0.3 \text{ MeV}; \; i = 1,6$$
$$2.0 \text{ MeV}; \; i = 7,12$$

The longitude, ϕ, is used here, not to infer a dependency, but to serve as an identifier between the different LANL spacecraft (really different parking ϕ's). Because of the nature of the satellites, (i.e., geostationary), it is much more efficient to defer the assignment of physically meaningful position coordinates to the analysis phase. For purposes of requirements, it is convenient to consider this quantity as a 5-index array. Thus J(i,j,k,l,m) will be used where

i	=	channel index, 1,12, i.e. defines the energy band,etc.
j	=	LT index, 1,24.
k	=	day of month index, 1,28,29,30,31.
l	=	month index, 1,M, where M can be as large as needed
m	=	parking longitude index, 1,6 or so.

With this notation the following quantities have been be produced:

$$J_k(i,j,l,m) = \frac{1}{N(i,j,l,m)} \sum_{k}^{N} [J(i,j,k,l,m)] \qquad (1)$$

the sample monthly average;

$$J_j(i,k,l,m) = \frac{1}{N(i,k,l,m)} \sum_{j}^{N} [J(i,j,k,l,m)] \qquad (2)$$

the sample daily average which corresponds to a daily local time average;

$$J_{jk}(i,l,m) = \frac{1}{N(i,l,m)} \sum_{j}^{N} [J(i,j,l,m)] \qquad (3)$$

the sample monthly and local time averages.

$$\Phi(i,j,k,l,m) = \frac{J(i,j,k,l,m)}{Jj(i,k,l,m)} \qquad (4)$$

an empirical normalized local time variation function.

The LANL data sets also have the standard deviation accompanying each local time bin flux, which will be denoted here as S(i,j,k,l,m). This quantity is a standard deviation of lux measurements observed during one hour UT periods i.e. also LT periods.It is not directly useful in the planned study, but the quantity

$$SL(i,j,k,l,m) = \frac{S(i,j,k,l,m)}{J(i,j,k,l,m)} \qquad (5)$$

is approximately equal to the standard deviation of both the lnJ and logJ over the hourly periods of time;

$$SL(i,j,l,m) = \frac{1}{N(i,j,l,m)-1} \sum_{k}^{N} [J(i,j,k,l,m)-J_k(i,j,l,m)]^2 \qquad (6)$$

is the standard deviation (sigma for short) of the monthly sample used to create (1) above.

LANL data processing

The LANL data sets from 1979 to 1988 are available on six files names LANLn.DAT with n = 1,6.

Table 3-3 summaries LANL data available to TREND. The number of records is the number of valid records whereas the size refers to the total number of records (valid and invalid). The longitudes are calculated from the universal time and local time (available within each record).

The detailed description of the LANL data records is given in TN4, and will not be repeated here.

After reading and validation of the records, the longitude of the satellite is calculated from the Universal time and local time. Daily average flux have been calculated from the local time data. Similarly montly and yearly averages have been determined. Similar averages of the logarithm of the fluxes are also computed as explained in TN4, indeed the individual flux measurement follow generally a log-normal distribution.

Standard deviations associated with all these averages have also been determined using normal procedure. Various graphical plots of these averages and standard deviations have been generated. A few examples will be presented in the next chapter.

Omnidirectional electrons integral spectra are fitted with two exponential energy distributions (Cayton et al., 1989)

$$J(>E) = A \exp(-E/E_a) + C \exp(-E/E_c)$$

where A, and C are constants, E_a and E_c are exponential gradients and E the lower energy limit.

The differential flux is then given by

$$J(E) = (A/E_a) \exp(-E/E_a) + (C/E_c)\exp(-E/E_c)$$

The parameters A,C,E_a, and E_c,are determined by the least square method using the 12 electron energy channels available. The procedure is described in TN4.

The data have also been fitted to a power law

$$J(>E) = A\,E^{-C}$$

where A and C are again ajustable constants determined by the least square technique. The LANL data fit the power law less well than the exponential law.

The B-L coordinates of the LANL positions are calculated using the new software BLXTRA described in TN5. Since one of the objectives of this study is to determine the amplitude and phase of the local time variation of trapped electrons near geostationary orbit, the B-L coordinates are first determined using a magnetic field model which is not local time dependent (i.e. the IGRF model corresponding to the epoch of the measurements). In this case all measurements are characterized by nearly the same value of B-L. Indeed the satellites is fixed within the IGRF distribution used to model the geomagnetic field. In a second step, new B-L coordinates are computed with BLXTRA but with a magnetic field model which depends on local time and on the level of geomagnetic activity Kp. (i.e., the same IGRF model as above; Tsyganenko's external magnetic field: T89). In this second case the geostationary satellite changes position with respect to the B-L drift shells.

The first approach is called the conventional approach; the second one is the approach with an external field model. In chapter 4 the results of both approaches are compared.

In the first case once all B-L values are available a grid of points is determined in B-L space.

-four B bins [0.00102,0.00106],[0.00106,0.0011]
[0.0011,0.0014],[0.0014,0.0018].
-five L bins [6.5,6.6],[6.6,6.7],[6.7,6.8]
[6,8,6.9] and [6.9,7]

The omnidirectional fluxes for each B-L bin, and for each local time bin are then averaged; this is repeated for each energy treshold.

The observed local time variations are then compared to those of the AE4 models which are described analytically by the formula....

$$\Phi_T(E,L,\phi) = K_T(E,L)\, 10^{C_T(E,L)} \cos(\pi/12)(\phi - \Omega_T(E,J))$$

where:

- T denotes the epoch dependence,
- E is the energy level,
- L is the McIlwain shell parameter,
- U is the local time,
- $X_T(E,L)$ is the phase (constant and taken equal to 11 in AE4 model),
- $K_T(E,L)$ and $C_T(E,L)$ are dimensionless.

parameters (amplitudes of the LT variation)

- $K_T(E,I)$ is a normalisation factor such that,

$$\frac{1}{24}\int_0^{24} \Phi_T(E,L,\phi)\,d\phi = 1$$

Physically, Φ_T represents the normalized amplitude of local time variation of flux levels. In AE8-AE4 models, it is linked to the integral flux $J_T(>E,B,L,\Phi)$ by the formula

$$J_T(>E,B,L,\phi) = N_T(>E,L)\,\Phi_T(E,L,\phi)\,G(B,L)$$

where :

- J_T is the time average omnidirectional flux above energy E,
- B is the magnetic field strength,
- N_T is the spectral function,
- G is the model B-dependence. (described in TN2)

LANL data are used to update coefficients C_T, K_T, and Ω_T for the geostationary orbit at epochs T covered by LANL satellites (that is, 1979 to 1988) keeping the same analytical expression for Φ_T but including a B dependence for these 3 coefficients.

The values coefficients C,K, and Ω are determined by a least square technique, and stored on file. Their values determines the local time variation which will be discussed in chapter 4.

Assuming the logarithm of the electron flux is normally distributed at all points of observation in space, a standard deviation can be computed and compared to those from the earlier AE8 and AE4 models.

The details of this calculation are presented in TN4. The standard deviation is provided for each B-L bin, ϕ-bin, and energy threshold E : $\sigma(>E,B,L,\phi)$. Provided the statistical distribution of fluxes is log-normal, the value of σ can be used to compute the probability distribution.

The result will also be discussed in chapter 4.

In order to preserve compatibility with AE8MIN/MAX, the new values for the flux obtained from the LANL observations are stored in block data file called TREM-G.FOR. The internal organisation of AE8MIN/MAX models is also used for the TREM-G.

It may be useful to mention here what this new acronym stands for : TREM-G means Trapped Radiation Environmental Model for Geostationary orbit. The same procedure is followed to determine the alternative model TREM-GX. The X in the acronym means that an eXternal magnetic field model (T89) has now been used in BLXTRA to determine B-L coordinates.

Since Tsyganenko's model depends on the value of the geomagnetic index Kp, the transformation from geodetic coordinates to B-L coordinates will depend on K_p. All observations have been binned into 4 internals of Kp :

$$K_p<2^+,\ 2^+\leq K_p<3^+,\ 3^+\leq K_p<5^+,\ 5^+\leq K_p$$

These four geomagnetic activity levels correspond to quiet, mean, strong activity and magnetic storm conditions. Wider ranges of B and L values are now covered as a result of the local time dependence of the magnetic field distribution and the K_p dependence. The B-L grid is now divided in

- eight B-bins [0.00094,0.00098],[0,00098,0.00102]
  [0.00102,0.00106],[0.00106,0.0011]
  [0.0011,0.000114],[0.00114,0.00118]
  [0.00118,0.00122] and [0.00122,0.00126]

- eight L bins [6.6,6.75],[6.75,7],[7,7.25],
  [7.25,7.5],[7.5,7.75],
  [7.75,8],[8,8.25],[8.25,8.5]

The integral electron spectra $J_T(>E,B,L,K_p)$ for each B-L bin, are now given for 4 K_p intervals instead of 24 local time intervals. Similarly, the standard deviation is $\sigma(>E,B,L,K_p)$ is now a function of K_p, the local time dependence being averaged out. This is a reasonable procedure, since introducing an appropriate external magnetic field should cancel or at least reduce the local time variation of the flux $J_T(>E,B,L,K_p)$.

The objective of this analysis is to build new trapped electron flux tables for the geostationary region of B-L space. The model matrix is stored in a block data files names TREMGXn.FOR, where n refers to the number of the four K_p ranges considered above.

The results obtained are displayed and discussed in chapter 4.

The IUE particle flux monitor (PFM)

The IUE instrument

These data are being supplied to TREND by NSSDC on a demand basis on tape that contains the orbit elements, the attitude of the spacecraft roll and pitch axes in the geocentric equatorial inertial (GEI) coordinate system [given as Euler angles], the median voltage reading from the instrument count ratemeter for intervals of about 5-minutes, and the number of voltage readings that were made during each interval. The PFM is comprised of a lithium-drifted silicon detector, a 16° half-angle collimator with the opening covered by a 0.357-g/cm^2 Al absorber, pulse discriminator, associated electronics, a logarithmic count ratemeter, and overall shielding of 2.31 g/cm^2 except for the collimator opening. The electron threshold energy is 1.0 MeV and the proton threshold is 15 MeV.

IUE is in a 24-hr elliptical orbit at an inclination of 31.6°. The apogee altitude is 42,413 km and the perigee height is 29,155 km. These parameters have varied somewhat over the lifetime of the satellite.

Data have been collected in digital form since Nov. 6, 1980 and continue to be deposited in NSSDC by the IUE project at the present time. The tapes are 9-track, 1600-bpi, EBCDIC, and multifiled. Each tape contains approximately 15 files. Three tapes covering the time period Nov. 6, 1980 - March 27, 1981 were supplied to MATRA prior to the Dublin meeting and initial reading of the first few records has been accomplished by using the EBCDIC read utility.

IUE Data analysis

A program (IUESYS) developed by Vette and Abdul Doyle in 1981 is capable of handling this data set but some modifications had to be made.

Since the IUE data provides a measure of the directional flux > 1.0 MeV off the magnetic equator in the 20 - 40° range, the position tagging to physically meaningful coordinates cannot be postponed until the analysis phase. Since IUE only generates one data point every 5 minutes. The only requirement that takes some new logic, is to trace the total field line from the position of the satellite to the position of the miror point corresponding to the pitch angle (i.e. the angle

between the direction of the particle detector with respect to the magnetic field direction.

There are fourty-three IUE data files at present in the possession of TREND and these cover the period November 6th 1980 to March 27th 1981. The files in EBCDIC format have been converted to ASCII format prior to using them. The characteristics of the IUE files is given below.

From the 43 IUE files provided to TREND we have built 25 'sorted' IUE files, each being characterised by a set of constant orbital elements. Indeed, after examining IUE data, it has been observed that different files had the same orbital elements whereas in the same file one finds occasionally several times the same set of orbital elements. The format of these files is the same as the original ones; only the list of records is different.

As IUE files do not provide the position of the satellite at start and stop times, an orbit generator has to be used to relate date and time to the geographical spacecraft position. The SAPRE module is utilised for this purpose.

For each IUE file, we read the (constant) orbital element and the starting date/time and create the associated SAPRE namelist file. Then, SAPRE generates an output file containing the geodetic coordinates of the points of data observations. This file is used as input by program IUESYS.

The main objective of the processing these data prior to there analysis is to bring the data set to the same level as the LANL data. This process was done at Los Alamos National Lab.before the LANL data were made available to TREND via NSSDC. In brief, the processing tapes starts from the raw data. Also involved are transformation matrices to obtain e.g. geographic coordinates and solar magnetic coordinates.

The preprocessing program provides the following variables, which do not contain B,L nor the pitch-angle information.

YEAR	- year, (integer)
T	- Starting date/time of the logical record, (decimal days)
DT	- Time increment,

	(decimal minutes)
FLUX	- Directional flux of electrons with energies larger than 1 MeV, (electrons/cm^2-s-sr)
NQUAL	- Quality index, number of samples for median.
GLA(K,1)	- GEO x-component of detector, look angle unit vector.
GLA(K,2)	- GEO y-component of detector, look angle unit vector.
GLA(K,3)	- GEO z-component of detector, look angle unit vector.
GLA(K,1)	- GEO s/c radial distance, (km).
GEOP(K,2)	- GEO s/c latitude, (degrees).
GEOP(K,3)	- GEO s/c east longitude, (degrees).
GLT	- GEO local time or s/c, (hours).
ISLEW	- The slew flag.

The contents of these processed IUE files allows to plot :

- the omnidirectional flux versus local time assuming an isotropic flux (multiplication of variable FLUX by 4π),

- the cumulative distribution of the log flux, that is the probability to exceed a given flux treshold.

Some of these plots will be shown and discussed in chapter 4.

For each record B and L are then computed with and without external magnetic field. In both cases, we use program BLXTRA with IGRF-85 internal field model (with BLTIME = Year of the IUE data measurements) and Tsyganenko-89 external field model. For each record, the value of K_p is read in the K_p file.

The following four tasks have been accomplished :

- determination of the B-L coverage of IUE satellites with B and L computed with IGRF-85 only,

- determination of the B-L coverage of IUE satellites with B and L computed with IGRF-85 and Tsyganeko-89

- mapping of flux in B-L coordinates with B and L computed with IGRF-85 only,

- mapping of flux data in B-L coordinates with B and L computed with IGRF-85 and Tsyganenko-89.

The graphics tools used are based on the MATRA graphics library GRAPHLIB. Results are described in chapter 4.

This processing of IUE data assumes that the pitch angle distribution of the particle is isotropic: i.e. that the omnidirectional flux can be obtained from the unidirectional flux by multiplying the latter by 4π. Although this procedure is rather questionable, it leads at least to an order of magnitude evalutation of the actual omnidirectional fluxes along the IUE orbit. As indicated in TN2 (chapter 4), since the particles entering the detector have in general a pitch angle not equal to 90° (i.e. corresponding to a miror point) a program had to be developed to compute the geodetic coordinates of the actual miror point associated with this pitch angle. This programme is currently under development at IASB but it needs to be tested before it can be implemented in IUESYS.

Once these coordinates are known the geomagnetic B-L coordinates can be determined using the BLXTRA programme which will be described in the following section.

Software tools developed by TREND

In order to analyse the LANL and IUE data a number of software tools have been developed by TREND. Some of these tools (e.g. BLXTRA) have been implemented in the new version of UNIRAD delivered to ESTEC as part of the present contract.

Fig. 3-1 shows a block diagram of the architecture of the UNIRAD software TREND has been concerned with.

A - The UNIRAD software package contains a suite of programs which computes the geocentric coordinates of a predetermined number of points along the orbit of a satellite. These coordinates are outputs of a program called SAPRE. Although, it was not part of the tasks for the present contract, additional features have been implemented in SAPRE to make it more userfriendly for occasional users of ESABASE/UNIRAD. These improvements have been explained in TN5 and will not been emphasized here, although it is a real improvement for UNIRAD, that was provided by TREND.

B - The UNIRAD software package contains a second chain of programs and subroutines which transforms the geocentric coordinates into magnetic B-L coordinates by using optional geomagnetic field models. This chain of programs is called SHELLG in the earlier version of UNIRAD. It uses one of a series of eleven optional internal geomagnetic field models. No local time dependent external magnetic field model was available in SHELLG.

It has been a major and important task for TREND to design, implement and test a new software package which includes now four different optional external magnetic field models which are local time dependent. (Mead-Fairfield, 1975; Tsyganenko's models, including the latest one of 1989; the short and long versions of 1987 are also included for the sake of completness).

The new software package replacing SHELLG in UNIRAD, is now calles BLXTRA. Figs.3-2 and 3-3 shows the architectural design of BLXTRA. BLXTRA is described in TN5 and delivered to ESTEC as a documented FORTRAN source

programs. The comparison of results obtained with BLXTRA and SHELLG are presented in TN5 and will be summarised in Chapter 5.

C - The UNIRAD software package contains a third chain of programs called TREP whose overall architectural design is shown by fig.3-4.

(1) This complex of programs calculates the omnidirectional flux of trapped electrons and trapped protons, using optional models like AE8 (for the electron flux distribution) and AP8 (for the proton flux distribution) for each pair of B-L coordinates determined as output of SHELLG or now BLXTRA. The trapped radiation models are stored in matrix form for a grid of B-L coordinates. Interpolation methods are used to calculated the fluxes at the intermediate B-L pair of values.

The fluxes are given both in differential form and integral form i.e. either for unit energy interval, J(E), and, for energies above an energy threshold, J(>E). Fig. 3-5 shows the architectural design for this part of TREP.

(2) The TREP chain of programs calculates also the fluence of these omnidirectional fluxes or orbital average flux values. (see fig. 3-6 for the architectural design).

(3) The fluences corresponding to the trapped protons, are added to the contribution due to the solar flare protons. In this part of the TREP software TREND has implemented, as the default option, the Feynman et al."s model described in TN1 and TN2.

The original fluence model of King which was the only choice in the earlier version of TREP is left as an option to the user of UNIRAD. Fig.3-7 gives the architectural design for that new part of TREP. The detailed description of these changes are given in TN5. A comparison of the numerical results obtained by both models is also presented in TN5 and will be summarised in chapter 5.

Software utility subroutines developed by TREND

A series of new utility subroutines have been developed by TREND and added to UNIRAD as part of this contract. They are called in SAPRE, BLXTRA or in TREP programs.

A- The following routines have been added; they are called directly by the main program.

- INIORB: initialisation of constants and commons,
- JD1950 (IYEAR,IMONTH,IDAY,IHRS,IMIN,ISEC,AMJD): computation of the modified Julian time AMJD as a function of date (IYEAR,IMONTH,IDAY) and time (IMIN,SEC,AMJD),
- GREMEQ (AMJD): function returning the sidereal time as a function of the modified Julian date AMJD.

These routines are called by the main program of the orbit generator SAPRE. They are described in more details in TN4.

B- The external magnetic field components are computed by the subroutine BEXT which calls the subroutine TSY89. This subroutine computes the GSM components of the magnetic field produced by the magnetospheric current system. It corresponds to Tsyganenko's empirical magnetic field model version published in 1989 which is K_p dependent and based on the widest data base ever used to construct an external field model. There are 6 different series of model coefficients which correspond to 6 different ranges of K_p values. The Earth's dipole tilt angle is another input argument which is however set equal to the zero, which corresponds to the daily averaged of this angle.

A more detailed description of the TSY 89 subroutines is given in TN. The difference of constant L-contours calculated with and without Tsyganenko's external field is shown in chapter 5. At geostationary orbit a maximum difference of the order of 20% is obtained.

C- The optional solar flare proton model of Feynman et al. has been implemented in TREP. The input and output arguments are similar and

compatible with those of King's model subroutine already available in TREP The duration of a mission in years during the active part of the solar cycle (TFLARE), and a confidence level, expressed in % (FLPROB), are the inputs as well as N values of proton energies E (as in the case of King's model). E is expressed in MeV.

P = 1-FLPROB/100 is the probability that the fluence does not esceed the calculated fluence during the time length of the mission. The outputs are the fluences (FLUEFL) calculated for each energy level E. The units are protons/cm^2

The program used to compute the Probability, P, as a function of the solar proton fluence, F, is based on a numerical method described in Feynman et al.'s paper. It is also described in TN2 and TN5. The numerical values of P = P(FLUEFL;TFLARE) for different values of TFLARE are found to be identical to those published by Feynman et al.(1988) (see fig.2 - X)

These values are stored as matrix elements which are used in TREP to calculate by interpolation the value of FLUEFL for any input value of TFLARE and P or FLPROB.

CHAPTER 4

DATA ANALYSIS & MODELLING RESULTS

Results obtained with Feynman et al.'s model.

The FEYNFL subroutines computes the probability FLPROB that the a given fluence 10^f is not exceeded during a mission which would last τ years during the active period of the solar cycle. This probability depends on the energy threshold E (in MeV) as well as on the values of τ and f.

The numerical method is based on a Monte Carlo technique which involves the generation of N random numbers. The value of N is large (up to 10^5); this implies that the calculation is very time consuming and cannot be performed directly for each point along the satellite orbit with this subroutine FEYNFL. Therefore, the calculation of FLPROB is performed once for a variety of values of τ, f and for two values of E : 10 MeV and 30 MeV. Conversely, the value of f can be determined for a given value of FLPROB. These values are then stored in matrix form which is then used in TREP by interpolation to determine the value of f or 10^f for given value of E,τ, and FLPROB.
Table 4-1 shows the values 10^f (in p/cm^2) for τ = 2 years, for E = 10 and 30 MeV, and for two values of the FLPROB : 80% and 95%. The four last columns give the results obtained by TREND for different values of N. The results given by Feynman et al. (1989) are also shown in the fourth's column. It can be seen that when N increases the results obtained with the FEYNFL program is consistent with that of Feynman et al. The third column gives the results obtained for the same input conditions with the model of King (1974).

Note that the CPU time required for calculating one value of the solar proton fluence f for FLPROB = 95% and τ = 2 years is equal to 30 s, 5 min, 45 min, respectively for N = 100, 1000, 10.000 with the FEYNFL.

This clearly indicated the need for interpolation tables to be used in TREP instead of a direct calculation with subroutine FEYNFL. The good agrement between the results obtained by TREND with the FEYNFL subroutine and Feynman et al.'s results is illustrated in fig.4-1.

In Feynman's statistical study only two energy threshold were selected 10 and 30 MeV. To obtain the fluence for other intermediate values of E an interpolation energy spectrum has to be assumed. Two different fit functions have been tried: an exponential law, and, a power law. Fig. 4-2 shows the fluence spectrum obtained with an exponential law (X) and with a power law (*) using Feynman et al's model. For comparison the corresponding results obtained with King's model for FLPROB = 95% and a 7 years spacecraft mission is also shown by (+). This figure confirms that the fluence prediction in King's model is more optimistic (lower values of the fluence) than Feynman et al's model at low energies.

But at higher energies the reverse is true, when Feynman et al.'s observation are fitted with a simple exponential law. The values of $P(\tau, f, E)$ are stored as matrice elements in a file called PSTORE.DAT which is used with a standard interpolation technique to determine in TREP the value of f or 10^f for a given mission length, and for a given energy range or energy threshold.

B-L coordinates with and without an external magnetic field.

Up to now only internal geomagnetic field models have been used to determine the B-L coordinates of particle mirror points or labels of drift-shells. The 11 models already implemented in UNIRAD/SHELLG did not include the early Jensen and Cain (1962) model (for epoch 1960) which was used to construct AE8 and AP8; it did not contain most recent IGRF model. These two models as well as the GSFC 11/87 model for epoch 1982, have been added by TREND to the UNIRAD software package.

When these models are used to transform the fixed position of a geostationary satellite, the B-L coordinates is then constant i.e. independent of universal time (UT) and local time (LT). But a geostationary satellite positioned at different geographical longitudes has its B-L coordinates located somewhere along the curve shown in fig.4-3. The double loop shape of this curve in B-L space is the consequence of the tilt angle of the magnetic dipole and of its eccentric distance with respect to the Earth center (see TN1). The B-L coordinates associated with the flux measurements of LANL geostationary satellites are then independent of UT and LT.

This is no more the case when a local time dependent external magnetic field component is added to the internal geomagnetic field. In this case the values of B-L coordinates of a geostationary satellite changes continously with UT and LT. This is a consequence of the day-night asymetry of magnetospheric currents which produces the observed LT asymetry of the magnetic field at geostationary orbit (see figs. 4-4 and 4-5). Since this LT asymetry in the B-field entails a LT asymetry in (B-L) drift shells (and in addition produces shell splitting) it is essential for mapping radiation environment at large radial distances to include in UNIRAD the best external magnetic field model currently available (see TN1) for a review of different such models.

Despite its limitations the model of Tsyganenko (1989) has been adopted as the default one for UNIRAD. It corresponds to OUTER=4 in the NAMELIST of UNIRAD. It describes in an empirical way the contributions due to
1) the tail current calculated in SM coordinates
2) the ring current calculated in SM coordinates
3) the return current of the tail
4) and the Chapman-Ferraro current both calculated in GSM coordinates.

The coefficients of the equations describing these different contributions depend all on the value of the geomagnetic index K_p which determines, for every tri-hourly period of time, the amplitude of the short time variation of the geomagnetic field.

TREND has pointed out that it would have been preferable to parametrize the Ring Current component as a function of the D_{st} geomagnetic index instead of Bartels K_p tri-hourly index. TREND has also recommended to construct future external magnetic field models which are directly dependent of solar wind plasma

and field parameters instead of K_p. But since such more elaborate models are not yet available, the latest version of Tsyganenko models has been adopted by TREND. The equations used are described in Tsyganenko's paper and in TN1 and TN5. The subroutine implemented by TREND is called TSY89.

The TREND subroutine TSY89 was tested with respect to the published results to Tsyganenko's own software. A software package has been received subsequently from Tsyganenko himself (personal communication 1989). Both codes give the same outputs. TREND's code is slightly faster on the computer available at IASB than the original version of Tsyganenko.

Fig 4-6a and b show isocontours of the magnetic field intensity at a surface of constant altitude (36.000 km). The latitude and longitude of points forming constant B-lines are superposed on a mercator map of the Earth.

Fig.4-6a corresponds to the case where an internal geomagnetic field model is used to determine B. Fig.4-6b is obtained for the case when Tsyganenko's model is added the same internal field model. These figures clearly illustrate the significant effect of the external field on the B-field intensity at large distance.

Fig.4-7a and 7b show in a similar format contours of constant values of L corresponding to all points of the same constant altitude surface (36.000 km). The limit between "open" and "close" magnetic field lines (i.e. where $L>20$) is strongly local time dependent. It is in the mid-night local time sector that the latitude of the trapping boundary is closest to the equator. Note also that the introduction of an external field lowers considerably the latitude of constant L contours.

Beyond this trapping boundary the magnetic field lines extend to infinity (at distances larger than 20 R_E); the second adiabatic invariant, I, of particles spiraling along these field lines is not defined; therefore L cannot be defined either. In this region of the magnetosphere, outside the trapping region B-L coordinates are not defined. No valuable alternative to B-L coordinates has been found yet, in this case.

TREND recommends that a commission of scientists including theoreticians, modellers of the Earth radiation environment, and experimentalists from different space agencies meet to discuss this issue of coordinatie systems to be used in future modelling efforts. This question merits serious attention now that the introduction of external magnetic field models in UNIRAD raised this

question. It must be recognized, however, that the flux of trapped particles in the region of open magnetic field lines (and in the quasi-trapping regions) drops to zero and needs not to mapped here. In this region solar flare protons contribute occasionally very large fluxes for short periods of time, and constitute the major hazard for microelectronic device.

It should be pointed out, that the amplitude of LT variation of L for a geostationary satellite is of the order $\Delta L = 1$ (i.e. one Earth radius); this remains relatively small ($\Delta L/L$ = 10-15%); furthermore at these larger L values the trapped radiation fluxes in the AE8 model are given at L-intervals of ΔL = 0.5 ! This implies that only two bins in L are concerned by the LT variation resulting from the asymetry of the external magnetic field at geostationary orbit.

Distribution of LANL data in B-L space.

Since LANL satellites are geostationary their position in B-L space is a single point when B and L are determined with an internal magnetic field model. This point corresponds to $B = 1.09\ 10^{-3}$ Gauss and L=7.00 for LANL1. For the five other LANL satellites located at other fixed longitudes along geostationary orbit the B-L coordinates correspond to five other points of the curve shown in fig. 4-3.

When Tsyganenko's external magnetic field is introduced to recalculate B and L at each instant of time, the position of the satellite moves along a closed curve which is fixed in B-L space provided that the external field is constant in time: i.e. when the geomagnetic index K_p does not change. However, in reality the value of K_p changes almost every three hour of UT, consequently the orbit of LANL satellites is not a close curve, but the positions of the satellites wander in a rondom manner within extended areas of B-L space. This area is shown in fig. 4-8 for LANL1. The different color scale (or grey shading) shows the relative number of data (in %) available in each small bin of B-L space.

This figure clearly illustrates how the LT variation of the external magnetic field and furthemore its dependence on geomagnetic activity (K_p - index) scatters the positions of a geostationary satellite like LANL1 into a range of B-L bins around the single point corresponding to its position calculated with SHELLG, the former software of UNIRAD.

Distribution of LANL electron flux measurements.

Let us now concentrate on all measurements made in a selected bin of B-L space : e.g.
$0.001045 < B < 0.001065$ Gauss and
$6.85 < L < 6.95$.

Figs.4-9 and 4-10 give the cumulative distributions (in %) of the relative number of flux measurements whose value is smaller than x (i.e. the abscisa in these figures). Fig. 4-9 shows this distribution for fluxes of electrons in selected energy intervals (30-300 keV... 200-300 keV). In fig. 4-10 the flux above different energy thresholds are considered (i.e. E>200; >1400 keV).

There are no flux measurements with values smaller than 10^2 cm^{-2} s^{-1} (instrumental limitation). On the other hand 100% of the flux measurements (i.e. all of them) have values smaller than 10^8 cm^{-2} s^{-1}. From these distributions one can test wether the observed fluxes satisfy a log-normal statistical distribution or not.

Energy spectra deduced from LANL electron flux measurements.

The (X) in Fig. 4-11 shows the observed electron fluxes per cm^2 per second and per unit energy internal (keV), when all the LANL1 data available for all B and L are averaged. This differential energy spectrum has been fitted by the sum of two exponential functions (see TN4, and chapter 3 of this report). The solid line marked by (*) is the best fit obtained by a least square technique. The free parameters A,C,E_a and E_c of this fit function have been determined by TREND.

Once these constants are known it is easy to calculate the integral spectrum using the expression given in chapter 3 (see also TN4). The upper curve in fig.4-11 marked (+) shows the mean integral flux, J (>E) in cm^{-2} s^{-1}, averaged over all LANL1 electron measurements.

Fig. 4-12 has the same format as the previous figure but it shows only the integral spectrum (not the differential spectrum) averaged over a subset of LANL1 data. This subset is obtained by taking only those measurements for which $0.001085 < B < 0.001105$ Gauss and $6.95 < L < 7.05$. The lower curve is the best fit obtained by the least square technique applied to the log of observed flux

fit obtained by the least square technique applied to the log of observed flux values. The upper curve, marked (*), corresponds to the sum of the mean value of F and the calculated standard deviation (σ_F). This value of $F + \sigma_F$ is a maximum value that is not likely to be exceeded (at the probability level of 75%).

It can be seen that the double exponential function fits very well the measurements over a wide range of energies : from 30 to 2.000 keV. The flux values vary by 5 order of magnitudes over this range of energy. No attempt is made by TREND to explain the origin of the two populations of electrons which form this composite energy spectrum. Furthermore, it has been found that the energy spectrum is harder for large K_p values.

The large value of the standard deviation results from the large amplitude time variations observed at geostationary orbit and in general beyond L = 4 in the magnetosphere, over a time scale of several days. These variations are attributed to adiabatic as well as non-adiabatic acceleration processes which were first pointed out by McIlwain (1963). The source of these electrons as well as their loss mechanisms are no yet satisfactory modelled. In this respect TREND wishes to recommand that renewed efforts should be encouraged and supported by national laboratories and space agencies, to study these basic physical mechanisms.

Indeed, the eventual goal of modelling efforts should be to build physical models instead of empirical ones. But to build a physical model of trapped electrons in a given energy range, the source and sinks of these electrons need to be well understood and modelled. This remains to be done in the future. Unfortunately, since late 1960's there is a characterized void of interest for such basic studies, except recently by Baker and colleagues and within the CRRES team of investigators. TREND recommands that a new generation of modellers attack these unsolved issues on the origins and sinks of energetic electrons, that they develop physical models and compare them to empirical models like AE8, or those like TREND is working on.

Local time variation of LANL electron flux measurements.

Fig.4-13 shows a scatter diagram of all LALN1 electron flux measurements for energies between 30 and 300 keV. It can be seen that at any local time there is a large dispersion of values, up to three orders of magnitudes near 00.00 LT.

When LANL data are sorted according to K_p values, one obtains slightly different scatter plots. When the mean values of log J are computed (this corresponds to calculate a geometrical mean value instead of the arithmetic mean value) for each local time hour a clear local time variation appears in the data.

This is illustrated in fig.4-14 which shows (+ marks) the relative values of all observed fluxes J(>30keV) as a function of LT, for $0.001085 < B < 0.001105$ and $6.95 < L < 7.05$. This LT variation is normalized to unity corresponding to the mean value of the sample considered. The solid line and * marks determine a best fit to these mean values using the same fit function as used earlier in the AE4 model (see TN4 and chapter 3 of this final report).

The parameters K_T, C_T and Ω_T of this function have been obtained by least square fit. The values deduced with LANL data are very much like those obtained earlier by Vette et al. for the AE4 model. The LT time variation for the mean integral flux of electrons is of the order of 50% of the average value, with a maximum around Ω_T = 11.00 LT and a minimum near midnight. Note however that Ω_T changes from one set of data to the next. In this calculation all LANL1 data have been included. When too small bin sizes are taken the statistics becomes poor in certain local time sectors and a satisfactory LT variation can hardly be deduced with one set of data,only.

Distribution of electron flux for a constant L-value.

Fig.4-15 shows the scatter plot of J(>E) of all LANL1 data for which $6.9 < L < 7.0$. The integral flux is plotted versus B/B_0 where $B_0 = 0.311563/L^3$, is the equatorial magnetic field intensity associated with L. This scatter plot shows again the large variability of electron flux measurements at large radial distances. The straight line indicates the mean value of J(>E) near the equator where B = Bo.

This value can be compared with that given in the AE8 model for $B/B_0 = 1$ and for $6.9 < L < 7.0$. Owing to the large standard variations the agreement between the LANL data and the AE8 model is satisfactory, although the AE8 are shlightly more pessimistic in certain cases.

TREND has found a slight increase of this mean value when K_p increases. However, owing to the large standard deviations this small difference is not of paramount significance.

In this chapter we have mainly shown the results obtained with the LANL1 data set collected during the year 1979. In TN4 results for the 5 other LANL data set are also presented. They confirm the conclusions outline above and all these additional figures need not to be presented again in this report.

Results from IUE data.

With IUE a much wider range of B-L space is covered than with the geostationary LANL satellites. Indeed IUE is on a 24 h elliptical orbit with apogee at 42,413 km perigee at 29,155 km, and an inclination of 31° 6, variable over its lifetime.

Fig.4-16 shows the local time distribution of the log (J(> E) for the IUE data. As indicated in TN2 and TN4 the B-L coordinates to be considered are not those of the satellite but those of the mirror point of the particles penetrating the unidirectional detectors i.e. with a pitch angle not necessarily equal to 90° .

As it stands BLXTRA program is not designed to determine the position where particles are expected to mirror. This modification of BLXTRA is currently under study by TREND but has to be tested and implemented in the IUE data software package. This additional task will not be completed before the term of this study, but could be executed subsequently if requested.

In any case TREND recommends that the exploitation of the IUE data, and of the other data sets identified in TN3 be pursued or undertaken to extend the coverage in B-L space beyond the region which has been sampled by the series of LANL satellites.

CHAPTER 5

FLIGHT MEASUREMENT REQUIREMENTS

With the exception of galactic cosmic rays (GCR) the only types of particles that are important from the point of view of radiation hazards are the energetic electrons and protons trapped in the Van Allen Belts. These particles provide a hostile environment for space systems.

Spacecraft missions are heavily impacted by the trapped energetic particle environment in several ways. Electrical charging which occurs as a result of hot plasma (20 keV magnetospheric electrons) can produce surface discharges that result in spurious operation or damage to the spacecraft. Energetic electrons of 0.5-1.5 MeV embed within dielectrics, producing optentials in excess of the breakdown potential of the material, again tesulting in discharges damaging sensitive components. Radiation dose effects, which are observed at all altitudes, limit the operational life of microcircits, and solar cells. They cause single event upset (SEU), latch up (LU), which produce spurious signals, and are a nuissance for the operation of all sensitive microelectronic devices which are onboard. In certain cases these particles constitute and additional heat input to low-temperature systems, especially those with passive radiators designed to operate at temperatures under 100 K. For ultra-low-temperature infra-red red sensors, such as those of IRAS, a transient additional heat load of 5 W/m^2 due to energetic particle population, must be considered in the design of the thermal management system; this could be a major constrain in the spacecraft design. For manned missions the radiation flux in space is a major element in planning orbits and extra-vehicular activies of the astronauts.

It is true that too optimistic models for the radiation dose would be fatal to certain sensitive devives, to man, as well to the mission operation. While too pessimistic radiation models would lead to design spacecraft too heavily shielded, too heavy, and too costly.

All this indicates how serious it is to have a continous monitoring of the radiation environment and to obtain a comprehensive mapping for the omnidirectional fluxes of energetic electrons and ions which are trapped in the geomagnetic field.

In this chapter we resume the main ideas and conclusions contained in TREND's TECHNICAL NOTE 6. It will be split into three main sections :

Where is there need for additional or new data;

What are the future flight opportunities for incorporating radiation monitoring detectors;

What is a 'minimally intrusive' detector to achieve cost effective monitoring.

Spatial regions of importance for the space radiation environment

The present knowledge has been derived mainly from the data obtaned during the first twelve years of the space erea along with the theoretical analytical, and modelling efforst associated with them. It should be pointed out that the first area of dicovery and scientific effort in space involved energetic paticles. The instruments were readily available out of nuclear physics, high-energy physics, and balloon borne/rocket borne cosmic-ray work. It took nearly a decade to develop instruments for other areas, such as plasma, astronmy, and earth resources where the main thrust has been for the past two decades

Knowledge of galactic cosmic rays

The basic work in GCR in the energy range of interest for TREND is essentially finished. The energy spectrum, composition and solar cycle modulation have been studied for more han 60 years by ground-based, balloon, rocket, and satellite instruments. The omnidirectional flux of GCR (> 100 MeV/nucleon) is about 4 particles/cm^2-s at solar minimum, and 2 particles/cm^2-s at solar maximum. More details are given in TN6.

The knowledge gained from this work is adequate for all foreeeable spacecraft engineering work. This is why the study of GCR has not been included in the work packages of TREND.

Knowledge of solar protons

These particles have been monitored nearly continuously since the launch of IMP 4 in May 1967. Of course earlier satellites also measured them on a research basis. Ground based observations go back to 1956. Recently a model has appeared that incorporates data that covers the 1956-1985 period containing most all of the 19th, 20th, and 21st solar cycles. These particles appear on a random event basis when looked at from a predictive aspect. There were 140 solar proton events in this period, which resulted in a total fluence of 1.06×10^{11} protons > 10 MeV and 2.8×10^{10} > 30 MeV. Converting these numbers into skin dose one obtains 55 and 6.2 krads, respectively. The average flux is about 118 and 31.1 p/cm^2-s, respectively.

Except for man and films these numbers are tolerable even for solar cells on a 10-year mission. Within an 11-year solar cycle there are seven years in which proton events are most likely and four years when the events are less likely and produce lower fluence events. The difference in yearly fluences between these two periods is about a factor of 25-50. By starting with a zeroth index year centered at solar maximum and running from year +6 down through -4, the active proton event years are -2 thru +4 and the less active ones are -4,-3, +5, and +6. Although the GCR do not contain protons of such low energies, their integral flux above such thresholds produce fluences which exceed those of the less active years for E > 30 MeV and are comparable for E > 10 MeV.

The observation of these particles far out in the solar system by Pioneer 10 and 11 and Voyager 1 and 2 spacecraft have provided further unterstanding of the propagation process so that flux levels measured in the vicinity of the Earth can provide some estimates for the outer reaches of the solar system.

The events can be treated much like terrestrial weather in that enough is known about the behaviour of the solar atmosphere that crude short term predictions of the order of a week can be made. In addition, large active regions

live longer than a solar rotation so that monthly predictions also have some credibility. However, these only benefit short manned missions. Most missions extend for 5 years or longer. Consequently, there are other models which can be made with the wealth of data.

Although monitoring by high altitude geocentric spacecraft is fast disappearing (IMP 8 is likely to be the last), there is monitoring on the NOAA series of polar weather satellites that cover the energy range from 16 - 850 MeV with a number of channels. These satellites spend about 40% of the time in the interplanetary medium over the polar cap. The present set of instruments provide coverage back to October 1978. In addition, the geostationary meteorological staellite series, GOES and GMS, have high energy proton detectors for covering the range 0.6 - 500 MeV in 7 channels. This set of instruments provides coverage back to September 1980.

Consequently, the outlook is good for continuing coverage of these types of particles and, as the low altitude weather instruments move to the Polar Platform, it is expected that the monitoring detectors will also be flown there. The LANL satellites also monitor solar protons in the 0.4-140 MeV band and this set of instruments started operating in July 1976.

In the case of solar protons there has been and will be a wealth of data. The modeling for these has not been very active. From the doses they deliver, it seems clear that SEUs are the major concern relative to spacecraft now that devices have 10 krad or higher hardness. Of course manned flights at higher latitudes are still quite vulnerable to solar protons.

Knowledge of trapped protons

This element of the radiation environment is in much poorer shape than that of the two previously discussed. Part of the problem is the difficulty in obtaining coverage with a single satellite, and another is the complexity of understanding the source and loss mechanisms in quantitative detail. The AP-8 model, which covers all energies above 0.1 MeV, used essentially all of the proton observations made by non-Soviet satellites. This covered the time period July 1958 - June 1970 but with many time gaps. There were 29 experiments flown on 24 different spacecraft and a total of 90 energy channels were available from this assembly of data. Even with this, the low altitude regions were never sampled

simultaneously by two satellites and the equatorial region 3-4 Re was only sampled by Explorer 26.

There are protons of at least 500 MeV trapped in the magnetosphere. Once protons get too energetic, their gyroradius gets too large for trapping to occur; this sets the upper energy limit. The most energetic protons peak around 1.4 Re. By the time the energy drops to 40 MeV the peak has moved to 1.5 Re. This trend continues so that 5 MeV protons peak at 1.8 Re. The outer boundary also has the same trend. 400 MeV protons reach the background flux at 2.1 Re, 50 MeV do at 2. Re, and 10 MeV reach to 3.7 Re. At any given L shell the energy spectrum hardens as one goes away from the equator. The more energetic protons have a flatter equatorial pitch angle distribution than lower energy ones. The peak fluxes are quite high relative to anything discussed far. For example, 30, 15, and 10 MeV protons have peak fluxes of 4x104, 1.1x104, 4x106 which means skin dose rates of about 32, 152, 760 rads/hr or 0.28, 1, 3, 6.6 Mrad/yr.

The sources are believed to be cosmic-ray albedo neutron decay (CRAND) protons for the highest energy protons down to about 10 MeV and from the solar wind through the geomagnetic tail, with inward radial diffusion producing acceleration from the solar wind energy (~ 1 KeV) to that observed. There is some difficulty getting enough acceleration to achieve the right energies. The CRAND source has been studied extensively and detailed calculations have been made, but the energetic protons that exist are larger by about a factor of 20 than the calculation predicts.

There is somewhat better agreement with the loss of protons to the atmosphere. However, there remain significant problems. The secular changes of the magnetic field possibly produce an addition source that decreases with increasing altitude.

At any rate there is no reliable way to extrapolate the existing AP-8 model to low altitude to correct for the problem of having increasing fluxes as one extrapolates to later times. The dosimeter results from manned flight missions show no increases in the doses except for the known solar cycle effect. Thus the combination of the source and loss terms plus the transport/acceleration produced by the changing field all seem to cancel at the inner boundary, but what is the underlying process and what do things look like at higher altitude?

The DMSP/F7 data covering the time period from November 1983 - July 1988 show about a 6-7% increase over this time period, which is probably a solar cycle effect, since the period concerned coincides primarily with the interval when the density of the atmosphere is decreasing at low altitude. These data are becoming available for modellers soon but no plans are known for undertaking a proton study. The energies covered are > 20, > 35, >51, and > 75 MeV. The limited equatorial coverage is the same as the NOAA series discussed below.

In reviewing the outputs from TN3 it was noted that there are no mesurements of protons in the energy region for solar cell damage. Nor are any being planned that TREND is aware of except for the CRRES satellite. This spacecraft will touch all the bases and one hopes it will have a long and successful life. Fortunately, in its near equatorial orbit with detectors that measure pitch angles all the particles on the field line will be sampled twice per period. There is not a CRRES follow-on planned, so the long term outlook is rather bleak. Maybe the outputs of CRRES will have to satisfy environment users in many regions of phase space for the next twenty years.

At energies > 15 MeV, the NOAA Space Environment Monitor (SEM) has two sets of detectors, MEPED and HEPAD, which have proton channels. The first covers the ranges 16-80, and 80-215 MeV and the latter covers the interval 370-850 MeV in three ranges plus > 850 MeV. The satellite will cover a portion of the proton region but above about L=1.18 the equatorial region will be missed. At L=1.5 and 2.0 the sampling will stop at about 27° and 40° magnetic latitude.

The MEPED detectors are three separate "omni" detectors commonly used to measure the omnidirectional flux. These should be straightforward to use. The HEPAD is a counter telescope with a 24° half angle conical field of view. It is not clear at this time if the pitch angle of the measured particle can be ascertained. If not, the data from this instrument for trapped proton analysis may be difficult to interpret. The MEPED data may provide a way to perform a systematic relook at protons in important energy hands for spacecraft engineering. Six satellites in this TIROS-N series have been launched starting in October 1978; there are three more in this series. The MEPED data set should be used for modelling purposes and could be compared with the DMSP/F7 data. Unfortunately, equatorial coverage is missing but CRRES can fill in this gap.

Knowledge of trapped electrons

These particles are found throughout the magnetosphere depending on the lower energy limit. Even if one chooses 500 keV. as suggested earlier, the flux cutoff is around 10.5 Re but islands (in a sea of no flux) can be seen in the tail. Since the atmosphere is the cause of the low altitude boundary, this boundary is similar to that of the protons. However, the electrons are lost to the atmosphere through pitch angle scattering instead of by dT/dx. This causes one to see a longitudinal dependence in the these fluxes. This is known as the windshield wiper effect and results from the electrons drifting through the South Atlantic Anomaly (SAA). As the low altitude electrons encounter the atmosphere drifting from west to east, they are scattered out of the radiation belt. This hole is then filled on the eastern side where scattering is still occurring and this brings new particles down from higher altitudes. After the electrons clear this region, there is little scattering on the rest of the drift path until the SAA is again approached.

From this inner boundary the electrons have two main peaking regions. The first is around 1.6 Re for 1 and 2 MeV electrons, with the 500-KeV ones peaking at 1.7 Re. One should point out that there have never been good measurements of natural electrons in the inner zone. Throughout the period from July 1962 until late 1969, the Starfish injected electrons dominated this region. Peak fluxes here are about 10^6 for 1-MeV electrons, which means a skin dose rate of 120 rad/hour which is equivalent to the 15 MeV proton skin dose. However, the important thing here is the response of solar cells and the 1 MeV equivalent ratio for protons to electrons is 1.2×10^3. In addition, the electron spectrum is such that the proportion of particles that can penetrate into most spacecraft is small relative to protons. The bottom line is that inner zone electrons are not a problem - but only because the energetic protons are more of a problem.

The slot region lies between 2-3 Re and this shows a dip in the electron fluxes; one may recall that the protons showed no such behaviour. The higher the energy the deeper the dip. At 500 KeV the dip is less than a factor of two while at 2 MeV the dip is more than a factor of 100. The region below 2 Re shows hardly any time variations now that the Starfish residue has decayed.

The slot region has considerable time variations but nothing like these existing farther out. Only a few of the many injection events from the tail, as seen at the geostationary position, are seen in the slot. However, because the number is small, these events determine the long term average flux and as with small number

statistics, the averages are highly variable. Yearly averages differ by up to a factor of 10.

The electron lifetimes in the energy range of interest are lower in the slot than on either side of it. In fact one has to get near the geostationary position before the lifetimes are as low. The presence of VLF noise and other wave disturbances are believed to be the cause for this decay. Flux levels are low enough on average not to be a problem and in general it is the most benign region until one gets past 7 Re. One can see factors of 30-100 changes in the flux but the structure change is slower than in the heart of the outer belt. The higher energy electrons have a longer life so that for injection events that reach the slot, the spectrum gets harder with time.

Starting around 3.3 R_e one finds the maximum of the long term (~ 9-12 months) 7-MeV flux. Then as one goes to a lower energy this maximum moves farther out. For solar maximum conditions the peak of the 500-KeV particles is at 4.75 Re while in solar minimum it is found around 5.1 Re. The general effect is that the solar minimum peak flux is invariant but the inner side of the peak grows during maximum conditions and pushes the observed maximum inward and to a slightly higher value. This is a fine detail that is difficult to see with all of the time variations that are present.

Solar max peak fluxes are $3.5x10^6$, $5x10^5$, $4.5x10^3$ at 1, 2, 4 MeV while solar min peaks are $3x10^6$, $3.5x10^5$, $4.5x10^3$ at 1, 2, 4 MeV while solar min peaks are $3x10^6$, $3.5x10^5$, $2.2x10^3$. Thus, the relative change increases with energy. Comparing with the inner zone peak at 1 MeV, one sees there is about three times the flux in the outer zone. This ratio rises rapidly above 2 MeV, being about 100 at 3 MeV. The inner zone has no 4 MeV electrons any more while the outer zone has them up to at least 7 MeV, possibly to 15.

The time variations in this 3.3-5 Re region show large injection events with the flux rising abruptly by as much as a factor of 1000. Then there is a period of exponential decay until this is interrupted by another injection type of rise. The decay times at 4 and 5 Re are nearly the same but, at 5 Re, one sees about three times the number of injections. This pattern continues as one moves higher, except the decay times become less. When one looks at the geostationary region, the exponential decay pattern is essentially gone and the time structure can be characterized by many injection events of varying size (rarely exceeding a factor of 100) that appear as jagged top rectangular waves. As one moves on to greater

distances the pattern looks more chaotic and there are periods where there is no discernible flux.

At geostationary orbit there is no solar cycle effect so the average fluxes are essentially constant. The flux levels at 1, 2, 4 MeV are $4.5x10^5$, $3.5x10^4$, $5x10^2$. The skin dose rate is 54, 4.2, 0.06 rads/hr or 471, 36, 0,52 krads/yr and the 1-MeV equivalent electron fluence is about $1.4x10^{13}$. This is more benign that the trapped energetic proton region, but the environment here is still a factor to consider. There is no compelling evidence that the very energetic electrons seen by the LANL satellites are trapped. If one considers that the Jovian electrons have access to the geostationary region without attenuation then eqn (6) indicates that these electrons would start to dominate the trapped spectrum somewhere around 5 MeV. Except for the LANL SEE experiment there have been no good electron measurements > 3.9 MeV at geostationary orbit. According to TREND information from LANL, the experimenters are still sorting out the energy calibration on this detector system, so the data are not yet available to modellers.

As in the case of solar protons, the geostationary region is well covered for electrons except with respect to the particles cited directly above. The LANL Charged Particle Analyzer measures electrons between 0.2 - 2 MeV in 6 bands. A lower energy system measures 6 other bands between 30-300 KeV. Their combined time coverage is from July 1976 to the present. The GOES/GMS series of geostationary meteorological stallites carry detectors that measures electrons > 2 MeV, while Meteosat P2 carries the low energy LANL system. It is expected that the geostationary meteorological satellites will continue to carry similar monitors for the foreseeable future. Hopefully, higher energy electron channels can be added to provide a comparsion with the LANL SEE data and shed more light on the deep dielectric discharge problem. The whole region from 3-7 Re should be considered as a region of danger.

There is a tremendous amount of data available in the geostationary region that covers all energy ranges of interest. Additionally, much of it is easy so use. The main things needed to be done are model the time variations using global knowledge; study the cause of the local time behaviour (mostly from the external field), and analyze variances of the log of the flux in more detail than the previous work.

For the regions beyond geostationary, one should first mention the synchronous satellites, SCATHA (officially STP P78-2) and IUE. These satellites

were in similar orbits with a period very close to 24 hours. The perigee was ~ 27.000 km and the apogee was ~44.000 km. SCATHA had an inclination of 7.9°, IUE was about 31°. IUE was launched in January 1978 and SCATHA in January 1979.

The main goal of SCATHA was to study spacecraft charging and as such it covered a full complement of energetic electron detectors. One covered the 0.05-1 MeV range in 16 channels and the other covered the 0.6-5 MeV range in 4 bands. The L shells from 5.4 to 8.6 were sampled within the magnetic latitude range from 0-18.8°. Although the satellite was operated for at least 6 years most of the data that has been processed only covers the period from March 79 - May 1980.

IUE is an astronomy satellite but a Particle Flux Monitor (PFM) was placed on board to indicate the electron flux near perigee so that the maximum exposure time that could be taken with the camera would be known. The PFM is a solid state detector with a 16° half angle conical field of view. It is a threshold detector; the pitch angle can be determined since the satellite is three axis oriented. The instrument is still producing data. The spatial coverage is similar to SCATHA except that the magnetic latitude range goes to about 42° and the L value goes about 14°. However, the intensity threshold is equivalent to about 10^4 electrons/cm2-s so coverage past L=10 or 11 is rare.

The synchronous region described above is an ideal one for study in conjunction with the geostationary satellite to understand drift shell splitting and the effects of external magnetic fields. TREND has made a start on such a study.

Complementing this, to round out the story over the whole flux tube, are the electron detectors on DMSP/F7 and the NOAA series. DMSP has > 1 and > 2.5 MeV channels while the NOAAs cover >30, >100, >300 KeV as well as lower energies that are not of interest here. As mentioned earlier the NOAA series has three more to be launched and continuation on a new series is hoped for. Unfortunaly, the DMSP series does not fly energetic particle detectors very often.

Finally, the distant reaches of the magnetosphere are not covered well in the energy range of interest. Beyond 8 Re there is usually not enough flux to cause any radiation damage problems but certainly background counting rates for some missions can be a problem. In the past 12 years only the ISEE and AMPTE (CCE and IRM) spacecraft have traversed this region with appropriate instruments. ISEE 1 and 2 lasted nearly 10 years and their termination was re-entry not a

radiation problem. ESA has been processing the ISEE 1 electron data in the 22-1200 KeV range in 8 channels for application to their space-based astronomy missions that will use synchronous orbits with apogees in the 12-20 Re range. It is unlikely that the future particles and fields spacecraft will carry energetic particles detectors.

Since the boundaries of the magnetosphere are so variable at these distances and much of the flux seen is related to solar events, a more logical solution than trying to model such a region would be to fly a simple particle detector system appropriate for operational needs in the same manner that IUE did. The solar Maximum Mission did the same thing to sense the SAA so that the large X- and gamma-ray detectors would turn off appropriately so as not to suffer degrading saturation effects.

In summary, in respect of looking towards the future, there seems to be good coverage of the energetic particle environment in the polar weather orbit and in the geostationary orbit from both meteorological and other operational missions. The polar orbits provide sampling at the foot of all the magnetospheric field lines but the electron coverage does not go to high enough energies (i.e. 7 MeV).

These satellites also provide reasonable coverage of the trapped energetic protons except for the important 5-15 MeV range for solar cells, where there is a complete gap. There has been nothing in the past 10 years (really more like 20) relative to electrons in the remainder of the magnetosphere. This includes the slot, the outer zone (except near geostationary) and the far reaches of the cavity past 7 Re.

ESA's future missions and flight measurements requirements

In the Appendix of TREND's TECHNICAL NOTE 6 background informations on measurements, and missions are presented with a comprehensive list of recent and future satellite missions. Based on these inputs, we outline in this section the requirements TREND has identified in the course of this study for future ESA missions.

As far as radiation hazards are concerned, there are several aspects to be considered.

First : what are the radiation problems for different types of space missions;

Second : how to combat these problems; can mission specific radiation environment monitoring with "minimally intrusive" detectors attached to future payloads resolve these problems ?

Thirdly : what are the carriers and future flight opportunities where such radiation detectors would be required and most appropriate ?
What is a "minimally intensive " system ?

Finally : How to make efficient use of all the data banks collected during future missions to update Earth's Radiation environment models and produce new ones.

What are the radiation problems for space missions?

In the introduction to this chapter it has already been emphasized that electrostatic charging of spacecraft surfaces in outer space, deep-dielectric charging of space vehicles exposed to energetic charged particles trapped in the inner and outer radiation belts or injected into the magnetosphere during solar proton events consitute a major problem for engineers involved in building shielded carriers for scientific instruments; the same is true for technical equipment of commercial and military interest (see Frezet et al., 1989).

The detrimental effect of hard corpuscular radiation is not limited to engineering technical aspects (e.g. degradation of solar cells) It impacts on and spoils also the measurements taken by scientific instruments in orbit around the Earth. Astronomical measurements are sometimes hampered by such detrimental effects (e.g.on HIPPARCOS). Indeed, detectors flown on astronomy satellites are very sensitive to the damage caused by the ambient trapped particles. Primary particles as well as secondary particles reduce the efficency of these detectors and shorten their life times. X-ray detectors using grazing-incidence mirror systems are, for instance, very sensitive to primaries and secondaries scattered through these mirrors.

But in addition to the detrimental effects on the spacecraft material, equipment and instrumentation, the bombardment of energetic electrons and ions from outer space poses critical problems for manned missions as well. Safeguarding astronauts from adverse biological radiation effects inflicts stringent requirements on the length of manned mission, and on orbit selection and the planning of EVAs (Extra Vehicular Activities). For occupations involving radiation hazards, (e.g. nuclear reactor enginnering, radiology..), The U.S Environmental Protection Agency guidelines set the acceptance dose rate limit at 5.000 mrem/year over the natural background experienced at the surface of Earth (60-160 mrem/year). This implies a careful planing of all manned especially when EVA are required.

An accurate prediction of the radiation dose expected during any (manned of unmanned) mission requires therefore reliable trapped radiation models. Indeed, too optimistic model predictions must be avoided for obvious reasons, while over-pessimistic ones are leading to unnecessary, heavy and costly shielding of the spacecraft or costly alternative orbits.

In this respect it has been shown by Gussenhoven et al. (1987), Vampola (1989) and others that the average fluxes given by current models, like AE8, are in certain instances misleading. Although AE8 remains a basic reference model describing the energetic electron environment, it is poorly suited to evaluate radiation effects on high altitude eccentric orbits where external magnetic fields are predominant, as well as at low altitudes where atmospheric cut off and secular variations of the geomagnetic field are important (see TECHNICAL NOTES 1&2).

Evaluation of the extreme values or standard deviations of the high altitude fluxes are needed in addition to the average values. The AE8 model provides average omnidirectional fluxes for electron energies ranging from 40 KeV to 7 MeV. Fluxes at the upper energy limit are mainly extrapolated from lower energy data. Extrapolation from lower altitude data is often used to provide values up to 11 Earth radii.

TREND has contributed to improve the model for the outer zone electrons by adding confidence levels and standard deviations for the predicted fluxes in the vicinity of geostationary orbit; the geomagnetic activity dependence, as well as local time dependence (similar to that existing in AE4) have also been incorporated in this updated environmental model.

These new implementations have usefully improved the earlier models. However, like all previous radiation environmental models, the new ones remain static models and take no account of the many dynamic processes which occur in the magnetosphere over periods as short as days and even hours. No dependence on interplanetary field and solar wind conditions has yet been included. But, as emphasized in TECHNICAL NOTE 2,(Chapter 6), more detailed dynamical models can only be built into the framework of long term modelling efforts backed up by continued multi-satellite observations of particles of high energy, in all regions of the magnetosphere.

In the following section we outline a strategy to achieve this goal within the framework of future European space activities.

How to manage these problems?

As indicated above, there is need for the European space community to devote some effort towards improving the radiation environmental models beyond the point where TREND has carried this effort already. Such a long-term effort could be envisaged in parallel with that of other Space Agencies. The CRRES mission dedicated to the study of the radiation belt environment is a good example of such an effort undertaken in the US.

Although, CRRES detectors covers a wide range of particle energics, and a wide range of B- and L-values, there are regions of space which will not be visited by this spacecraft. Sampling the environment with a single spacecraft will always be limited in B-L space. Simultaneous and multi-point observations are necessary to obtain the required time and spatial coverage. The more synoptic observations will become available for the future modellers, the more detailed and reliable will the new generation models become.

These are good reasons for all space agencies, including ESA, to consider now the incorporation in a number of their future missions, of "minimally intrusive", mission-specific radiation environment monitoring. It is worth pointing out here that such "minimally intrusive" monitors had been added (at the last 'minute'!) to the payload of the astronomical satellite IUE (International Ultraviolet Explorer); these unsophisticated particle detectors monitor continously since 1978, the trapped particle radiation background. They are still in operation and provide already over one solar cycle worth of data. These data are useful

indicators for evaluating the background noise spoiling the UV telescope measurements; but they happen also to constitute a most valuable and inexpensive data bank of directional flux measurements for trapped electrons over a whole solar cycle. These data have been analysed by TREND for the purpose of evaluating the AE8 trapped radiation model. It has been demonstrated in TECHNICAL NOTE 5 that these directional electron flux measurements collected by an astronomical satellite (i.e. not a magnetospheric satellite) can be usefully exploited to improve existing trapped radiation models.

Dependable and cost effective background monitors (like those of IUE) or radiation monitors should be incorporated not only in manned missions, (like Space Sation / Columbus) or geostationary environment monitors (ERS), but also in most scientific missions (like ISO, LYMAN, and possibly REGATTA, and the Polar-Platform), in application satellites (Polar Earth Resources, Communications, and Meteorological satellites), or in TDP missions...

The addition of radiation monitors to any such satellite allows its operation to be optimised. Furthermore, provided there are built-in alert procedures triggered on board by such radiation detectors, these simple devices could be very valuable to protect vulnerable instruments of the payload.

Note also that such radiation detectors on a particular mission yield data (average fluxes, maximum flux or fuence, integrated values, standard deviations ...) which are directly useable in planing follow-on missions on similar orbits (for instance had the EXOSAT X-ray astronomy satellite carried a radiation monitor, it would have made planning of the follow-on X-ray mission XMM much easier and fail-safe).

In order to be more specific we present a list of future flight opportunities where planners should encourage to fly dedicated monitors to understand and model the Earth's radiation environment

The modelling of climate or weather systems rely on data collected all over the surface of the Earth at the same time, at different locations; why should it not be the same in the case of modelling the radiation environment in outer space?

In order to be more specific TREND has presented in TECHNICAL NOTE 6 a list of future flight opportunities which are becoming available and should be encouraged to carry dedicated monitors to get more comprehensive

models of the Earth' radiation environment. These opportunities are discussed there in some details. In the following section we only will mention a few of them fro illustration.

What are the future opportunities which could be used to monitor the earth's radiation environment?

Monitoring the Earth's radiation environment should not only be carried and aboard magnetospheric missions like CLUSTER, REGATTA, or CRRES. Indeed, the science objectives of such missions are not necessarily compatible with environment modelling & monitoring. The IUE spacecraft which is not a magnetospheric satellite, is an illuminating case showing that other types of missions benefit from having onboard "minimally-intrusive" background particle detectors. Magnetospheric satellite are usually dedicated to investigate specific plasma phenomena occuring in the magnetosphere; in recent missions these scientific objectives had little to do with monitoring the Van Allen radiation Belts which, these days is an out of fashion activity for space physicists. This is the case for CLUSTER whose main scientific objective is to study the bow shock and magnetopause boundary layers (see the CLUSTER description in the Appendix).

Therefore, it would be inefficient to leave the role of monitoring the Earth's radiation environment to magnetospheric scientists and to the missions they are proposing. There are other SCIENCE missions as well, MANNED missions, APPLICATIONS missions, and missions belonging to the Technological Demonstration Programme (TDP) which are ideal carriers of radiation detectors.

Let us now first examine the opportunities to carry such monitors on spacecraft dedicated to scientific investigations.

Science missions

Science payloads become more and more sophisticated, employing new technology for their sensors, microproces- sors, mass memories, and basic components. In general, these become more radiation sensitive, so it is imperative to remain aware of the radiation environment and its effect on space flight payloads.

IUE, the International Ultraviolet Explorer, is an astronomical mission (as already mentioned above); it coverd very simply built small background monitors which contributed significantly (since 26 January-1978 for more than one solar cycle), to knowledge of both the radiation environment and its background.

HIPPARCOS could have done with such a particle detector since its optical astronomy payload is susceptible to radiation-induced background. This is especially true now that HIPPARCOS is in a near-GTO orbit instead of operating at GEO where it was originally planned to be. In Geostationary Transfer Orbit (GTO), the radiation background is continously variable. Large amounts of important environmental data could have been acquired had HIPPARCOS carried a "minimally intrusive" radiation monitor like that of IUE. This would have been useful, also if it had been sucessfully injected into geostationary orbit where it would still have experienced the radiation background.

XXM, ISO, FIRST are future astronmical missions with orbits traversing regularly the Van Allen trapping regions; TRENDS wishes to recommend that "minimally intrusive" particle detectors onboard of these mission if there are spare budgets in mass, power and telecommunication.

QUASAT, LYMAN, GRASP/INTEGRAs which had not been selected previously, but which may arise again, would be on highly elliptic orbits, very well suited for long-term monitoring the inner and outer radiation belts with "minimally intrusive" detectors.

Although in a relatively benign radiation environment, except as always during solar proton events, CLUSTER has generally light shielding and sensitive components, including transputers. This is because down-link limits mean that much processing has to be done on-board. Radiation housekeeping would obviously be prudent to monitor device health!

SPACE-STATION Payloads. Astronomy, geophysical as well as biology payloads which are sensitive to corpuscular radiation are envisaged to be flown on SS, both external or internal to the Space-Sation/Columbus Attached Laboratory. Although, this facility will be used primarily for payloads and experiments in material science, fluid physics and life sciences, important investigations on nuclear disintegrations 'stars' resulting from energetic trapped protons interactions can also be considered; these nuclear interactions lead to single-event upsets in electronic devices and to (still uncertain) radiobiological effects.

Since the module axis of Space Station Freedom and of the attached Columbus module will be closely parallel to the direction of their orbital velocity, the East-West asymmetry of the flux of inner zone protons could easily be observed and studied from this orbit. Note that ESA's module end will be located on the West end of the Space Station structure; this means that it should, in principes, be exposed to the highest energetic ion fluxes. Secular variation of the low altitude distribution of inner radiation belt protons can also be studied as part of a Columbus long-term environmental programme.

These effects are strong candidates for study by the US and European scientific communities. In parallel or in collaboration with the NASA Neutral Environment with Plasma Interactions Monitoring System (NEW PIMS) for Space Station Freedom (SSF), ESA is considering to develop a Columbus-PIMS (C-PIMS) package to provide significant contributions to monitoring of the SSF environment. A radiation monitor is strongly recommended for such a system.

In the meanwhile, it is proposed that a C-PIMS package be deployed from the Scientific Airlock and that a PIMS prototype be carried on Spacelab Pallet or a Hitchhiker structure, to include the radiation monitor for preliminary evaluation of the E-W asymetry, SAA variations and STARS.

COLUMBUS POLAR PLATFORM. Although the Columbus polar platform, the third element of the COLUMBUS DEVELOPMENT PROGRAMME, is mainly driven by its prime customer, the Earth-observation community, it will accomodate various Solar-Terrestrial Physics (CSTP) experiments including a Particle and Field Package (PAFP) with an electron spectrometer in the energy range of 10-600 keV. This package will be very useful to study the low altitude (500 km) radiation environment in the region of the South Atlantic Anomaly (SAA). NOAA proposes the Space Environment Monitor (SEM) for the ESA polar platform.

Space Station Freedom (SSF) payloads cover a wide range of disciplines; probably biology and astronomy interests are the most sensitive to radiation. The most important data in this orbit are stars, the highly ionizing secondary products produced by energetic protons and GCR. Nuclear emulsions, plastic track, and solid state detectors with pulse height analyzers are used to study these interactions. One cannot avoid SEUs from these stars and the rate is quite dependent on the payload mass and composition. Monitoring is clearly necessary.

Planetary and interplanetary missions are straightforward as concerns radiation. The solar proton environment is now well known and not extremely severe. Thus, Huygens, Rosette, and Vesta, require no further comment; SOHO and Ulysses both carry instruments to measure solar protons to which CCDs are sensitive.

Manned missions

Manned missions are confined to low altitude orbits to avoid the energetic protons, while both science and applications payloads cover a broader range of geospace.

SPACE STATION/COLOMBUS and HERMES. Unlike any on Earth, the environment where the european space shuttle Hermes, the Columbus Attached Laboratory, and the man-tended Free-Flying Laboratory will orbit, is unique in respect to the radiation hazard to man (low-level, high energy, nuclear interactions). It has been shown in TECHNICAL NOTE 1 that in this region the classical B-L coordinate systems used to model the Inner Zone Radiation Flux is the least reliable, (i) because of the atmospheric cut-off not properly described in this coordinate system, and (ii) because of the secular variation of the Geomagnetic Field. In TECHNICAL NOTE 2 it has been shown that there is an urgent need to reexamine the mapping of the low-altitude Earth's radiation environment with a new altitude like coordinate like the Hassitt shell height.

Standardized monitors on-board these manned vehicles would obviously provide an invaluable and unparalleled data bank for the next generation of mission planners and modellers of the low-altitude Earth's radiation environment. Such monitors would help solve some of the problems in planning and deciding on Extra Vehicular Activities for the astronauts.

This is why TREND strongly recommends also to add standardized "minimally intrusive" monitors on-board all manned missions.

Application missions

POLAR EARTH RESOURCES. Future Earth resources programmes of ESA are planned to be on polar orbits. Electronics, transputers which will be used

in future missions, CCDs are radiation sensitive devices whose environment requires constant monitoring.

The first ESA Remote Sensing Satellite (ERS-1) will fly in the familiar polar orbit that is well known relative to the radiation environment. The Columbus polar platform will also occupy this region later with the American and, later, the Japanese version. The need for the continuation of radiation monitoring was addressed already. It would seem that ESA should participate in that monitoring.

The Columbus free-flying laboratory will traverse space in the same region as the Space Station Freedom and so the remarks of the previous subsections apply here; the life sciences payloads are more susceptable than the rest but all electronics systems will be similarly vulnerable. Eureca will move up to 500 km in altitude. At those heights exposures of 5 krad skin dose can be expected, so radiation damage testing should be carried out.

COMMUNICATIONS. Data Relay Satellite, PSDE-SAT-2 communication technology project have increased on-board signal processing. Also under consideration are navigation satellites and high-latitude communication stallites which will be at lower altitudes than GEO or in inclined elliptical orbits. As a consequence, these spacecraft will be exposed to higher radiation levels: a radiation monitor would also be useful in these orbits for the reasons already given above.

There have been dosimeters with particle identification flown on several of the 12-hour US DOD navigation satellites but very little of that data is available. Depending on the exact orbits, these satellites might pass through the high energy electron region in the outer belt. This is important for studies of deep dielectric charging and constitutes a severe environment for payloads.

METEOROLOGY. Meteosat data have experienced problems with disruption, probably due to deep-dielectric charging. An on-board instrument like the LANL LoE detector for electrons should be on future Meteosat missions.

TECHNOLOGY DEMONSTRATION PAYLOADS. Given the aims and objectives of the Technology Demonstration Programme (TDP), a radiation environment monitor fits very well in the program and should be encouraged. This would provide environment data, flight-test a developed monitor for application on

many of the above missions, and provide engineering data if flown alongside radiation effects experiments such as components or solar cells.

Small-Sats, Spacelab, Small Payload-Of-Opportunity on Communication Satellites, ERS and Meteorological satellites will be availabe from time to time. If TDP leads to development of a unit which is available and minimally intrusive, it could be put on board at short notice. Environment monitoring, by its very nature, needs to be carried out on frequent flights in a variety of orbits over a long time span.

It may be of interest to the environmental community to mention here the UoSAT flown by the University of Surrey (UK). Inexpensive and cost-effective small satellites have been built by the University Company - Surrey Satellite Technology (SST) Ltd. Over eight years, this company has gained experience in the design, construction and orbital operation of two small spacecraft launched into polar, sun-synchronous, low Earth orbit by NASA in 1981 and 1984 (UoSAT-1&2). Two new low cost spacecraft are due for launch on ARIANE-ASAP. Such a 'standard' inexpensive small satellite bus can be used for a variety of mission payloads, including specific studies of the Earth's radiation environment.

Inter agency cooperation and stimulation

US MISSIONS. GOES-NEXT, Polar Platform, PHIDE AN SSF, CRRES are other ideal carriers for monitoring the Earth's radiation environment. Cooperation should be sought with those that are European. As far as we know there is no follow-on for CRRES which is the US mission specially dedicated to the study of the Earth's radiation environment.

ESA could consider a dedicated mission. It would fit with ESA's declared aim of autonomy in space, and the implication that this has to develop abilities to independently puersue areas of applied research such as environmental monitoring.

A CRRES follow-on type of mission could well be part of the TECHNOLOGY RESEARCH PROGRAMME, TDP, and/or of the PREPARATORY PROGRAMMES of ESA. So far, the technologies developed in these frames have been brought up to breadboarding status and ground tested. The need to carry out in-orbit flight demonstrations has become very strong

because of the increasing difficulty to perform realistic ground testing of a number of new technologies and to minimize the development risk of future ESA projects.

To cope with those needs ESA has planned to extend the ground testing of critical technologies to an orbital flight verification that is the In-Orbit Technology Demonstration Programme (TDP). It would be a pity if monitoring the Radiation Environment within the framework of these programmes would not be coordinated and analysed with those from other scientific and application missions of ESA, and of other Space Agencies.

What is a "minimally intrusive" system?

In the previous sections we suggested to have on future mission spacecraft "minimally intrusive" radiation monitors. A minimally intrusive system is one which is light (~ 1 kg; definitely less than 2 kg), consumes low power (~1 Watt; definitely less than 2 W), and needs low bit rate (less than 100 bps); it should be easy to meant, adn with very few interface problems including data system and telemetry interfaces.

In certain instances omnidirectional flux measurements are sufficient while in other case a directional monitor can be prefered. Fig. 2 illustrates how, with different bafle design, both types of detectors can be constructed most simply. The hemisphere dome geometry (on the left) returns omnidirectional measurements, while the cylindrical bafle on the right gives directional ones useful for pitch angle sampling. With hemispherical domes, magnetometer and spacecraft attitude is not needed. One may also consider either single or double silicon detectors with preamps, pulse-height analysis and discrimination.

Electrons as well as protons of different energies should be measured. Note that not too high energies several tens of MeV should be required to avoid sophisticated methods.

By using solid state detectors one avoids the high voltage problems of arcing, pump out, etc. and the weight of the detector is minimal. The system is made omnidirectional with hemispherical domes so that magnetometers and attitudes are not needed. With the use of just two discriminators a single integral electron channel and a single proton band measurement are possible with each detector. To obtain good energy coverage, four detectors have been used on

several occasions, e.g. ATS 1, ATS 6, DMSP/F1, DMSP/F7. For the last two a pulse height analyzer was used to determine the dose in the detector as well as to provide single channel information for each particle. Such systems have covered the range of electrons from 0.3-10 MeV and protons from 5-100 MeV. Stars are readily identified by even higher discriminator levels. Thus, the important range of particles identified earlier can be covered quite nicely.

New technology may permit other ways of doing the above, but the important characteristics will be the same. Thresholds can be changed easily by dome thickness and discriminator triggering level. Certainly one should also be prepared for more sophisticated opportunities, but one must realize that more lead time would then be required. For an opportunity on the Technology Demonstration Program (TDP) one could use a pulse height analyzer with the above system and have a good spectrometer for all the important heavily ionizing particles. Such a measurement fits in with the aims and objectives of TDP and would provide a good flight test for such an instrument.

Example of such units are the DMSP/F7 dosimeter and its forerunner flown on DMSP/F1. The IUE PFM was a similar instrument except there were two major differences; the project needed it at the last minute (about 3 weeks before launch) and it was a directional detector. In earlier times it was possible to build very small piggyback satellites (~2-5 kg) with fundamental particle detectors. In that case the satellite hitched a ride instead of an experiment. Examples are ERS 12,13,17,18,27, which all traversed the radiation belts from 300 km to 18 RE. (Note: the ERS name was first used for this US satellite series in the '60s).

In TREND's TECHNICAL NOTE 6 a few examples of "minimally intrusive" monitors have also been given (see for instance Fig.5-2). Their descriptions will not be repeated here. There are different types of detectors : Energetic particle detectors, Space "dosimeters" (counting dosimeters), RADFETS (integrated dosimeters, the new Radiation Monitor developed in the Technology Demonstration Program.

How to use future radiation data to update the Earth radiation environment models and produce new ones?

Of course it is not just enough to build "minimally intrusive" monitors for future European and possibly US and Japanese spacecraft, and to transmit their

centers they should be used for updating and renewing the earth's radiation models. However, after collection, there is often not enough manpower, available to examine such large amounts of new data, or to make use of them for updating radiation environmental models; most experimentalists are by then already busy constructing the next instrument for the next space project.

Furthemore, ESA does not effectively support multi-disciplinary scientists to analyse data which have become available. For the time being, there is not a concerted strategy to cross-fertilize data obtained during different missions, nor to make the best use of all the efforts put into particular missions by individual scientists and consortia of experimentalists.

The lack of interest in cross-correlating and cross-fertilizing data from different missions and using them to develop more reliable environment models does not come only from lack of encouragement and financial support by the Space Agencies for this sort of multi-disciplinary activity, it results also partially from the lack of coordination between Science Departments and Application Departments or Directorates. Perhaps more importantly, it results from the lack of interest of space scientists themselves for such 'tasks' which are unfortunately considered by some people as being of minor interest for 'their Science'. It is noteable that in the US, many institutes encourage the exploration of space acquired data for applied purposes (NOAA/SEL, NSSDC, AFGL, Aerosp.Corp.)

It is true that modelling the Van Allen Trapped Radiation Belts, or Predicting the Fluence of Solar Proton Events for the next solar cycle has become a less exciting scientific endeavour than investigating 'reconnection or Flux Transfer Events'; but for future scientific, applications, manned and commercial spacecraft design it is more urgent to obtain more precise and more reliable models of the Earth's radiation environment... Indeed, these environmental models have a direct impact on the shielding, weight and cost of future space transportation systems.

Note that not only the radiation environment should be modelled on a continuing, reliable and concerted basis by the different Space Agencies, but also neutral atmospheric and ionospheric models, as well as model distributions of natural and artificial debris in orbit around the Earth, should be developed.

As a consequence of the present situation in Europe and within the international Space Science Community, outer space environment modelling

efforts have not been encouraged, unlike in climatology and oceanography. In consequence most of the useful corpuscular radiation data now available and those which will become available in the future will not be exploited as they should.

It seems clear that a concerted and coordinated effort will be necessary to deal with the routine, special data analysis and modelling tasks which are an inevitable result of the present need (i) to update models based on existing data, and, (ii) to cope in a similar fashion with the data which will flow from the proposed future monitors. AFGL who are responsible for much of the CRRES data dissemination and analysis tasks are keen for ESA to cooperate in such activities.

The long-term format of the European effort needs to be established. Some continuing funding is obviously a prerequisite. Coordination with national and/or private efforts (if such ever exist) would be obviously benificial.

Final recommendations

ESA has declared its aim of autonomy in space. This implies that it is willing to pursue the updating and extension of knowledge of the space environment. Consequently, it seems appropriate to make some recommendations relative to the energetic particle environment. It should be clear at this point that our knowledge has been eroding for a decade or two in some facets of this field. It is important to understand what is lacking (as has been pointed out above) and how to be effective in filling the gaps. The latter topic is treated next.

It is doubtful that there will be a follow-on to CRRES for many years, so dedicated missions for radiation studies are highly unlikely. The way in which radiation monitoring has proceeded in recent years has been in two directions. The first is quite visible in this report. It is part of an ongoing program as exemplified by the NOAA, GOES, GMS, LANL satellites; the rationale : it is part of space weather. The second way is to have a monitoring flight unit that is minimally intrusive; this means it should be light, low power, easy to mount with very few interface problems, including data system and telemetry interfaces.

Where besides TDP could such a monitor be flown ? Certainly the 71,000 km astronomy orbit would be useful and the outputs could be of operational use to the mission, as pointed out previously. The navigation satellites would be another

somewhat provide data from an unexplored region. To cover the geostationary orbit Meteosat would be preferable to the communication satellites because of the operational environment but, in either case, the emphasis should be on high energy electrons.

The ERS and Columbus polar platform provide access to the polar weather orbit; however, it is recognized that this orbit is quite well monitored now. On Eureca it should be possible to test components for radiation damage since skin doses of 5 krad or $1.4x10^{13}$ 1MeV electron equivalents is produced by 10 MeV protons within six months. Thus such a monitor would be important in relating the incident flux to the damage measured.

In short, it is recommended that ESA establish a radiation environment program that is practical, useful to its aspirations, and pertinent to the extension of our knowledge of the radiation environment and its effect on space systems. Such a long term program would of course require first collecting Earth's radiation environment data simultaneously, in all region of space, over extended period of time with "minimally intrusive" systems. A second step would be to stimulate in the European scientific community coordinated activity to analyse and model the resulting data in dealing with the routine special data analysis and modelling tasks.

CHAPTER 6

CONCLUSIONS

The significant conclusions and results reached by the TREND team over these 15 months, should be useful for future developments in this area. Recommendations have been made all along this study. They are detailed in the six TECHNICAL NOTES which have been produced under this ESA contract.

But before summarizing the results and recommendations which have been recalled in the five previous chapters of the present FINAL REPORT, it may be suitable to re-emphasize the usefullness and benefits of having updated and comprehensive models for the Earth radiation environment. It is then appropriate to compare the situation before and after this study. The recommendations for the future will be given in the last section.

Why there is a need for environment radiation data and updated models

The detrimental effects of hard corpuscular radiation is not limited to engineering technical aspects e.g. degradation of solar cells, dammages due to electric discharges, a.s.o. It interferes and spoils also the measurements taken by scientific instruments in orbit around the Earth. Astronomical measurements programmes are hampered by such detrimentral effects (e.g. HIPPARCOS). Indeed, detectors flown on most astronomy satellites are very sensitive to the noise caused by the ambient trapped particles. Primary particles as well as secondary particles reduce the efficiency of these detectors and shorten their life.

But in addition to the detrimental effects on the spacecraft material, equipment and instrumentation, the bombardment of energetic electrons and ions poses critical problems for manned missions as well. Safeguarding astronauts from

adverse biological radiation effects inflicts stringent requirements on the length of manned missions, on the orbit selection and planning of extravehicular activities.

A factor of two (or more) uncertainty in the average value of the omnidirectional fluxes of trapped electrons and protons has therefore important consequences on the design of the spacecraft or/and on the overall mission operation, including the selection of orbits. Too optimistic flux models would be a disaster for obvious reasons. Over-pessimistic or too conservative models are leading to unnecessary heavy shielding of the spacecraft, or costly alternative orbits.

Accurate prediction models for the radiation dose is therefore mandatory. But this requires reliable and constantly updated models of the trapped particle environment both at low altitudes and at high altitudes beyond geostationary orbit. Collecting synoptic environmental data with "minimally intrusive" detectors is, like in meteorology and climatology, the safest way to go in space.

This would not only benefit to geophysicists (magnetospherists), but it would help the astronomers to plan the orbits and operation of their satellites and sensitive instruments. It would help the engineers to have more reliable dose predictions for scientific, and commercial satellites. It would certainly benefit the astronauts to know with greater confidence what is the dose of radiation they likely are going to be irradiated with.

All this leads to the conclusion that there is need for studies like the present one, and that this first effort from the european community has to be encouraged and continued in the future for the greatest benefits of all.

The situation before and after TREND

The present knowledge about the Earth's radiation environment has been derived mainly from the data obtained during twelve years of the space era along with the theoretical analytical, and modelling effort associated with them. It should be pointed out that the first area of discovery and scientific effort in space involved energetic particles. The instruments were readily available out of nuclear physics, high-energy physics, and balloon borne/rocket borne cosmic-ray work. It took nearly a decade to develop instruments for other areas, such as plasma, astronomy, and earth resources where the main thrust has been for the past two decades.

Unlike the Earth's radiation models, geomagnetic field models are updaded almost every five years by IAGA Division V. The latest update is IGRF-85. This version of the internal geomagnetic component was not yet implemented in the UNIRAD software package of ESABASE. TREND implemented this new IGRF-85 model as well as its secular variation.

TREND implemented also the Jensen and Cain (1962) geomagnetic field model for epoch 1960, which was missing in the former UNIRAD software. It is precisely the Jensen and Cain B-Field model which has been used to build the whole series of NASA trapped radiation models, including AE8 and AP8. It was interesting to have also this model available in UNIRAD since TREND came to the conclusion that the magnetic field model used for predictions must be the same as that used to build the trapped particle model.

Furthermore, TREND pointed out that, in order to avoid spurious secular evolution in radiation dose prediction, it is essential to use the same magnetic field model as that which was used to build a particular model for omnidirectional particle fluxes. To predict the radiation dose for a space mission planned in the year 2000, it was common practice to use the geomagnetic field model corresponding to the year 2000 while the AE8 and AP8 radiation models employed were built with a geomagnetic field corresponding to an epoch in the 60's. It has been shown during this study that this is a wrong method of calculation, and, that it should definitely be abandonned in future simulations. Therefore TREND recommends to use the same epoch for the geomagnetic field than for the radiation models used to make dose prediction calculation in the future.

Before TREND it was also suggested that the spurious secular variation in radiation doses pointed out by McCormack (1986), would disappear by replacing in McIlwain's algorithm the standard value for the magnetic moment, 0.311653 Gauss R_E^3, by the actual magnetic moment M at the epoch of time for which the prediction is to be made. As a result of the present study, TREND advises the user community not to adopt such a practice. Indeed, this would not resolve the embarassing secular variation mentioned above, because of the secular variation of the higher order moments in the geomagnetic field models. On the contrary, such a not standard practice would bring in even more confusion than there is already in this community about the true meaning and understanding of the B-L coordinate system.

Before TREND the calculation of McIlwain's L shell coordinate from the values of B and I, the geometric field invariant, was based on the orginal algorithm introduced by McIlwain (1961). Since Hilton (1971) published a simpler algorithm to obtain the same result, but in a more immediate manner, TREND has implemented the more recent Hilton's method in UNIRAD.

Before TREND there has been (and still remains) a dream of theoreticians to identify a generalized L^* parameter which would be 'truely invariant' (constant) along a given magnetic field line; indeed, McIlwain's L-parameter is not strictly the same for all mirror points along a given magnetic field line. Having investigated a quantitative formulation of this idea, TREND has concluded that this dream is beyond grasp. The reason is the high degree of complexity of the IGRF and external magnetic field models used in practice. The mathematical expressions for L^* or for the canonical Euler potentials characterizing a whole field line are untractable and difficult to determined for the 120 terms of the IGRF and sophisticated external magnetic field models.

Before TREND the UNIRAD software did not include any external magnetic field model which is local time dependent. Recognizing the need for such an external magnetic field component to calculate proper values of the B-L coordinates at large radial distances, TREND has implemented in UNIRAD four alternative external field options including the most recent model of Tsyganenko (1989). Tsyganenko's model depends on the level of geomagnetic activity which is determined by the value of the Kp-index. Therefore, after TREND's study the user of UNIRAD will have the option to select an external magnetic field model and to input the value of an additional free parameter corresponding to the value of Kp.

Before TREND the righteousness of B-L coordinates for low altitude mapping had never been seriously questionned. As part of this study TREND has pointed out that between 150 km and 1500 km altitude, the atmospheric density distribution must necessarily to be taken into account in modelling the trapped radiation fluxes. For these low altitudes TREND has suggested to replace B or B/Bo by a mean atmospheric density value which is an average over the drift shell of the particle. The Hassitt shell height has been proposed by TREND as an appropriate new coordinate depending both on the geomagnetic field distribution, and, on the actual atmospheric density distribution; the latter is a complex function of altitude, latitude, local time, season, solar and geomagnetic activity. Because of

the lack of man-power TREND has not updated, nor optimized the original programme designed at UCSD (La Jolla) by Hassitt (1965), and, kindly provided to TREND by Carl McIlwain.

Before TREND the UNIRAD user had only to rely on the NASA solar proton events model introduced sixteen years ago by King (1974). TREND has become aware of the existence of a recent probalistic model which is simpler and based on solar proton events observations extending over three solar cycles instead of one. This new solar flare proton model due to Feynman et al. (1989) has been implemented by TREND in UNIRAD, and is now available for ESABASE users as the default option. Since the NASA model will still remain a reference for some time, it is possible to access it as an option in UNIRAD.

Before TREND the NASA models AE8 and AP8 were the only trapped radiation environment models available to ESABASE/UNIRAD users. After the TREND study updated and new electron flux tables have been built using LANL electron omnidirectional measurements made at geostationary orbit. These tables are called TREM-G and TREM-GX where TREM stands for 'Trapped Radiation Environment Model'; G for 'near Geostationary region'; X means that it has been determined with Tsyganenko's eXternal magnetic field model. These tables are not made accessible by the programme TREP; nevertheless they can be used with additional data to build a new model similar to AE8.

The TREM-G table contains local time averaged integral fluxes. TREM-GX is Kp dependent; four different Kp ranges have been selected. Besides the average integral and differential energy spectra usually given by standard software packages, TREND has updated the standard deviations of these omnidirectional fluxes as a function of electron energy.

Interesting results have been obtained by TREND from the intercomparison of AE8 model predictions with TREM-G. Furthermore, the comparison of model predictions with and without the external magnetic field model (i.e. TREM-G versus TREM-GX) has also been a significant new contribution of TREND.

Comparison between the predictions made with Feynman et al.'s model and those obtained with King's approach have been made, and constitute an original contribution of TREND to this field of investigation.

This is a summary of most significant contributions that have been made by TREND within the rather short time span of 15 months. All these achievements could not have been accomplished without important investments in manpower and computer time made by MATRA-ESPACE, by JIV Assoc., by STI, and by IASB.

There are many possible extensions of TREND's work. Below, we are presenting recommendations for such future extensions, and, more generally,for Earth radiation environment modelling efforts to be undertaken or pursued by ESA or any other space agency.

Recommendations for the future

In the course of this study TREND has formulated a number of recommendations for future developments in the area of Earth's radiation environment modelling. These recommendations have been presented in the various chapters of TREND's TECHNICAL NOTES.

A first series of recommendations dealing with radiation environment monitoring have been recalled already in the previous chapter of this FINAL REPORT. They can be summarized in the following words:

- Propose a follow-up of CRRES mission dedicated to study the energetic particles injected or trapped in the geomagnetic field.

- Use the opportunity of future science missions (astronomical and magnetospheric missions) to monitor the energetic particle populations in the inner and outer magnetosphere.

- Use the opportunity of manned missions to collect data at the lower edge of the inner radiation belt.

- Use the opportunity of TDP, or small satellites to monitor radiation in space as frequently as possible to obtain, as in Meteorology, Climatology, or Oceanography, the best coverage in time and space of the Earth radiation environment.

To organise these various measurement surveys, standardized "minimally intrusive" detectors should be used on these different mission opportunities.

Minimally intrusive particle monitors have been described in TN6 as well as in chapter 5 of this FINAL REPORT.

To analyse the synoptic data sets which would be collected for over one solar cycle, the different space agencies, including ESA, should stimulate and support multi-disciplinary groups or teams to update and improve Earth's radiation models. Specialized laboratory departments and World Data Centers should promote this kind of application.

TREND recommends to pursue the data analysis of IUE data beyond the stage where TREND's resource sustained it. There are several other data sets which are available to extend these modelling efforts and extend the B-L coverage of TREM-G and TREM-GX. The DMSP data now being deposited at NSSDC, is another interesting set of energetic electron and proton flux measurements which has been considered by TREND, but which could not been handled within the time limits of this present contract. TREND recommends very strongly however the exploitation of these valuable DMSP data for the purpose of improving the reliability of low altitude radiation environment models. In TN3 TREND has produced a comprehensive catalogue of all mission associated data sets available for such modelling activities which would be able to extend and complement TREM-G and TREM-GX tables provided by TREND.

As far as modelling activities are concerned, TREND recommends that renewed interest and support for surveying and modelling the Earth radiation environment should be encouraged at more than one space agency, which was NASA until now.

Development of updated and new models has to be encouraged. There are many complementary directions to go in this respect. One first urgent improvement would be to develop a brand new model for the low altitude region between 150 and 1500 km height, taking into account the atmospheric density distribution. In this respect TREND has recommended in TN2 the 'Hassitt shell height' as a new coordinate to map the lower altitude region of the Van Allen belts.

Since the outer magnetic field distribution is directly dependent on the solar wind paramaters, TREND recommanded in TN1 to develop new external magnetic field models which are dependent on these solar wind parameters, in

addition to, or instead of Kp, the geomagnetic index, as it is presently the case for Tsyganenko's models.

Since the number of solar proton events taken into account in the stastistical analysis of King (1964) and even of Feynman et al.(1989) is relatively limited, TREND recommends that the prediction of both models should be tested using forthcoming data from the current solar cycle.

Development of space environment models must be considered as long term tasks by specialized teams of scientists and programmers. In chapter 6 of TN2 Jim Vette, TREND's consultant who has gained considerable experience and know-how in this field during a 26-year period employment at Aerospace Corporation and NSSDC/WDC-A-R&S, has outlined a possible progression for longterm developments in the area of model formalism. This strawman evolution starts with the simplified trapped radiation models currently available after TREND study, and extends in the far future when highly sophisticated dynamic models will be designed, like those now available in Meteorology and Oceanography or Earth Resources.

But before that final goal is reached much more synoptic observations must be collected. Serious and concerted incentive must be given to the space radiation modelling community, like that given to the climat modelling community during the recent years. The needs are similar and the returns are directly cost effective.

LIST OF REFERENCES

Adams, J.H. Jr., Silberberg, R. and Tsao, C.H., Cosmic Ray Effects on Microelectronics, Part I : The Near-Earth Particle Environment, NRL Memorandum Report 4506, 1981.

Baker, D.N., J.B. Blake, R.W. Klebesadel, and P.R. Higbie, J. Geophys. Res., 91, 4265, 1986.

Blake, J.B. and G.A. Paulikas, in Particles and Fields in the Magnetosphere, ed. by B. M. McCormac, D. Reidel Publishing Co., Dordrecht-Holland, p380, 1970.

Burrell, M.O., The Risk of Solar Proton Events to Space Missions, Proceedings of the 1971 National Symposium on Natural and Manmade Radiation in Space, edited by E.A. Warman, TMX - 2440,
Jan 1972, NASA, pp. 310 - 323 (printed separately as TND - 6379, June 1971, NASA).

Daly, E.J., Effects of Geomagnetic Field Evolution on Predictions of the Earth Radiation Environment at Low Altitudes, ESTEC/W.P.1531, 1989.

Daly, E.J., ESA Journal, 12, 229, 1988.

Feynman, J, Armstrong, T.P., Doa-Gibner, L. and Silverman, S., Preprint 1988.

Feynman, J., Armstrong, T.P., Dao-Gibner, L. and Silverman, S., Solar Proton Events During Solar Cycles 19, 20 and 21, Submitted Solar Physincs, 1988b.

Feynman, J., Armstrong, T.P., Dao-Gibner, L.V. and Silverman, S., A New Interplanetary Proton Fluence Model, accepted for J. Spacecraft, 1988a.

Fraser-Smith, A.C., Rev. Geophys. 25, 1, 1987.

Goswami, J.N., Mc Guire, R.E., Reedy, R.C., Lal, D. and Jha, R., Solar Flare Protons and Alpha Particles During the Last Three Solar Cycles, J. Geophys. Res., 93, 7195-7205, 1988.

Haerendel, G., in Particles and Fields in the Magnetosphere, ed. by B.M. McCormac, D. Reidel Publishing Co., Dordrecht-Holland, p416, 1970.

Haffner, J.W.: Radiation and Shielding in Space. New York: Academic Press, 1967.

Hassitt, A., J. Geophys. Res., 70, 535, 1965a.

Hassitt, A., J. Geophys. Res., 70, 5385, 1965b.

Hess, W.N. The radiation Belt and Magnetosphere, Blaisdell, New York, 1968.

Hilton, H.H., J. Geophys. Res., 76, 6952, 1971.

Hovestadt, D.G., G. Gloeckler, C.Y.Fan, L.A.Fisk, F.M. Ipavich, B. Klecker, J.J. O'Gallagher, and M. Scholer, Geophys. Res. Letts., 5, 1055, 1978.

IAGA Divisions I Working Group 1, J. Geomagn. Geoelectr., 37, 1157, 1985.

Jensen and Cain, J.C., J. Geophys. Res., 67, 3568, 1962

Jensen, D.C., and Cain, J.C., an interrim magnetic field, J. Geophys. Research, 67, 3568, 1962.

King, J.H., National Aeronautics and Space Administration, Special Publication NASA SP-3024 Vol.IV, 1967.

King, J.H., Solar Proton Fluences for 1977 - 1983 Space MIssions, J. Spacecraft, 11, 401 - 408, 1974.

Konradi, A., Hardy, A.C. and Atwell, W., J. Spacecraft, 24, 284, 1987.

Konradi, A., Sciences, 242, 1283, 1988.

Lemaire, J., Bull. Soc. Royale Sciences Lige, 31e anne, 7-8, 556, 1962.

McCormack, P.D.: Space: Opportunities for All Peoples. Oxford-New York-Frankfurt, Pergamon Press, IAF/IAA-86-380, 1986.

McIlwain, C.E., J. Geophys. Res., 66, 3681, 1961.

McIlwain, C.E., Processes acting upon Outer Zone Electrons, I; Adiabatic Perturbations, unpublished preprint, 1966c.

McIlwain, C.E., Space Sci. Rev., 5, 585, 1966a.

Mead, G.D. and Fairfield, D.H., J. Geophys. Res., 80, 523, 1975.

Mullen E.G. and Gussenhoven, M.S., SCATHA Environmental Atla, AFGL-TR-83-0002, 1983.

Mullen, E.G., Gussenhoven, M.S. and Hardy, D.A., Proceedings of NATO Advanced Study Institute "Terrestrial Space Radiation and its Biological Effects", Corfu, Oct. 1987.

Northrop, T.G., The Adiabatic Motion of Charged Particles, Interscience, New York, 1963.

Olson, W.P. and Pfitzer, K.A., J. Geophys. Res., 79, 3739, 1974.

Pruett, R.G., J. Spacecraft, 17, 270, 1980.

Reagan, J.B., Nightingale, R.W., Gaines, E.E., Imkof, W.L. and Stassinopoulos, E., J. Spacecraft Rockets, 18, 83, 1981.

Roederer, J.G., J. Geophys. Res., 72, 981, 1967.

Roederer, J.G., Rev. Geophys. Space Phys., 10, 599, 1972.

Roederer, J.G., Rev. Geophys. Space Phys., 7, 77, 1969.

Roederer, J.G.: Dynamics of Geomagnetically Trapped Radiation. Berlin-Heidelberg-New York: Springer, 1971.

Sawyer, D.M. and J.I. Vette, National Space Science Data Center, NSSDC/WDC-A-R&S 76-06, Dec. 1976.

Schulz, M. and Lanzerotti, L.J. : Particle Diffusion in the Radiation Belts. Berlin-Heidelberg-New York: Springer, 1974.

Schulz, M. and Paulikas, G.A., Bull. Amer. Phys. Soc., 2, 123, 1972b.

Schulz, M. and Paulikas, G.A., J. Geophys. Res., 77, 744, 1972a.

Schulz, M., J. Geophys. Res., 77, 624, 1972.

Shea, M.A. and Smart, D.F., Report N° AFCRL-TR-75-0185, Hanscom, AFB, Mass., 1975.

Shea, M.A., Smart, D.F. and McCracken, K.G., A Study of Vertical Cutoff Rigidities Using Sixth Degree Simulations of the Geomagnetic Field, J. Geophys. Res., 70, 4117-4130, 1965a.

Shea, M.A., Smart, D.F. and McCracken, K.G., A study of Vertically Incident Cosmic-Ray trajectories Using Sixth-Degree Simulations of the Geomagnetic Field, Environ. Res. Paper N° 141, AFCRL 65-705, September 1965b.

Shea, M.A., Smart, D.F. and Mooney, W.R., 13th Intl. Cosmic Ray Conf., 2, 1075, 1973.

Singley, G. W. and J.I. Vette, National Space Science Data Center, NSSDC/WDC-A-R&S 72-06, Aug. 1972a.

Singley, G. W. and J.I. Vette, National Space Science Data Center, NSSDC/WDC-A-R&S 72-13, Dec. 1972b.

Smart, D.F. and Shea, M.A., 15th Intl Cosmic Ray Conf., 11, 256, 1977.

Smart, D.F. and Shea, M.A., A Study of the Effectiveness of the McIlwain Coordinates in Estimating Cosmic-Ray Vertical Cutoff Rigidities, J. Geophys. Res., 72, 3447-3454, 1967.

Speldvik, W.N., J. Geophys. Res., 82, 2801, 1977.

Stassinopoulos, E.G. and King, J.H., An Empirical Model of Energetic Solar Proton Fluxes with Applications to Earth Orbiting Spacecraft, IEEE Transactions on Aerospace and Electronic Systems, Vol. AES-10, Nø 4, July 1974.

Stern, D.P., J. Geophys. Res., 73, 4373, 1968.

Stern, D.P., J. Geophys. Res., 76, 257, 1971.

Stern, D.P., J. Geophys. Res., 92,4437, 1987.

Stern, D.P., Rev. Geophys. Space Phys., 14, 199, 1976.

Störmer, C., Periodische Elektronenbahnen im Felde eines Elementarmagneten und ihre Anwendung auf Brüches Modellversuche und auf Eschenhagens Elementarwellen des Erdmagnetismus, Z. Astrophys., 1, 237-274, 1930.

Teague, M. J. and J. I. Vette, National Space Science Data Center, NSSDC/WDC-A-R&S 76-04, May 1976.

Teague, M.J. and E.G. Stassinopoulos, GSFC X-Document X-601-72-487, Dec. 1972

Teague, M.J. and J. I. Vette, National Space Science Data Center, NSSDC/WDC-A-R&S 72-10, Nov. 1972.

Teague, M.J. and J. i. Vette, National Space Science Data Center, NSSDC/WDC-A-R&S 74-03, Apr. 1974.

Teague, M.J., J. Stein, and J. I. Vette, National Space Science Data Center NSSDC/WDC-A-R&S 72-11, Nov. 1972.

Teague, M.J., Stein, J. and Vette, J.I., The Use of the Inner Zone Electron Model AE-5 and Associated Computer Programs, preprint NSSDC 72-11, 1972.

Tsyganenko, N.A., Planet. Space Sci., 35, 1347, 1987.

Tsyganenko, N.A., Planet. Space Sci., 37, 5, 1989.

Vampola A.L. and Gorney D.J., Electron energy deposition in the middle atmosphere, J. Geophys. Res. 88, 6267 - 6274, 1983.

Vampola, A.L., Balke, J.B. and Paulikas, G.A., J. Spacecraft Rockets, 14, 690, 1977.

Vette, J. I. and B. Lucero, National Aeronautics and Space Administration, Special Publication NASA SP-3024 Vol. III, 1967.

Vette, J. I., A. B. Lucero, and J.A. Wright, National Aeronautics and Space Administration, Special Publication NASA SP-3024 Vol.II, 1966.

Vette, J. I., in Particles and Fields in the Magnetosphere, ed. by B.M. McCormac, D. Reidel Publishing Co., Dordrecht-Holland, p 305, 1970.

Vette, J. I., National Aeronautics and Space Administration, Special Publication NASA SP-3024 Vol. 1, 1966.

Vette, J.I., Chan, K.W. and Teague, M.J., Problems in Modelling the Earth's Trapped radiation Environment, AFGL-TR-78-0130, 1977.

Walt, M., J. Geophys. Res., 69, 3947, 1964.

Spacecraft	Instrument	PI
ATS-1	ASC	Paulikas
ATS-5	UCSD	McIllwain
ATS-6	U. Minn.	Winckler
	NASA	Konradi
	MDAC	Masley
	ASC	Paulikas
SCATHA	SC3	Reagan
	SC5	Hardy
DMSP-F7	SSJ*	Gussenhoven
DMSP-F1	SSJ*	Blake
GEOS	S321	Korth
IMP	NOAA	Williams
	U. Md.	Gloeckler
	JHU/APL	Krimigis
	U. Ch.	Simpson
	Caltech	Stone
Los Alamos		
76-059A		Higbie
77-007A		Higbie
79-053		
SMS/GOES	SEM	Sauer
TIROS	SEM	
NOAA	SEM	
ISEE-1		Williams
ISEE-2		Keppler
ISIS-2		McDiarmid
S3-2		Fennell
S3-3		Vampola
		Yates
NTS		

Table 3-1 List of spacecraft missions with energetic particle detectors (from ESA statement of work, 1988).

Orbit Parameters	Spacecraft/Instrument Acronym	Electron Energies	Proton Energies	Time Coverage
Hi Elliptical i = 29 ha/p = 138000/281	ISEE1&2/L-GM	> 45 keV	> 600 keV	11/77 - 10/87
	ISEE1&2/EAP	8 - 200 keV 30 - 200 keV	8-200, 30-200 200 - 300 keV	11/77 - 10/87
	ISEE1/EEAP	0.02 - 1 MeV	0.02 - 1.2 MeV	11/77 - 8/79
	ISEE2/EEAP	20 - 300 keV 0.02 - 1.2 MeV	0.02 - 2 MeV	11/77 + 7 years
	ISEE1/LECR	75 - 1300 keV	66, 130 keV	11/77 - 10/87
Hi Elliptical i = 0 ha/p = 51000/5550	CCE/MEPA		0.01 - 1 MeV	8/84 - p?
	CCE/CHEM		1 - 300 keV	8/84 - p?
i = 29 ha/p = 113000/550	IRM/SICA	35 - 220 keV	10 - 300 keV	8/84 - p?
~Circular/580 i = 98	STPP78-1/GEE	0.04 - 2.5 MeV		3/79 - 2/80 ?
~Circular/850 i = 102	NOAA/SEM	>30,100,300 keV > 6 MeV	> 80 keV	10/78 - p
~Circular/840 i = 99	DMSP/SRD	> 1 & 2.5 MeV	>20,35,51,75 MeV	11/83 - 7/88
Synchronous i = 29 ha/p = 45000/26600	IUE/PFM	> 1 MeV		11/80 - p
Synchronous i = 8 ha/p = 43200/27600	STP P78-2/RSPD	0.05 - 1 MeV	0.05 - 7 MeV	3/79 - 5/80
	STP P78-2/PD		17 - 717 keV, 0.7 - 3.3 MeV	3/79 - 5/80
	STP P78-2/CPD	0 - 81 keV	0 - 81 keV	3/79 - 5/80
	STP P78-2/HEPD	0.3 - 2.1 MeV	1 - 100 MeV	3/79 - 5/80
Geostationary i < 1.9	LANL/CPA	30 - 300 keV 0.2 - 2 MeV	145 - 560 keV 0.4 - 140 MeV	7/76 - p
	LANL/SEE	3-5, 5-7, 7-10, 10-15 MEV		6/79 - p
i < 0.3	GOES/EPD	> 2 MeV		9/80 - p
i < 1.9	GMS/SEM	> 2 MeV	1 - 500 MeV	8/81 - p
i = 0	MTSAT P2/LOE	30 - 300 keV		6/88 - p

Table 3-2 Summary of data available and their characteristics.

File name	Identificator	Nb of records	Size	Longitude(s)	Time coverage
LANL1.DAT	1976-059	16 421	11 442 blocks	290° E 325° E	03/01/79 - 27/06/83
LANL2.DAT	1977-007	31 911	22 081 blocks	70° E	03/01/79 - 30/06/83
LANL3.DAT	1979-053	21 550	15 070 blocks	225° E	22/06/79 - 25/05/85
LANL4.DAT	1981-025	27 840	19 194 blocks	225° E 290° E 70° E	27/03/81 - 30/03/85
LANL5.DAT	1982-019	42 308	40 204 blocks	325° E 290° E	21/03/82 - 27/07/87
LANL6.DAT	1984-037	31 629	21 773 blocks	70° E 225° E	24/04/84 - 31/10/88

Table 3-3 LANL data sets available for this study.

E (MeV)	FLPROB (%)	King	Feynman	MATRA N=100	1000	10000	100000
10	80	1.3 E10	2.5 E10	2.28 E10	2.48 E10	2.35 E10	2.33 E10
10	95	4.0 E10	7.7 E10	1.12 E11	8.18 E10	7.89 E10	7.83 E09
30	80	4.9 E09	5.0 E09	5.99 E10	4.86 E09	4.80 E09	4.73 E09
30	95	1.7 E10	1.5 E10	2.11 E10	1.50 E10	1.51 E10	1.49 E10

Table 4-1 Comparison of different solar flare proton event models.

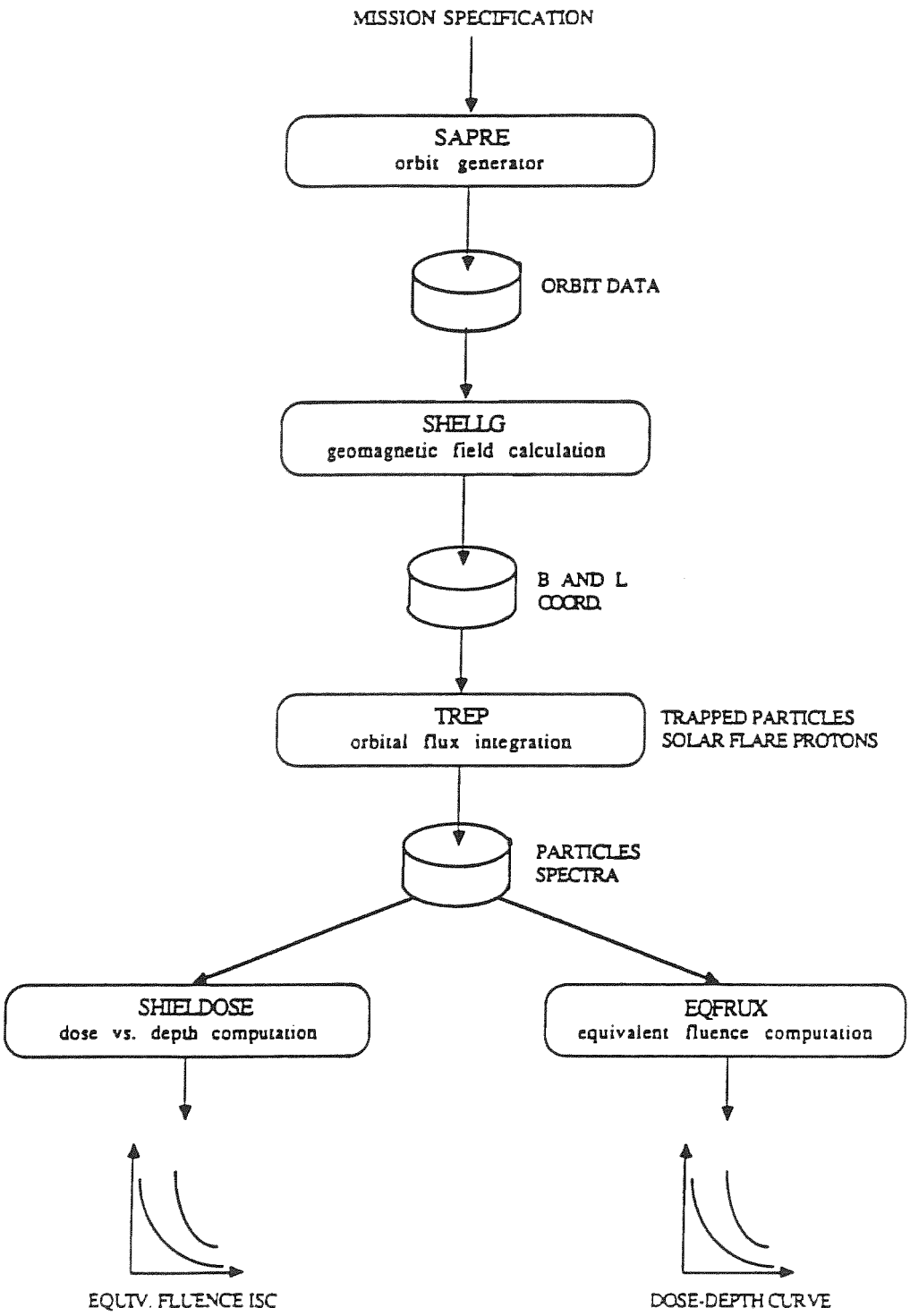

Fig.1-1. Block diagram of the UNIRAD software package.

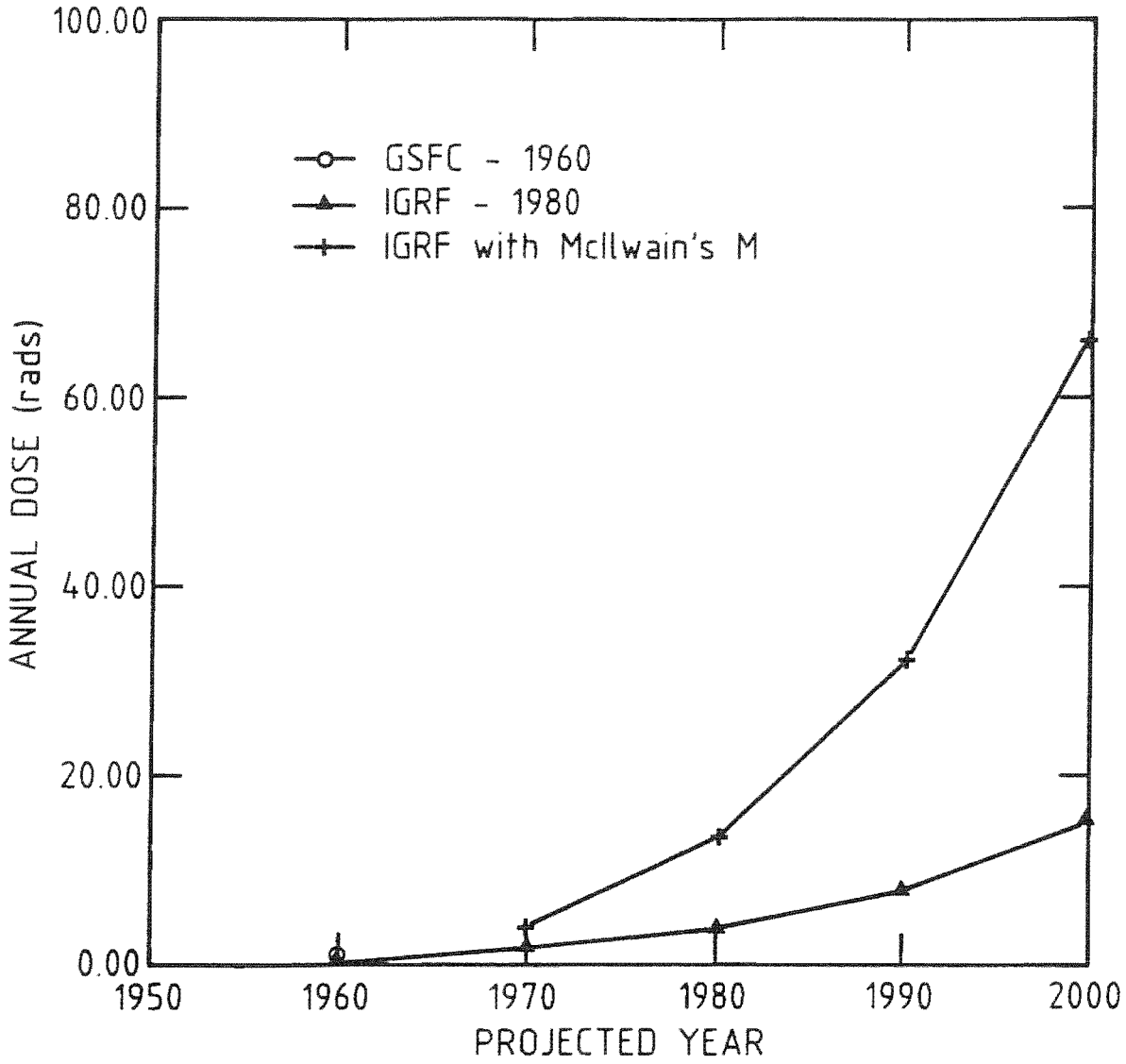

Fig.1-2. Predicted radiation dose as a function of the epoch of the internal magnetic field model used to calculate the B-L coordinates. AE8 and AP8 radiation models are used to calculate the fluxes of trapped electrons and protons along the 13 orbits of a satellite on a circular orbit at 300 km altitude, inclination of 28.5°. The orbit-averaged doses (inside a 1 mm Al sphere) are given in ordinate. (after Daly, 1989)

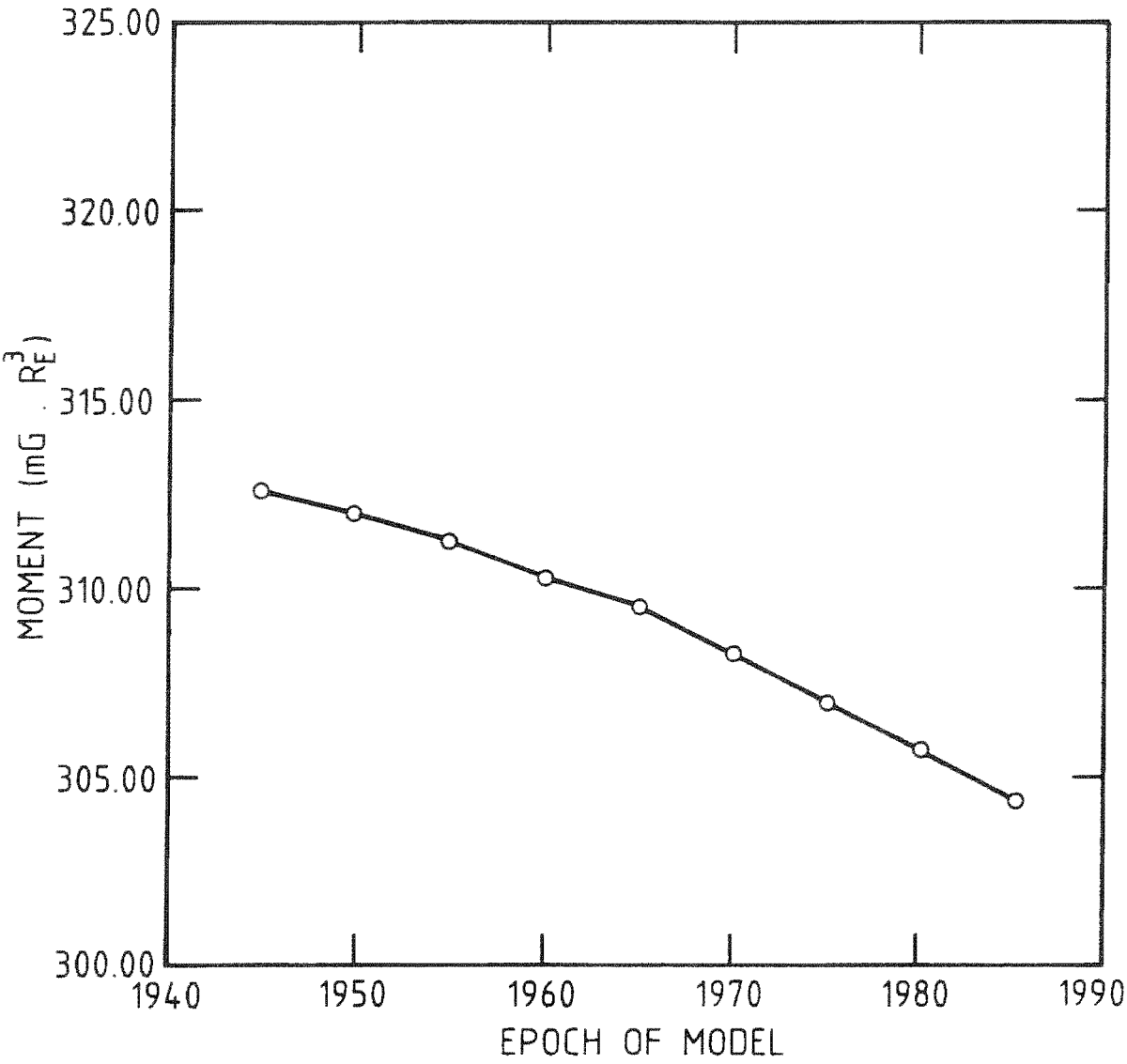

Fig.1-3. Secular narration of the geomagnetic dipole moment as a function of the epoch of the IGRF model (after Daly, 1989).

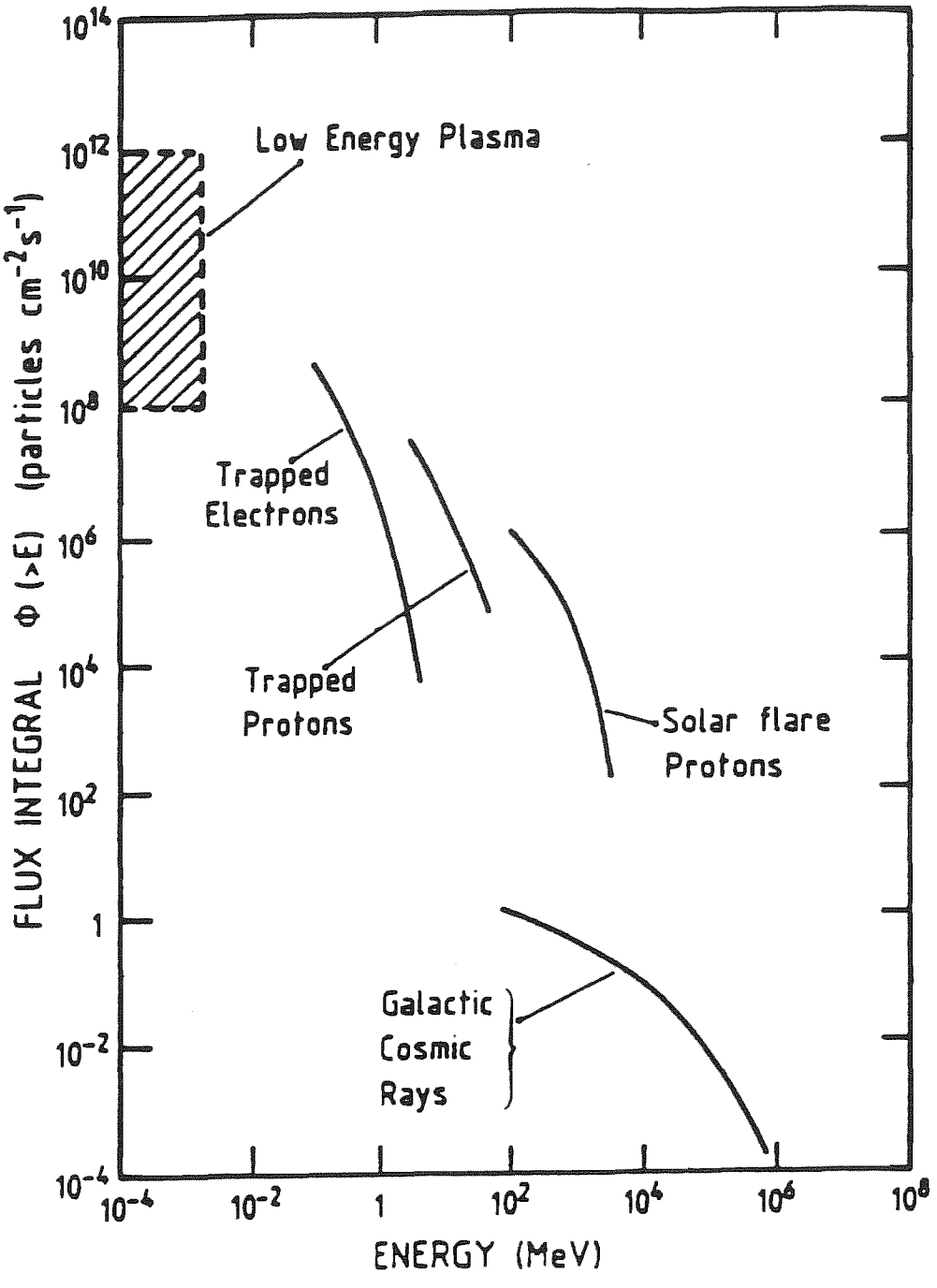

Fig.2-1. Typical energy integral flux of the different populations of charged particles in the Earth magnetosphere.

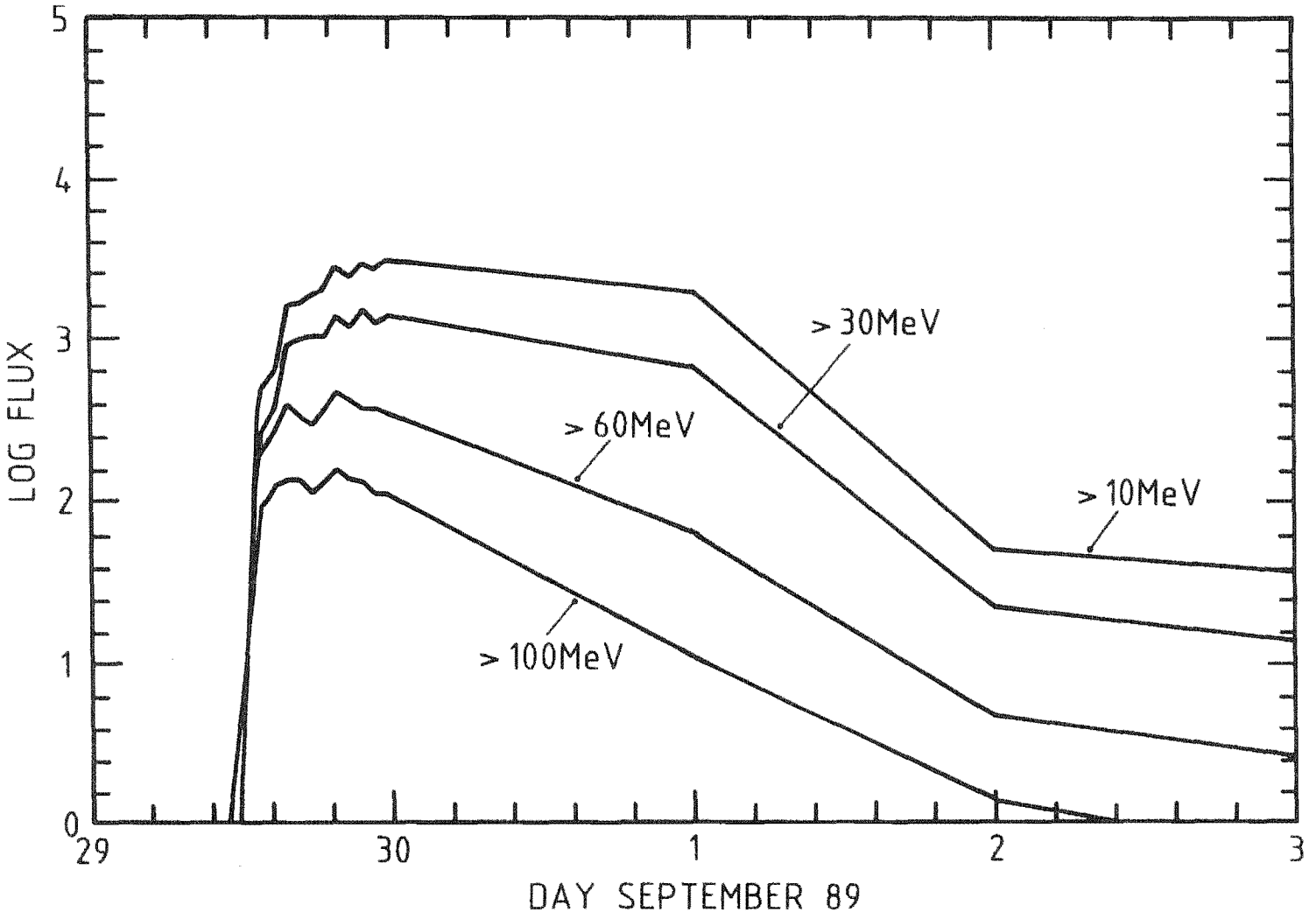

Fig.2-2. Integral flux above different energy thresholds for solar flare protons observed 29 september 1989.

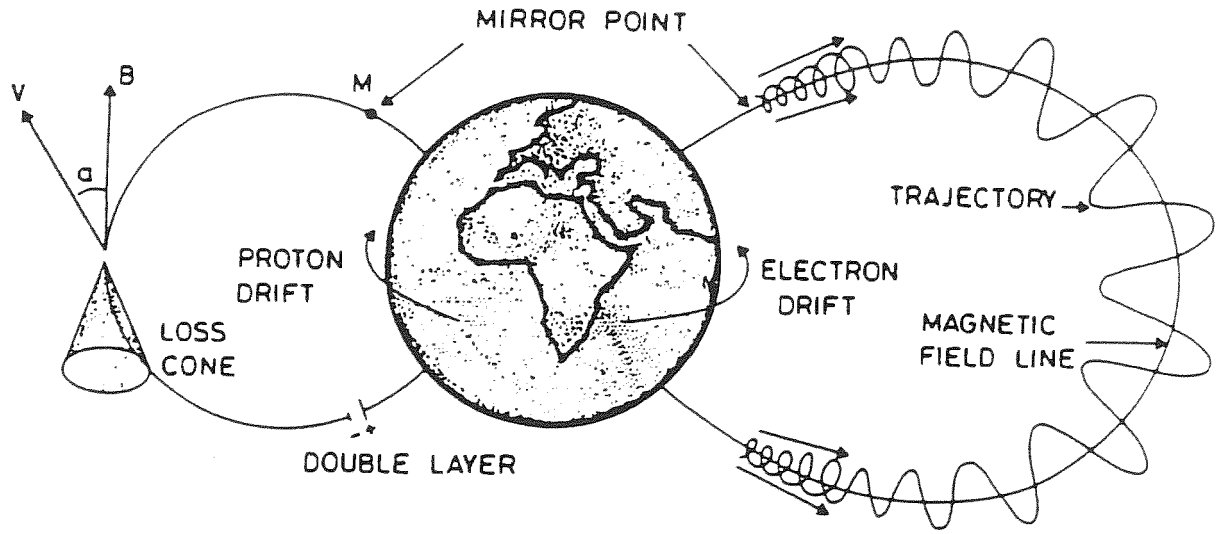

Fig.2-3. Charged particles trapped in the geomagnetic field gyrate around and oscillate along field lines. As a result of gradient-B and curvature drifts, electrons and ions drift also around the Earth, respectively, in the eastward and westward directions. Particles with small equatorial pitch angles (i.e. inside the loss cone) precipitate in the Earth atmosphere.

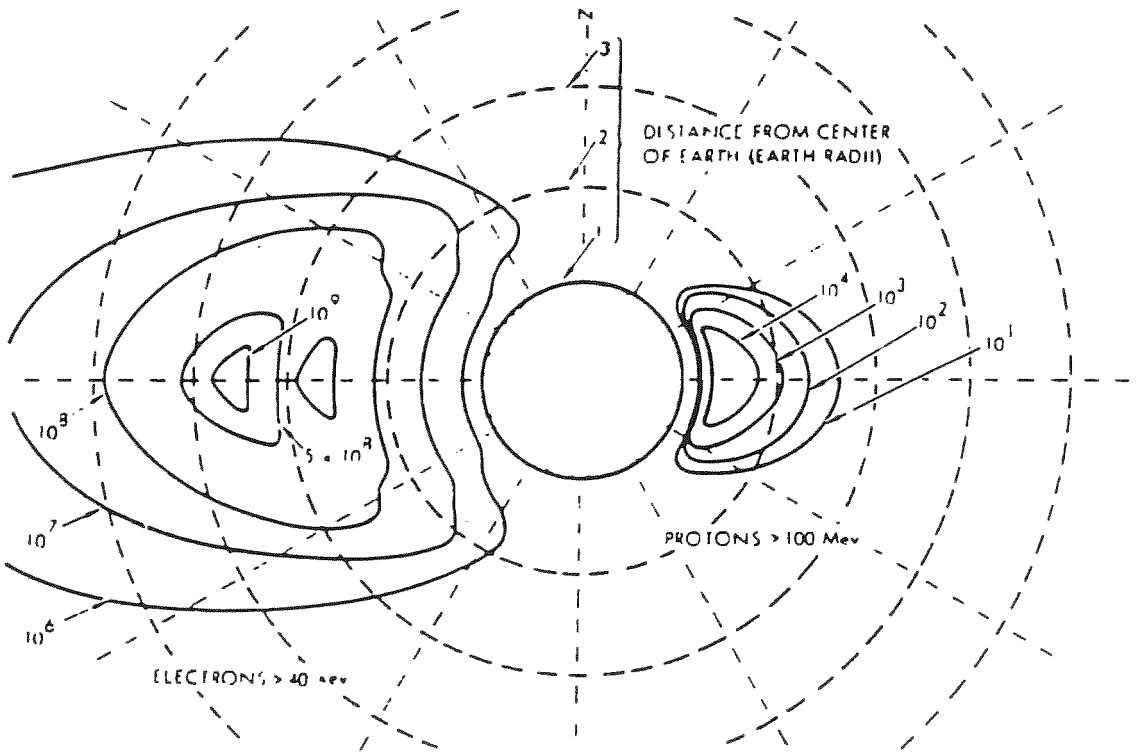

Fig.2-4. Meridional cross-section of the Earth magnetosphere. Isocontours of integrated radiation flux are shown for electrons above 40 keV and for protons above 100 MeV (After Haffner, 1967).

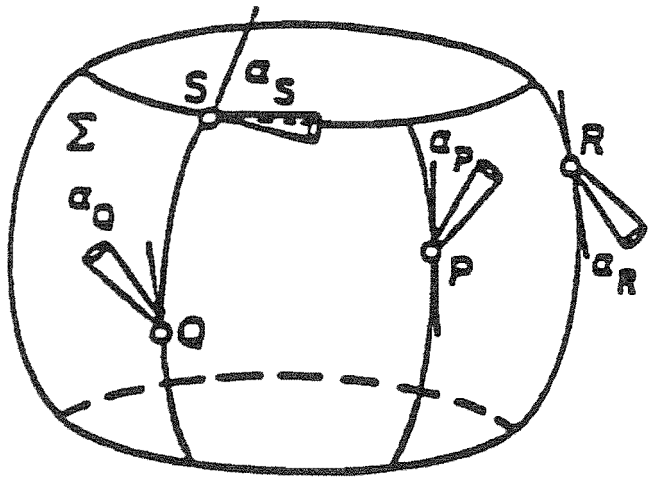

Fig.2-5. Drift shell and pitch angle of a particle (after Roederer, 1970).

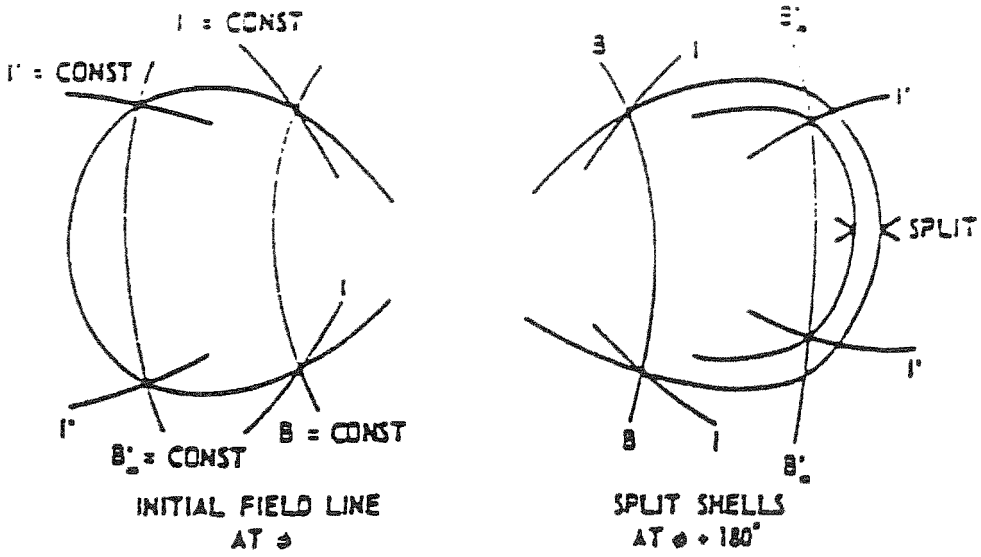

Fig.2-6. Constant B and Constant I contours.

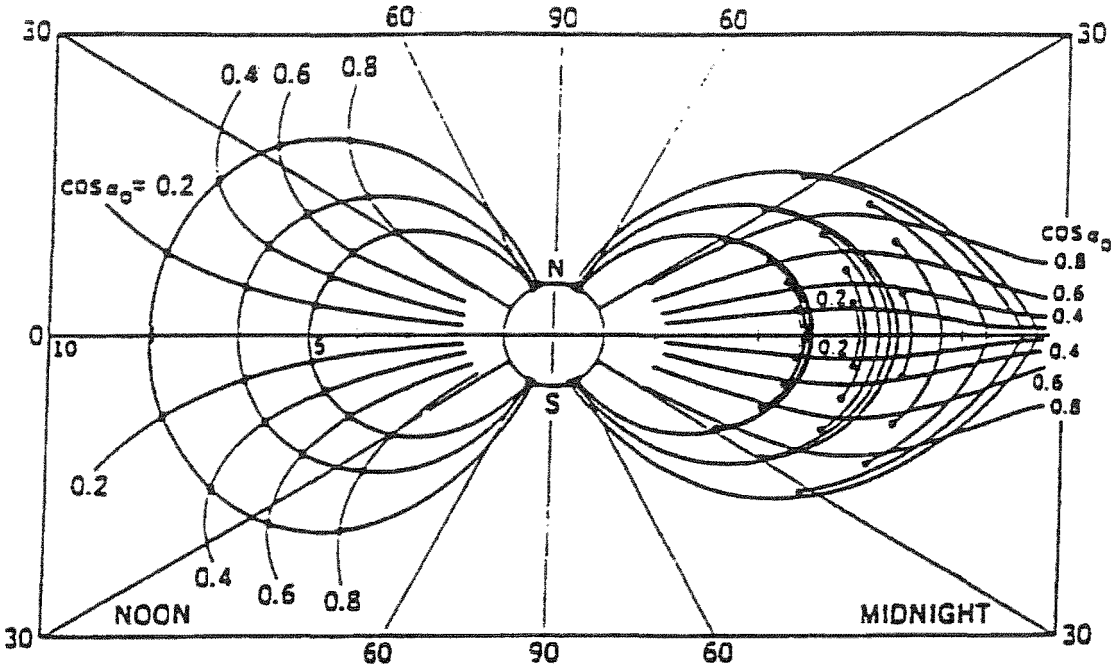

Fig.2-7. Computed shell splitting for particles starting on common field lines in the noon meridian. Dots represent particles mirror points. Curves giving the position of mirror points for constant equatorial pitch angle are shown. (after Roederer, 1972).

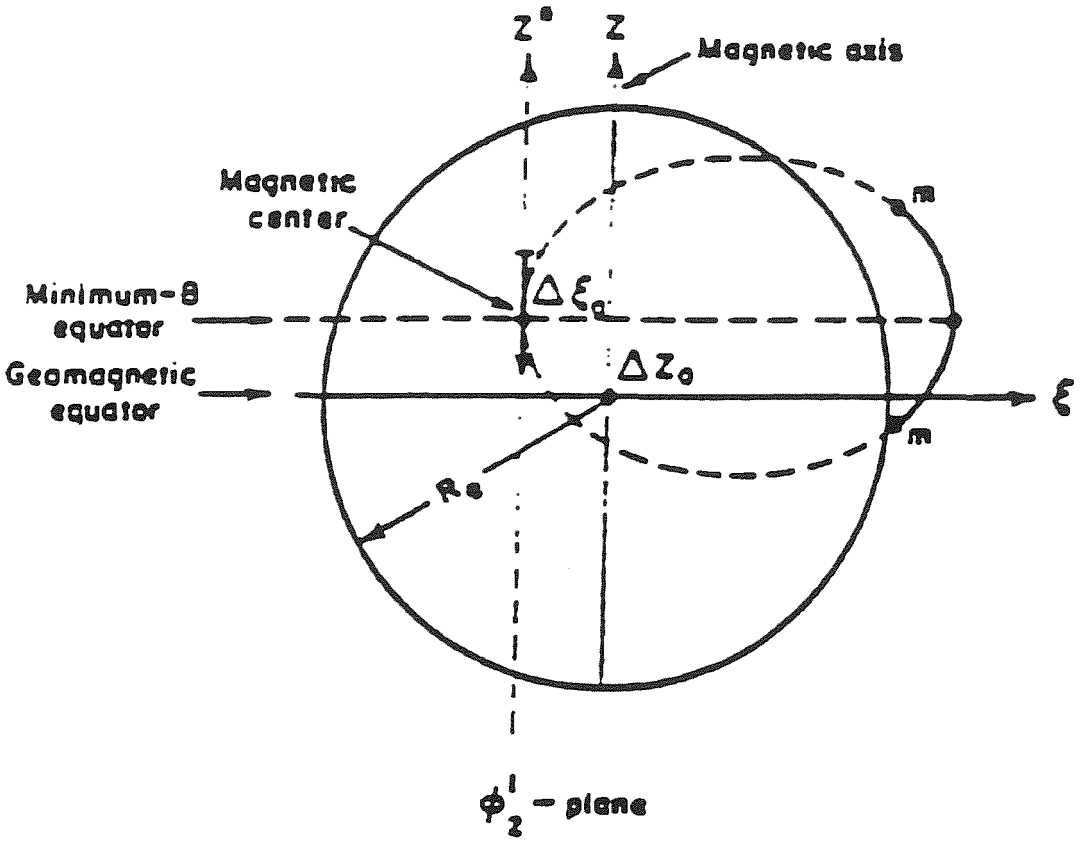

Fig.2-8. Schematic view (highly exaggerated scale) of the eccentric dipole position and its effect on a trapped particle shell (after Roederer, 1972).

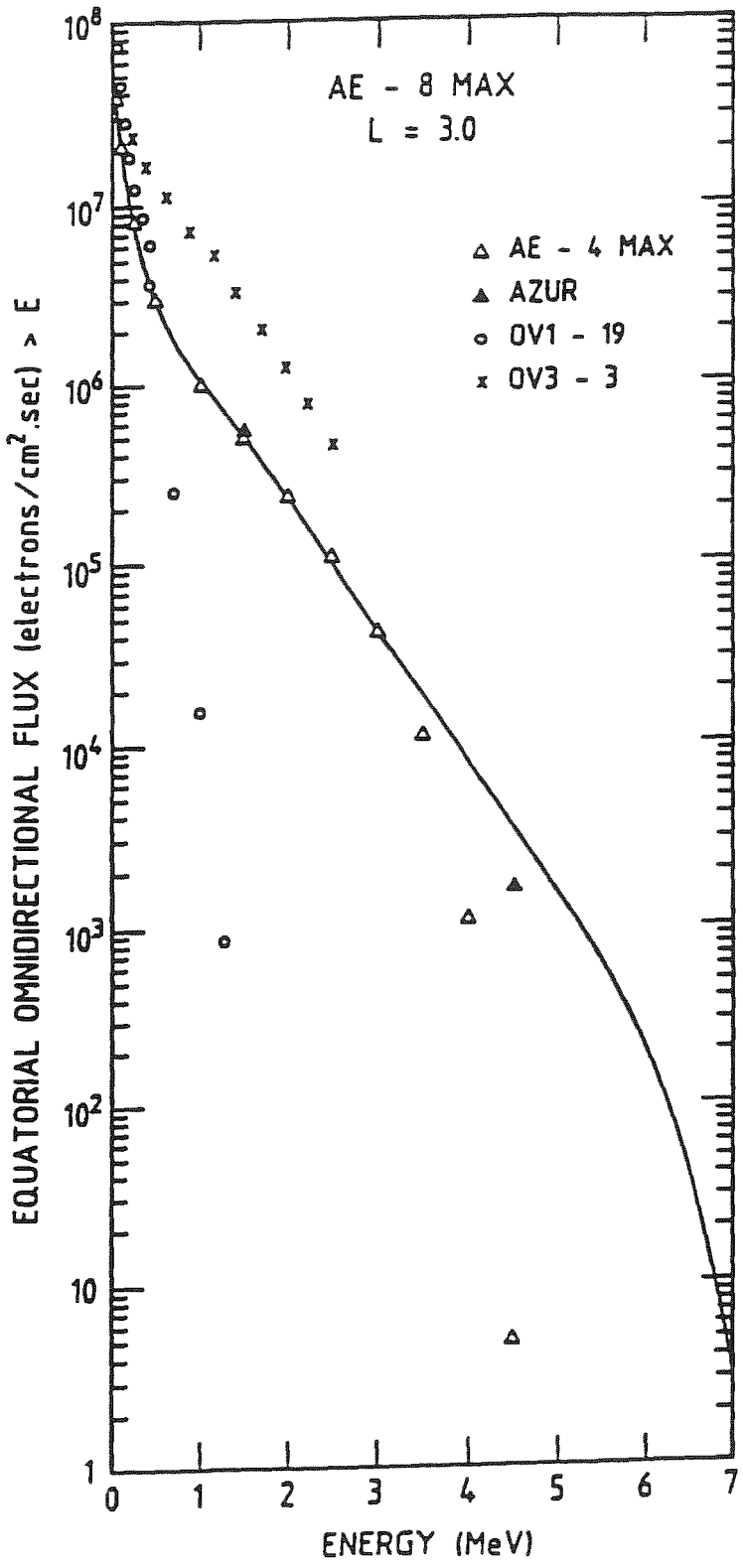

Fig.2-9. Comparison of AE-8 and data at L = 3.0.

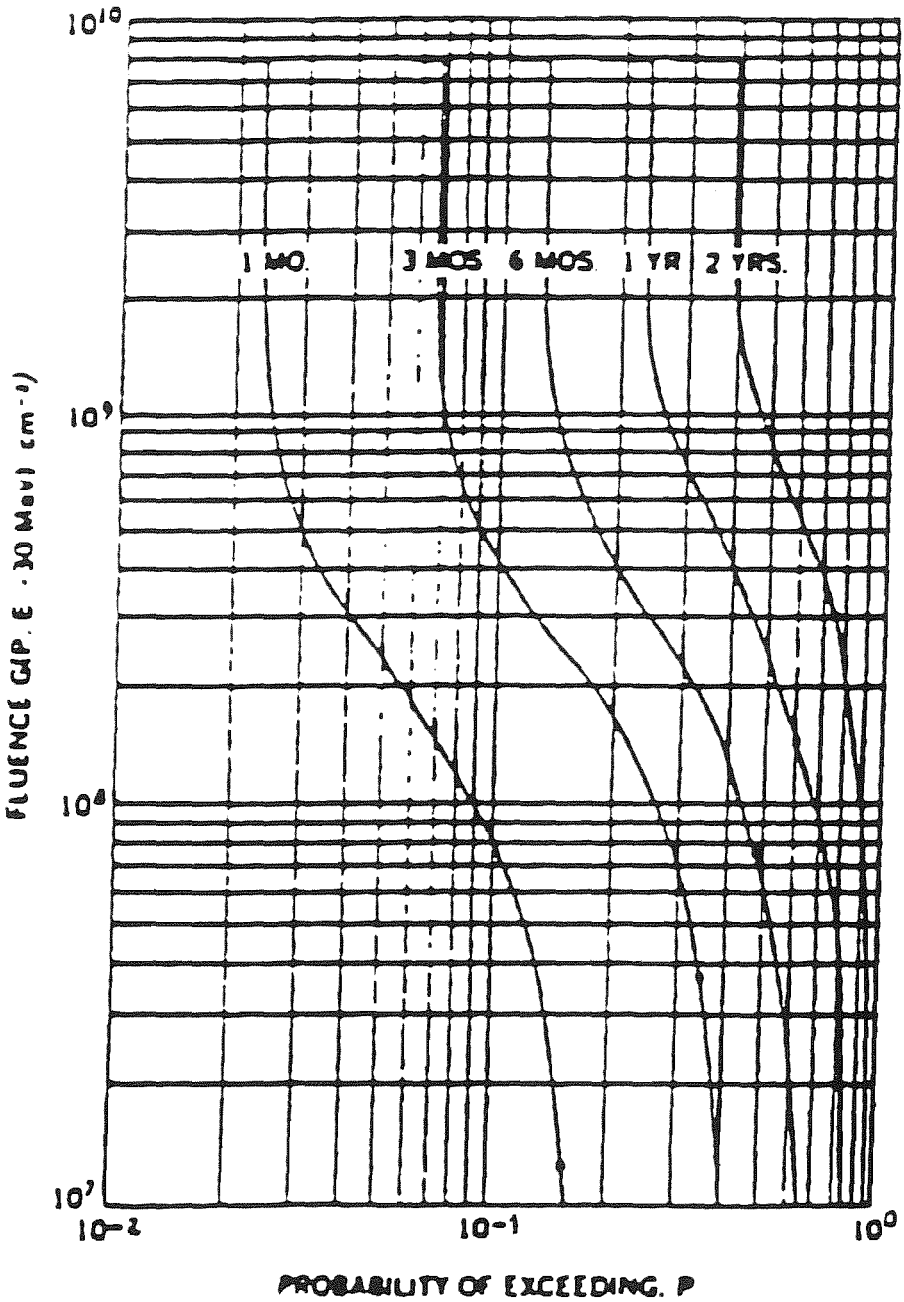

Fig.2-10 Fluence of solar protons above 30 MeV which will be exceeded (with probability P) for missions of varying durations and for fluence levels less than that associated with one AL event. Heavy dots on each curve indicate galactic proton fluence to be encountered (after King, 1974).

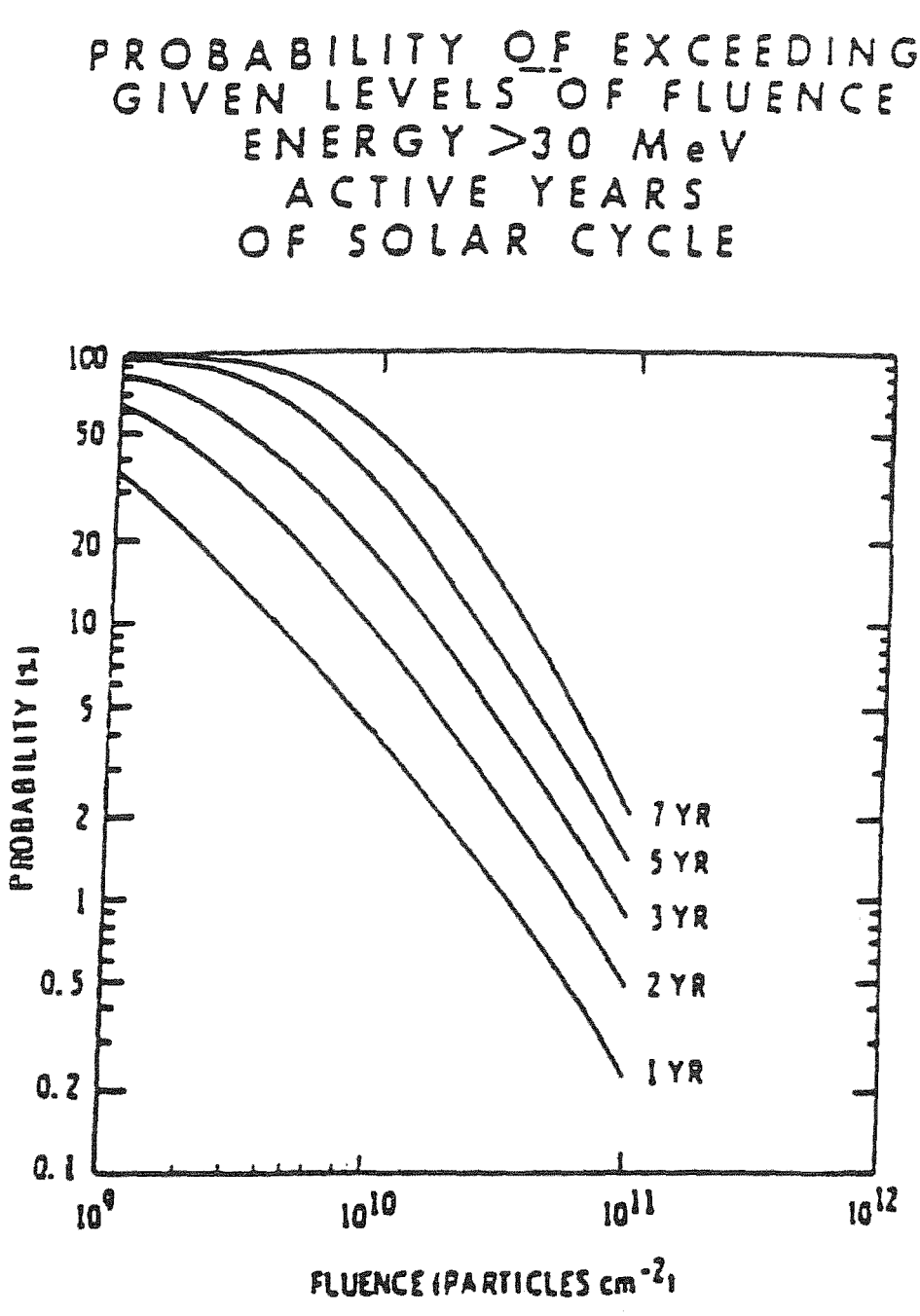

Fig.2-11. The probability of exceeding selected fluences for different mission lenghts for proton energies > 30 MeV (after Feynman et al., 1988a)

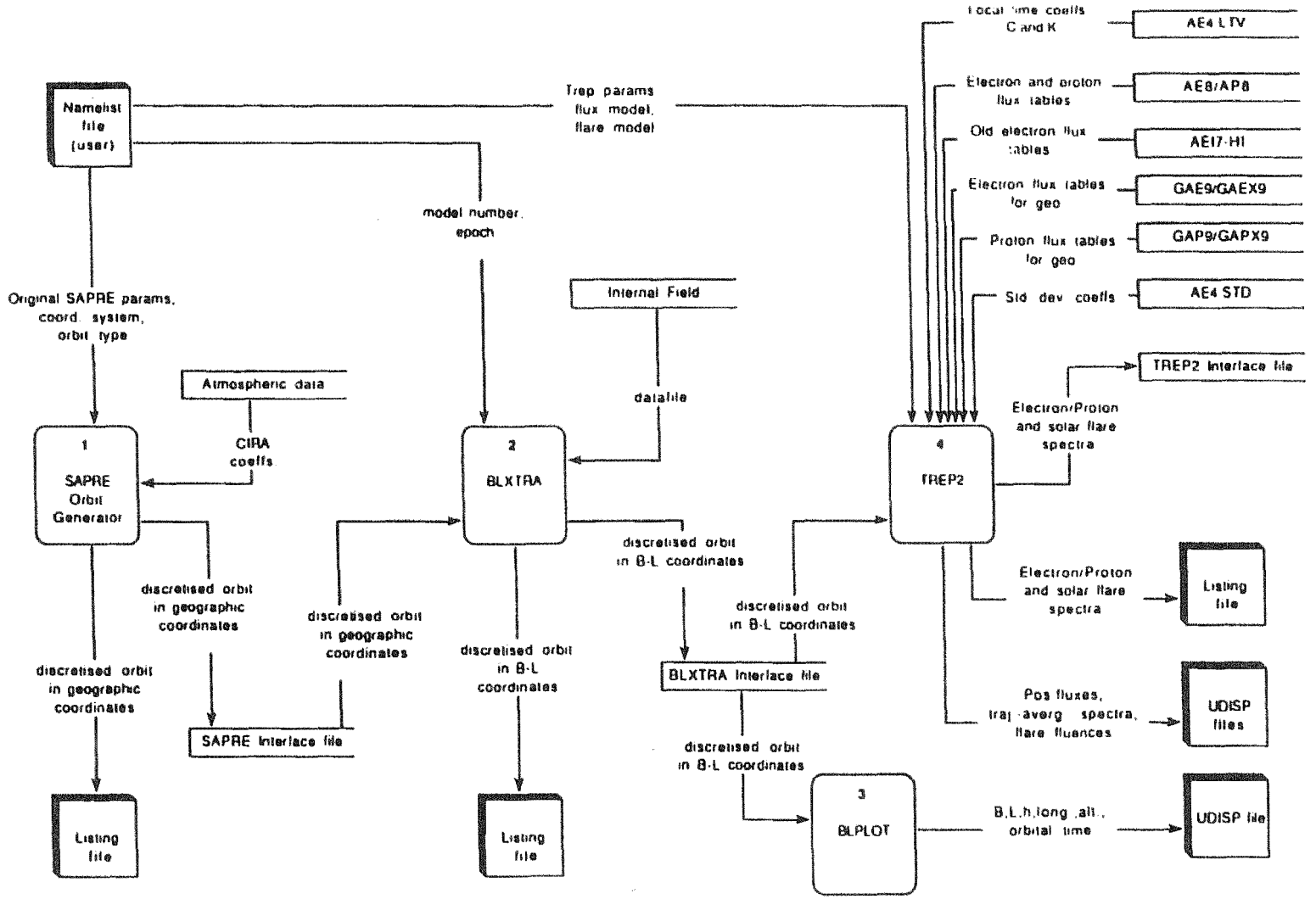

TREND

Fig.3-1. Architectural design of UNIRAD software showing the links between the orbit generator program (SAPRE), the B-L transformation program (SHELLG and now BLXTRA) and the radiation flux/fluence program (TREP).

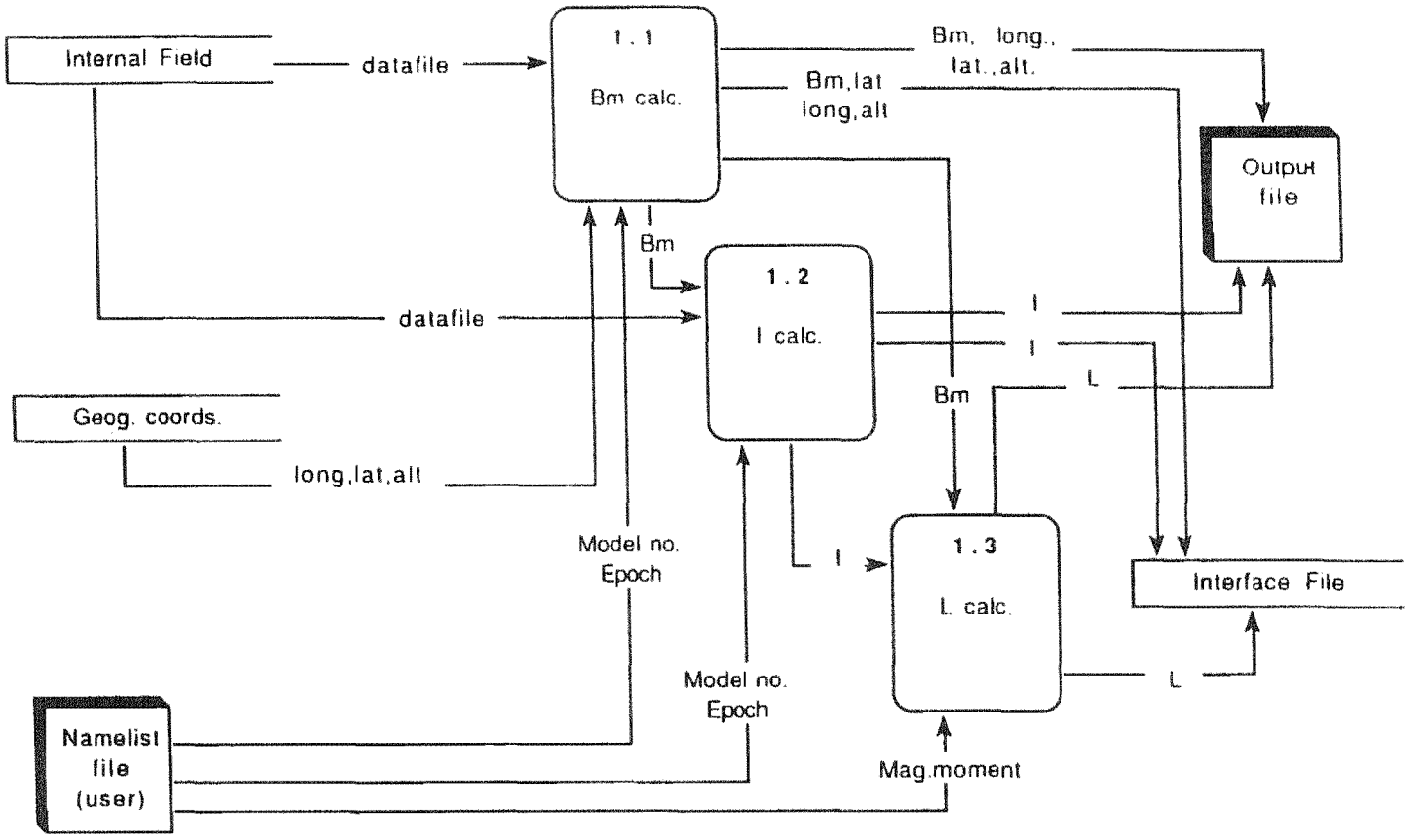

Fig.3-2. Architectural design of BLXTRA program used to transform geocentric coordinates into magnetic B-L coordinates (general overview)

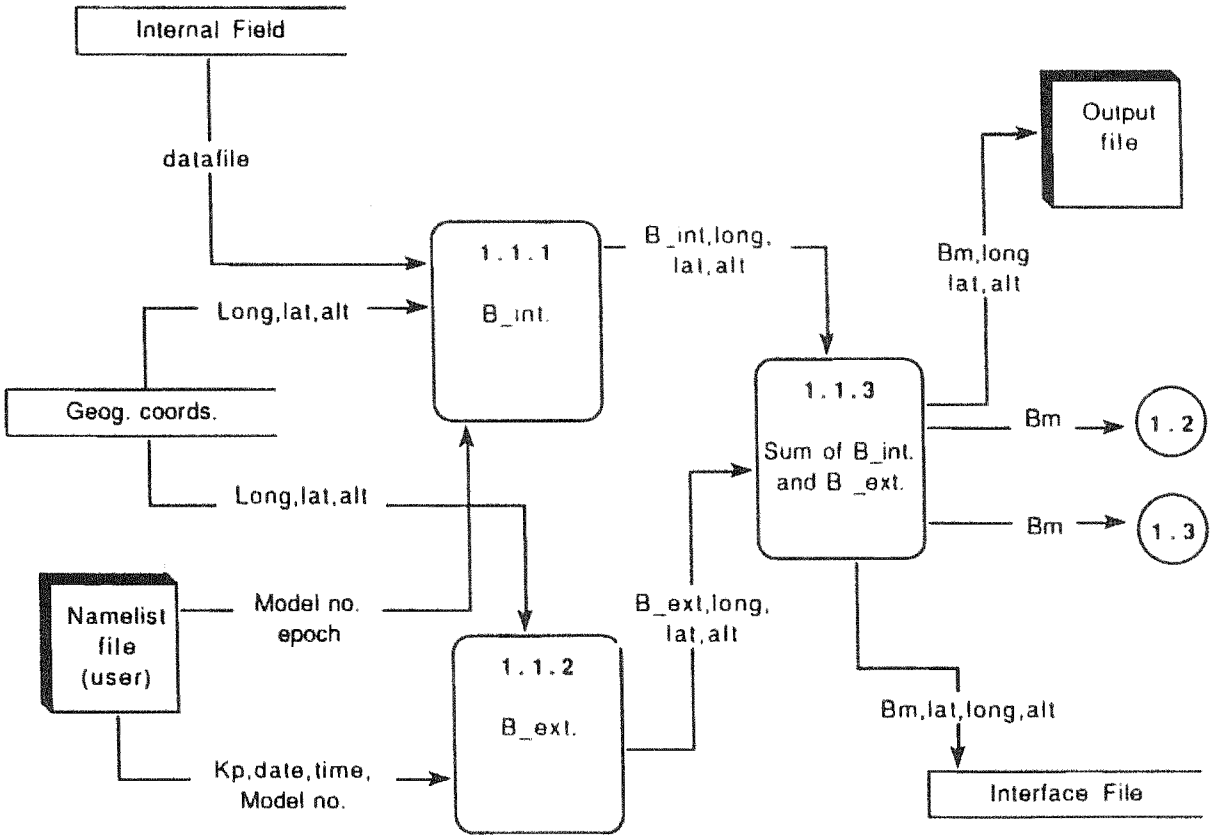

Fig.3-3. Architectural design of part 1.1 of BLXTRA, calculating the total magnetic field as the sum of an internal (B int) and external (B ext) magnetic field components.

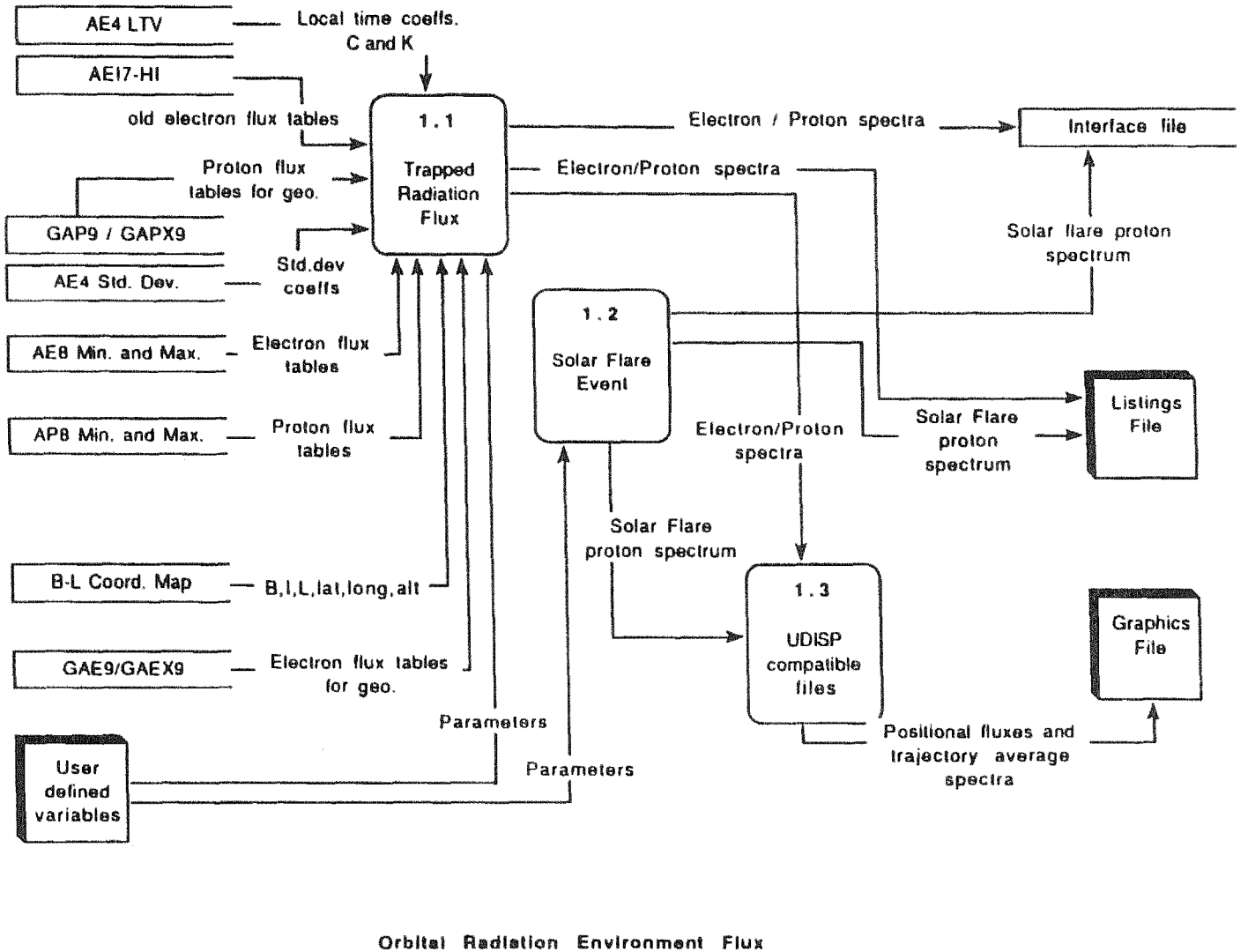

Fig.3-4. Architectural design of TREP (general overview)

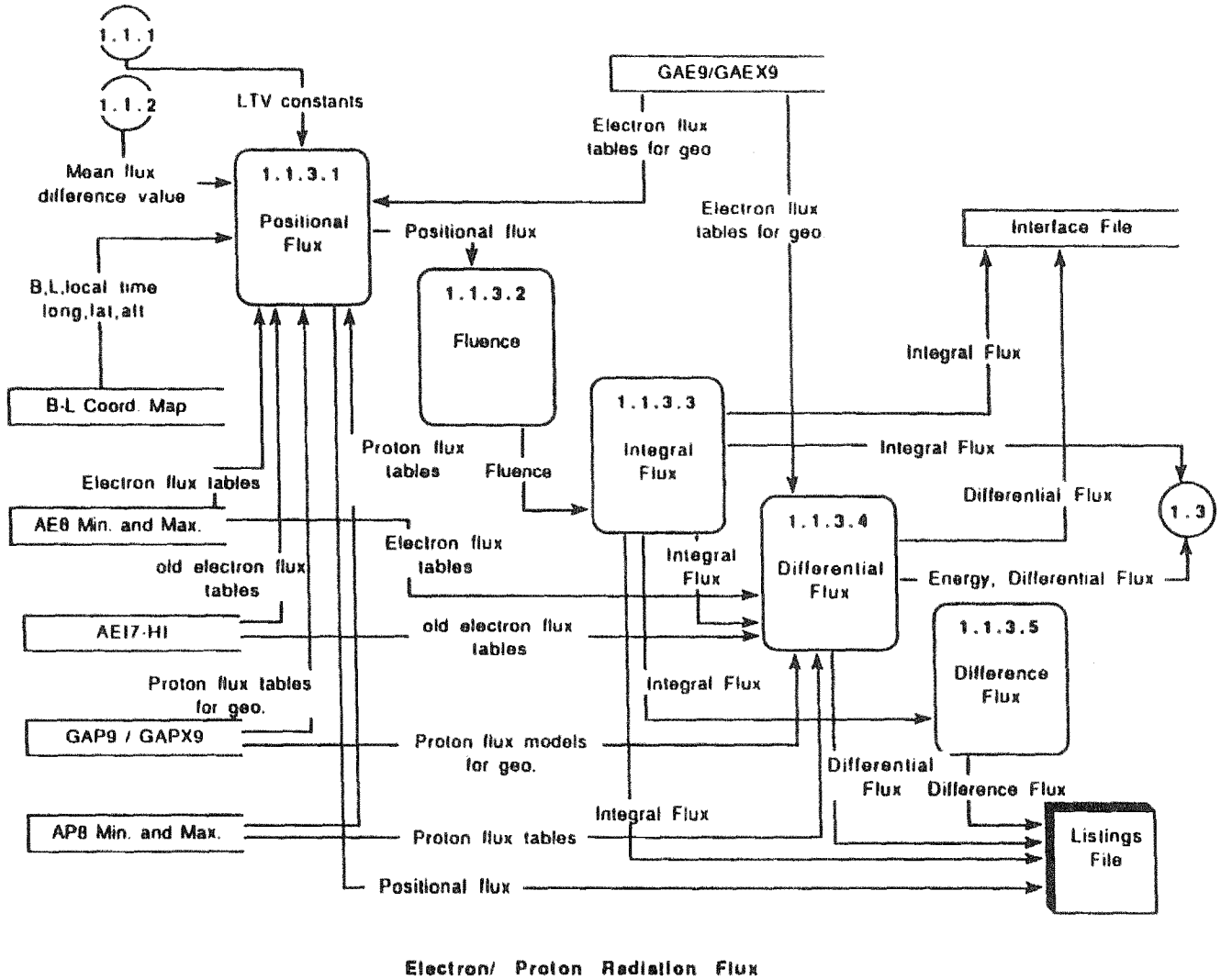

Electron/ Proton Radiation Flux

Fig.3-5. Architectural design of Electron and Proton flux calculation in TREP.

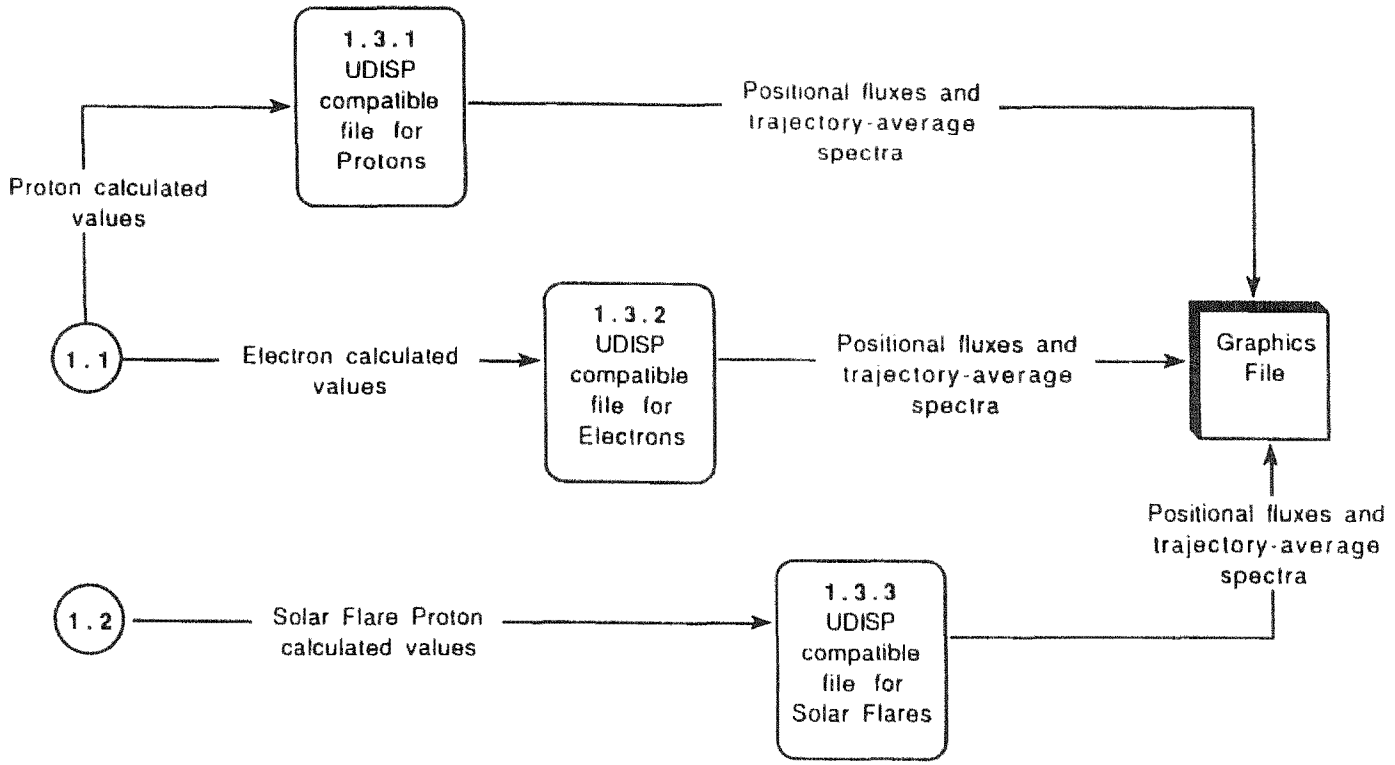

Fig.3-6. Architectural design of UDISP compatible files to determine trajectory-average energy spectra.

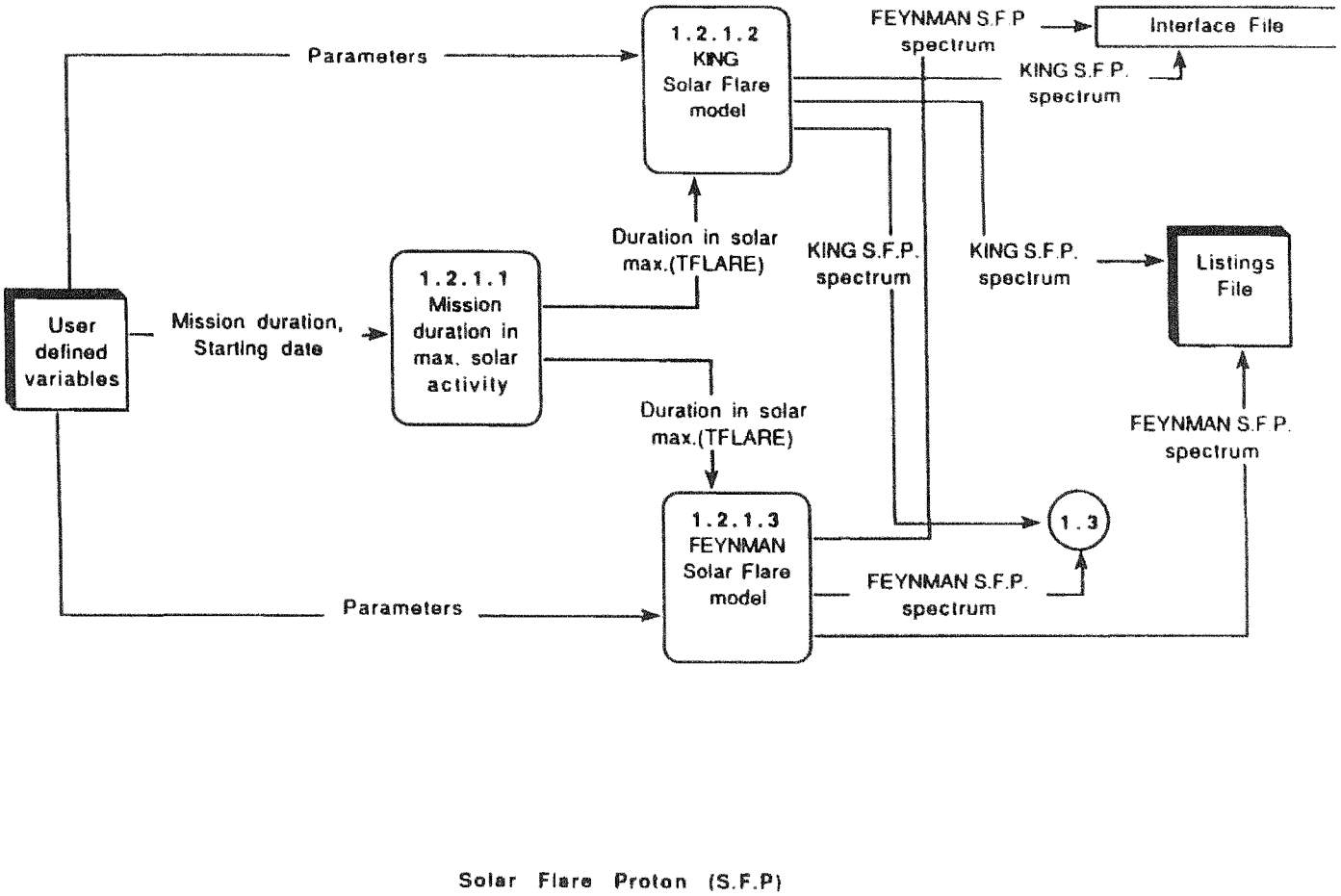

Fig.3-7. Architectural design for the calculation of solar flare proton spectra.

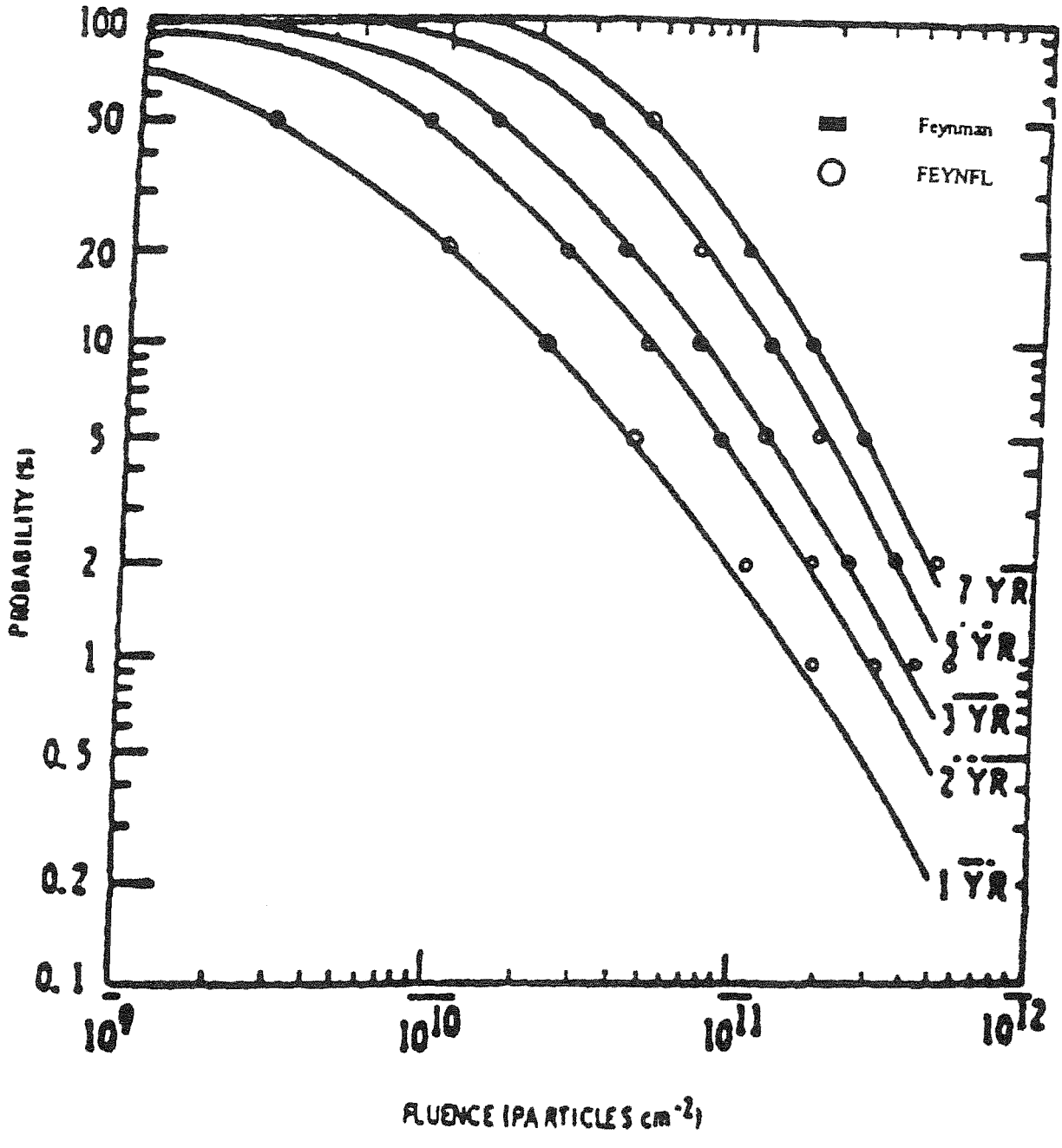

Fig.4-1. Comparison of Feynman et al.'s and TREND's calculation of the fluence of solar flare proton events for 10 MeV.

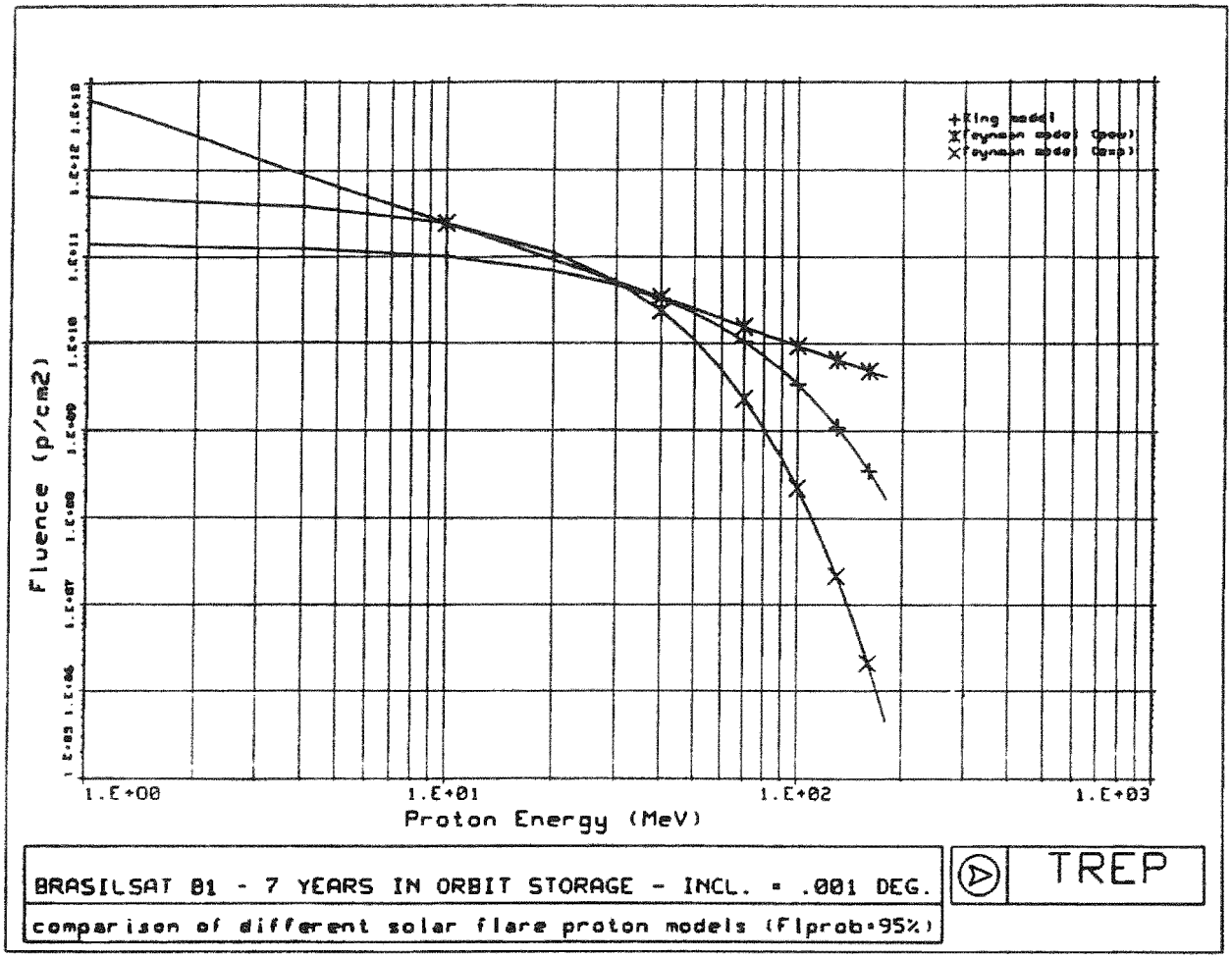

Fig.4-2. Comparison of the fluence spectra obtained from the Feynman et al's model for an exponential fit (X) and power law fit (*), for FLPROB = 95% and τ = 7 years.
The (+)'s give the fluence predicted by King's model.

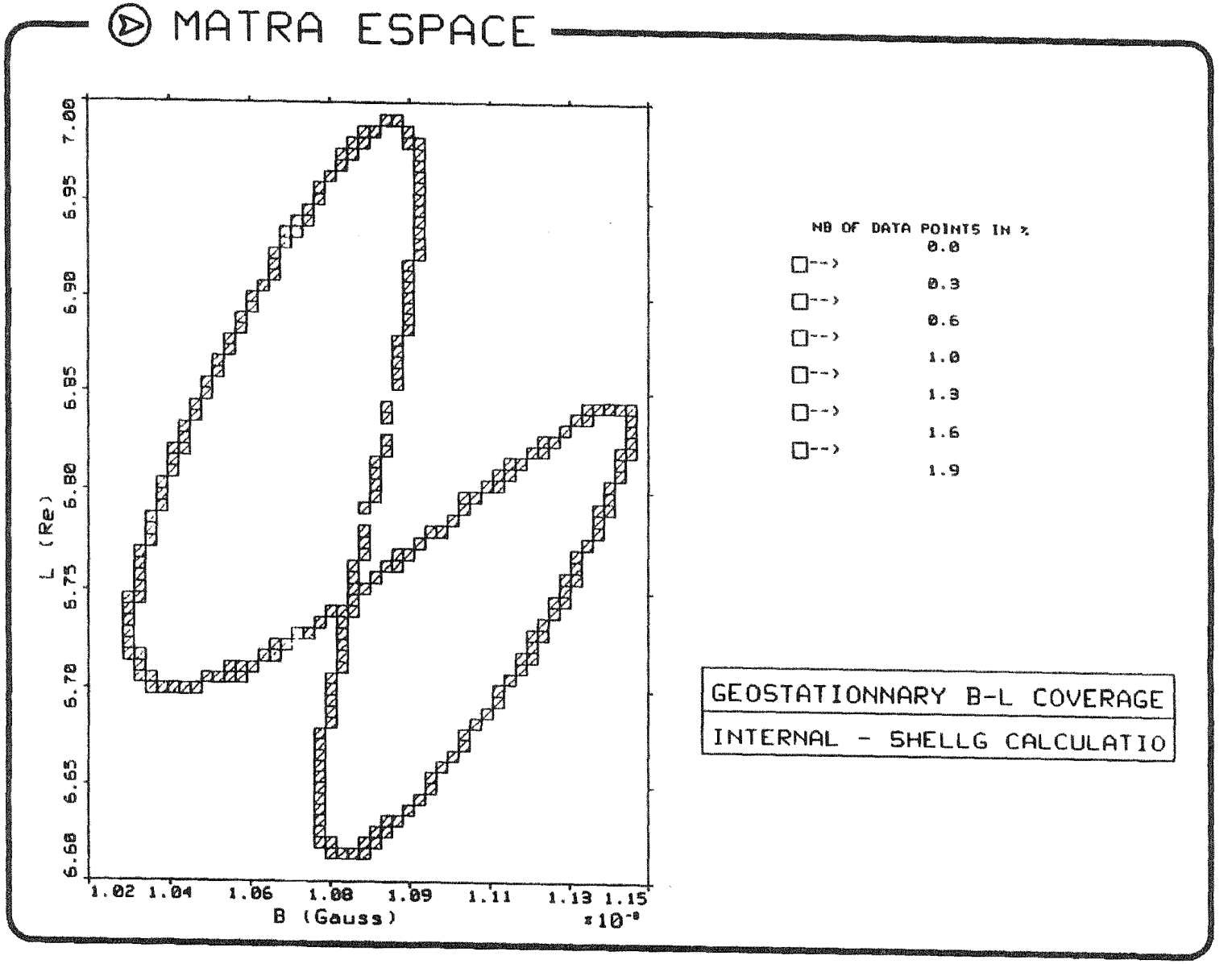

Fig.4-3. B-L coordinates of geostationary satellites located at different geographical longitudes, when the geomagnetic field is approximated by the IGRF-85 model for epoch 1979.

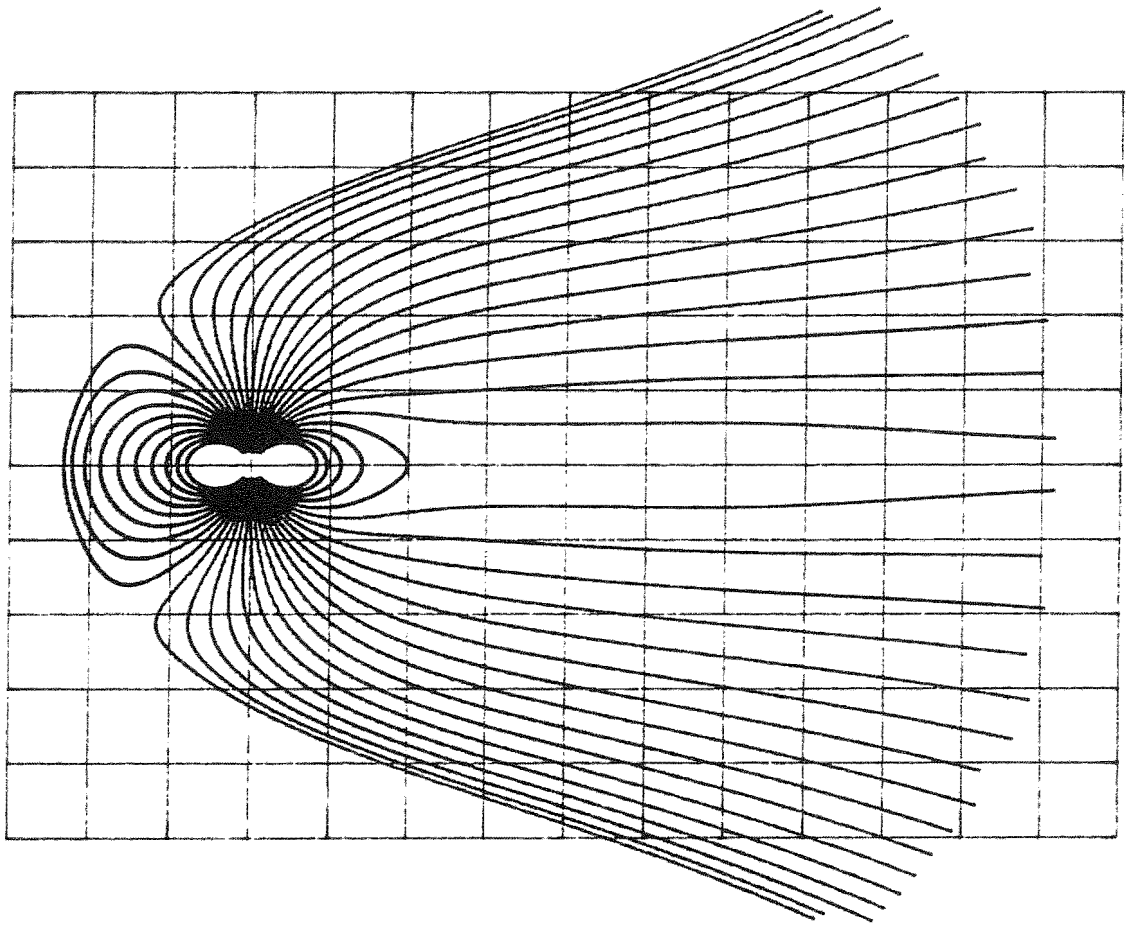

Fig.4-4. shows the magnetic field line distribution obtained with TSY 89 subroutine for zero tilt angle, and $K_p = 4$. The distortion of magnetic field lines at large distance is quite evident. This implies that the values of L corresponding to a fixed altitude in the midnight local time sector are larger compared to those calculated with an external field model. Near noon the values of L are reduced by the addition of an external field. The reverse is true for the magnetic field intensity which is reduced near midnight, but enhanced near noon local time by the presence of additional magnetospheric currents.

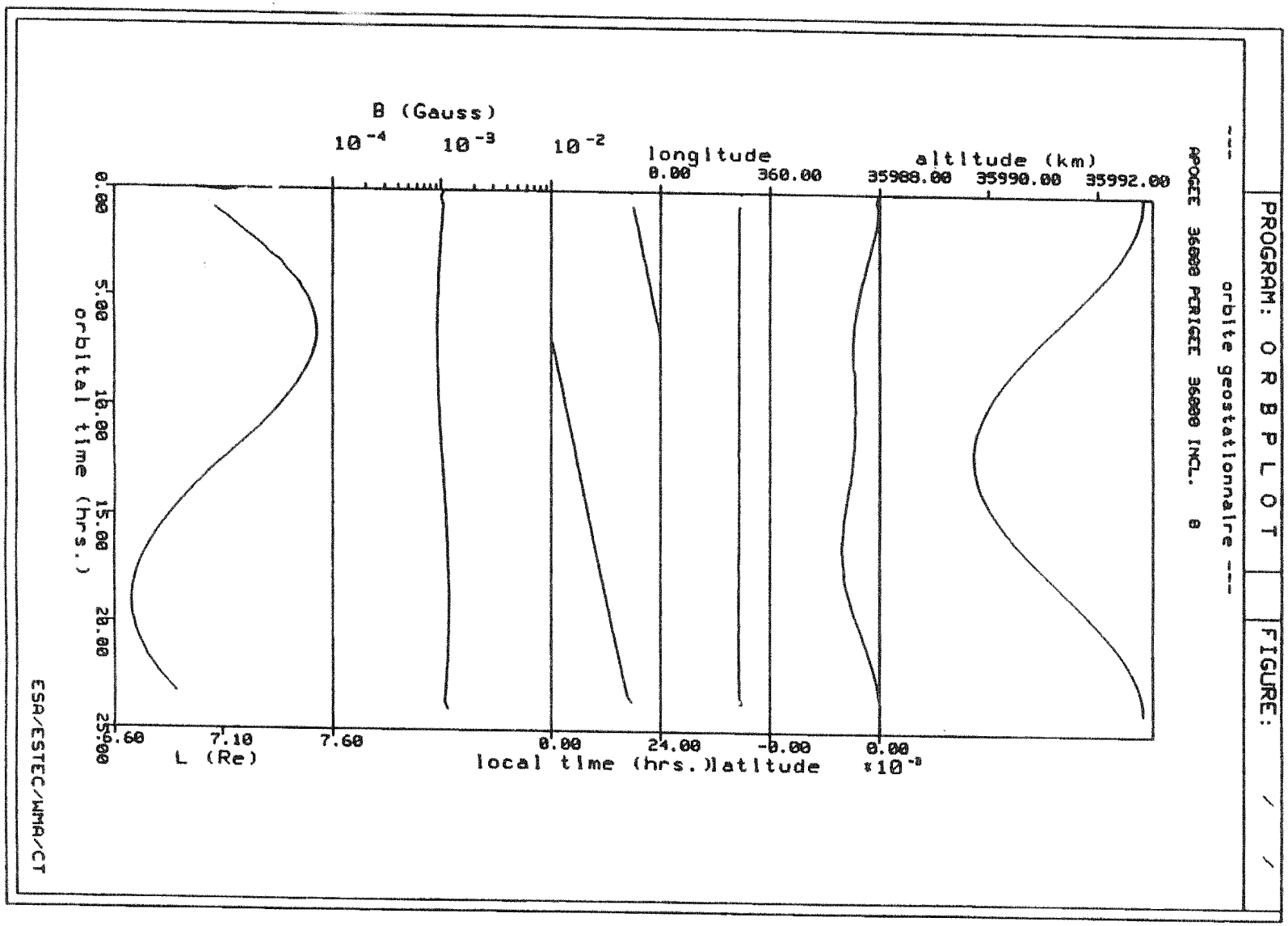

Fig.4-5. B-L coordinates of an equatorial circle coinciding with geostationary orbit.

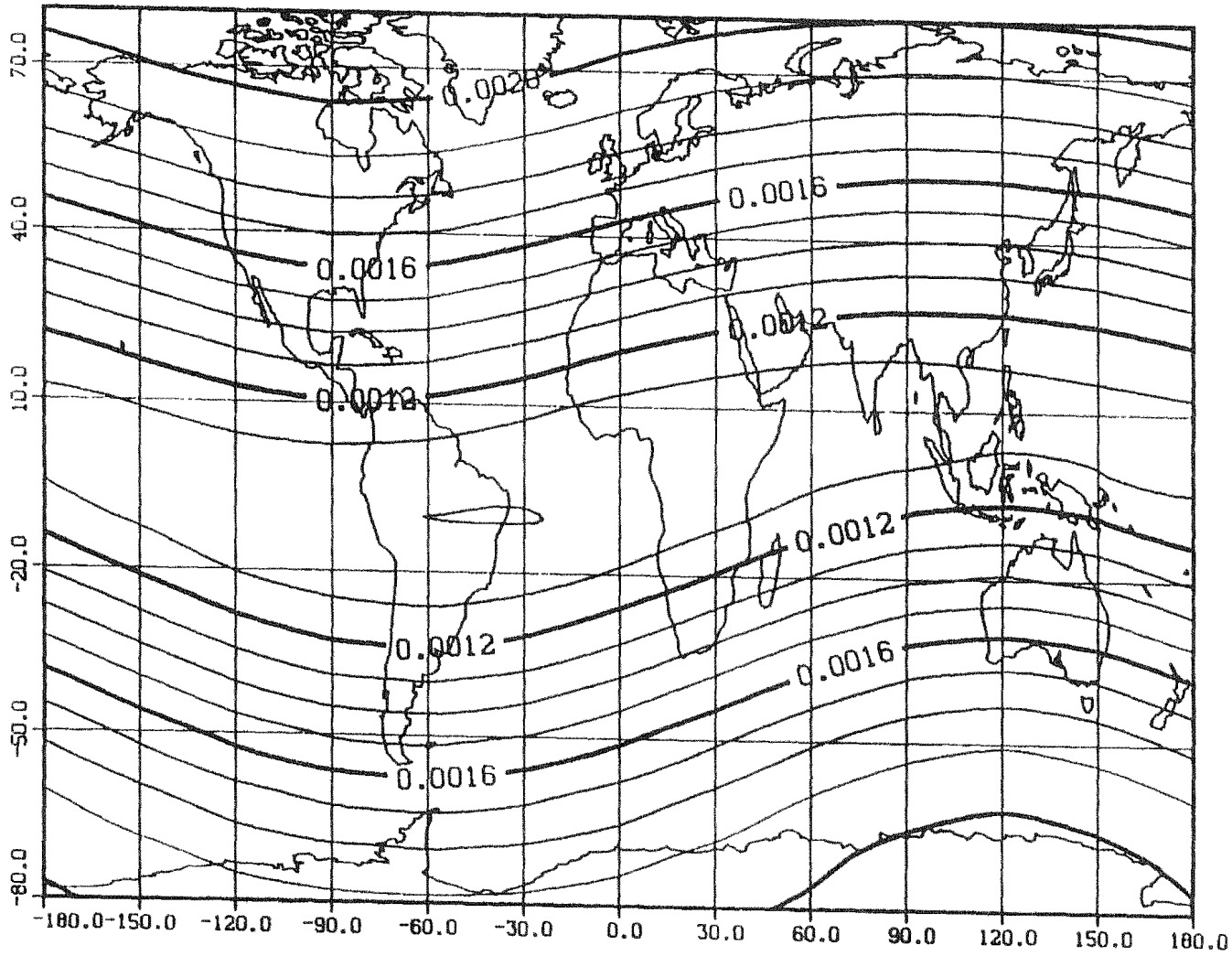

Fig.4-6a Intersection of a sphere of constant altitude (geostationary altitude: 35.677 Km) and surfaces of constant magnetic field intensity (B = 0.0016 gauss; 0.0012 gauss...) when the geomagnetic field is approximated by the internal IGRF-85 model for epoch 1979.

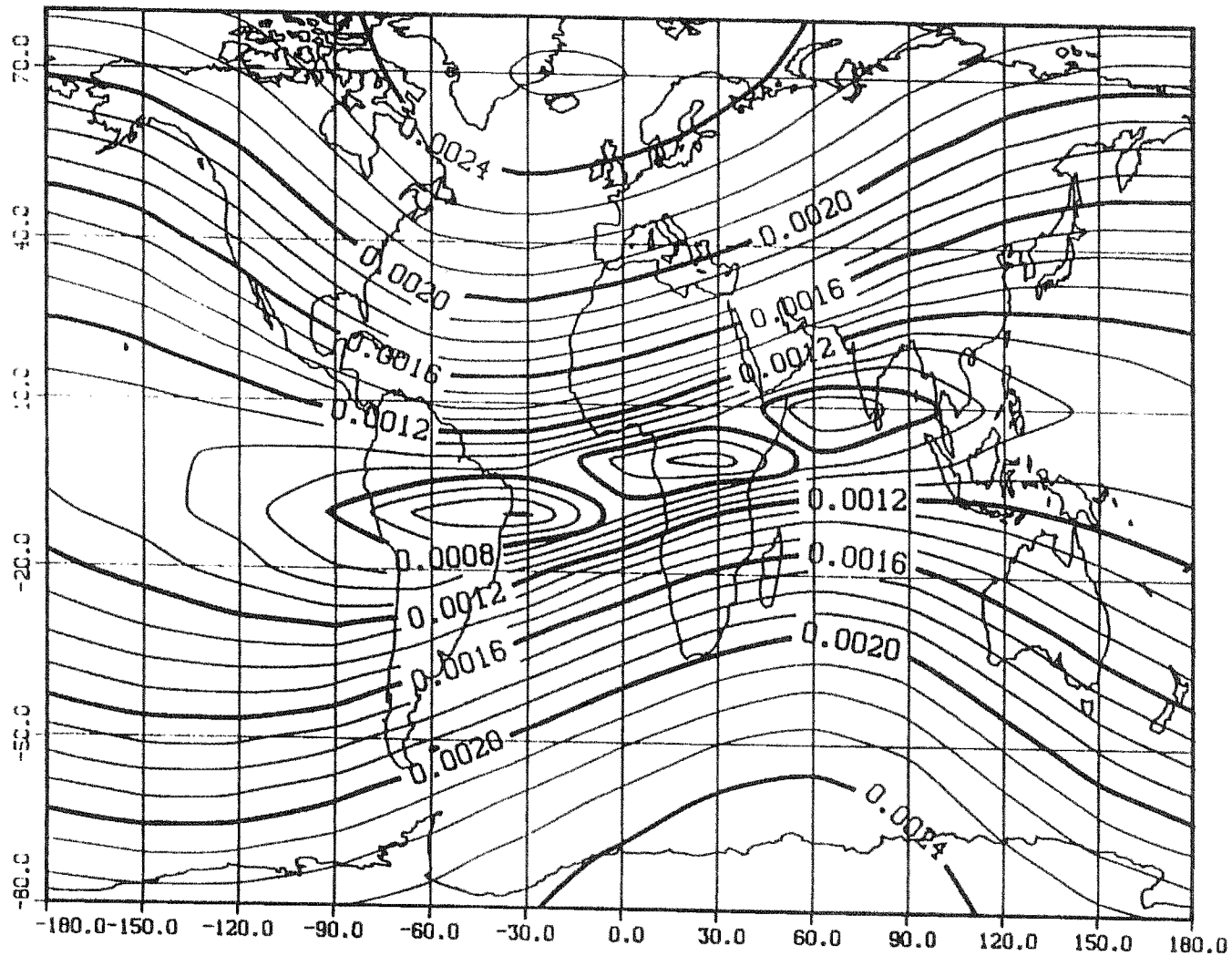

Fig.4-6b Same as fig.4-6a, except that in this case the external magnetic field model of Tsyganenko (1989) has been added to the internal field model IGRF-85.

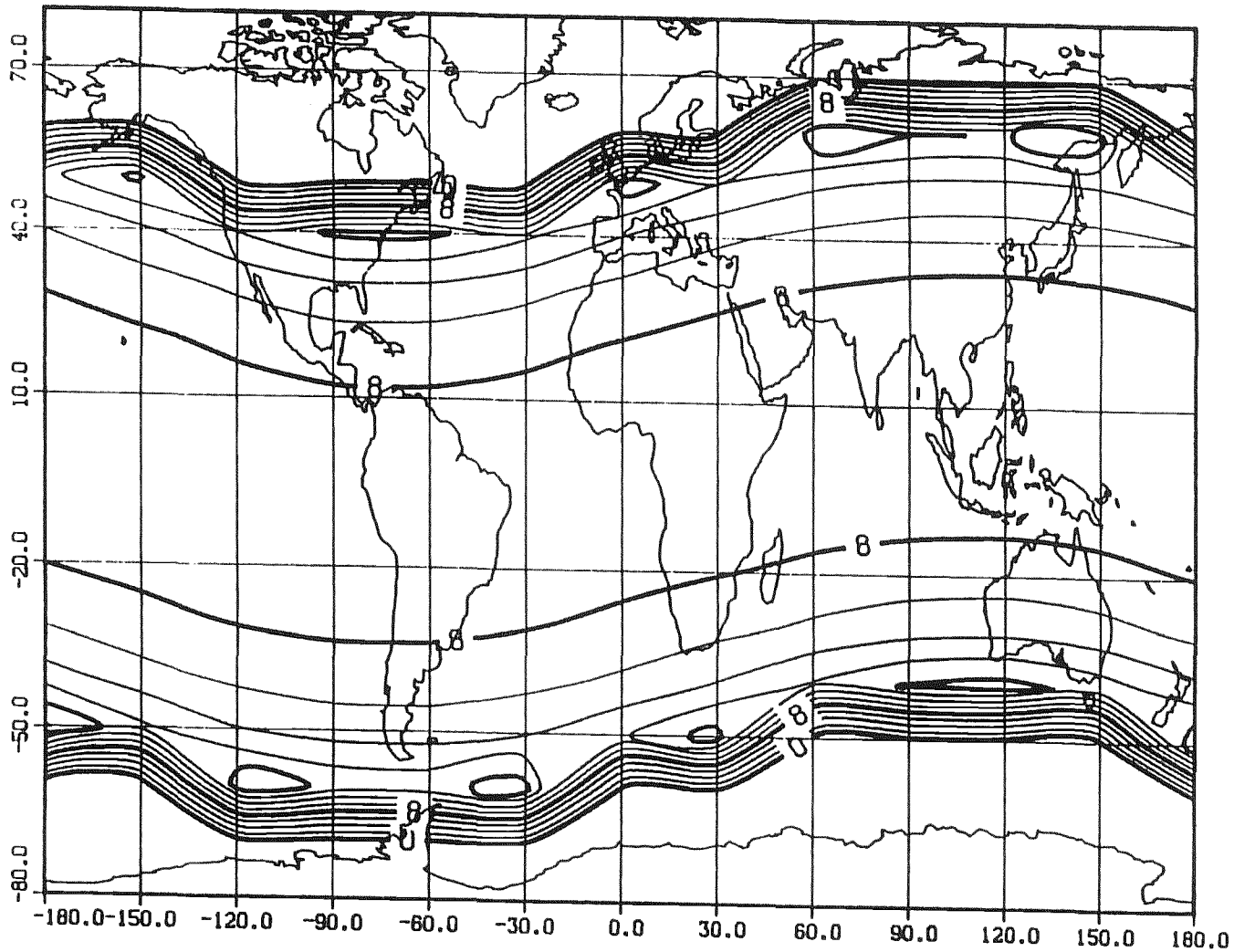

Fig.4-7a Intersection of a sphere of constant altitude (geostationary altitude: 35.677 km) and surfaces of constant L values (L=8,10...), when the geomagnetic field is approximated by the internal IGRF-85 model for epoch 1979.

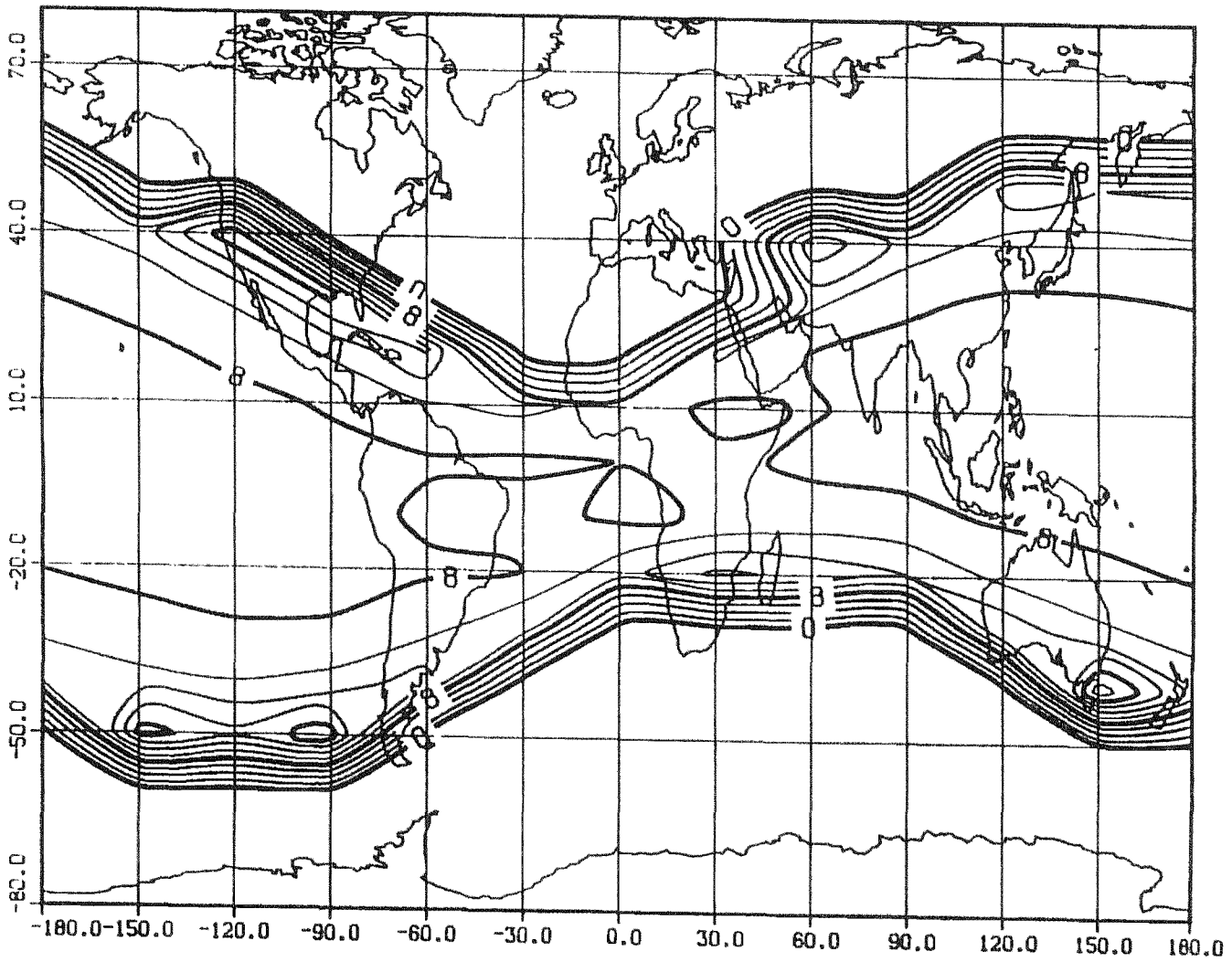

Fig.4-7b Same as fig.4-7a, except that the external field model of Tsyganenko (1989) has been added to the internal field model IGRF-85.

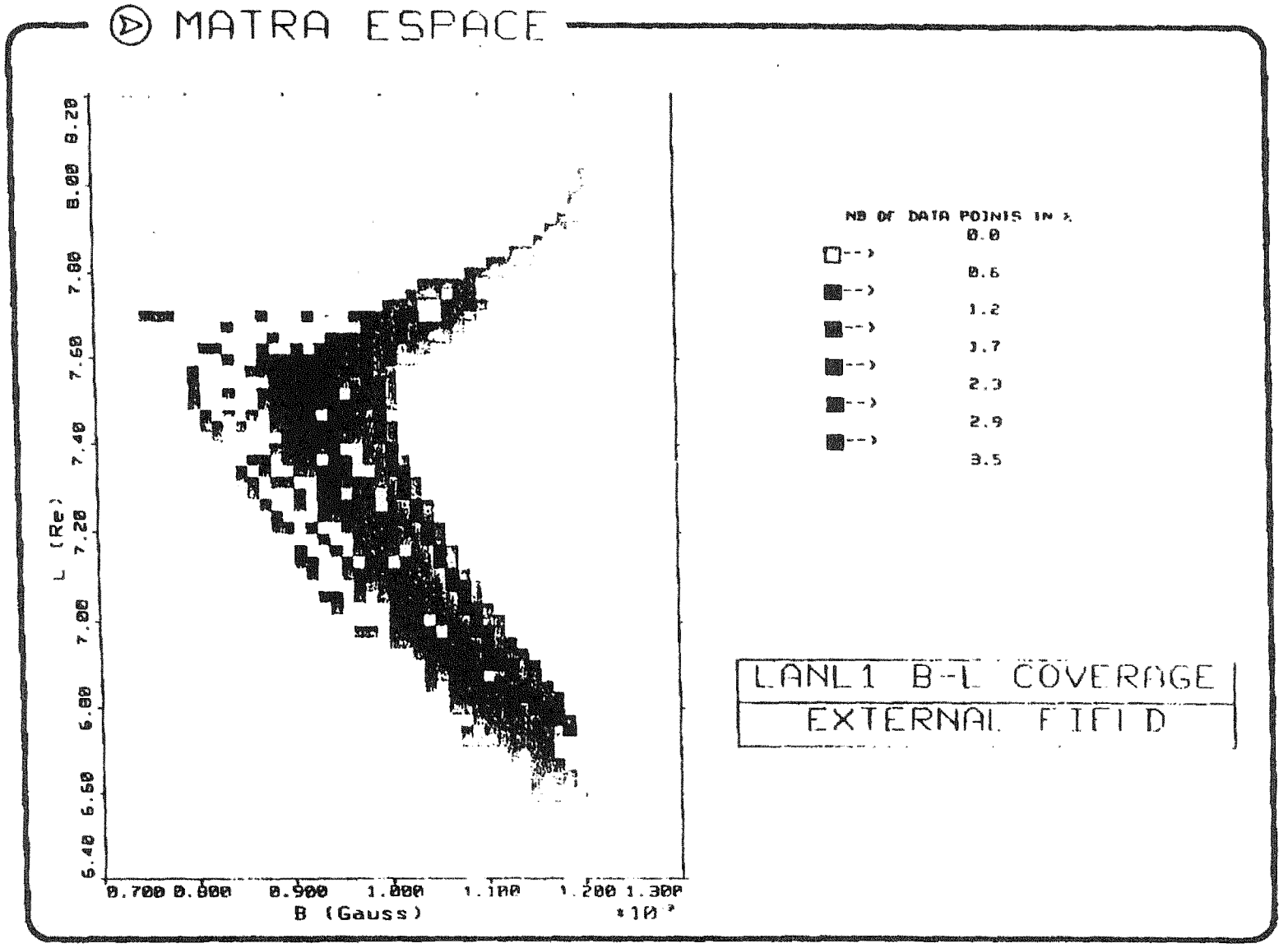

Fig.4-8. Distribution of LANL1 data set in B-L space. The geomagnetic field has been approximated by the K_p- and LT-dependent external field model of Tsyganenko (1989).

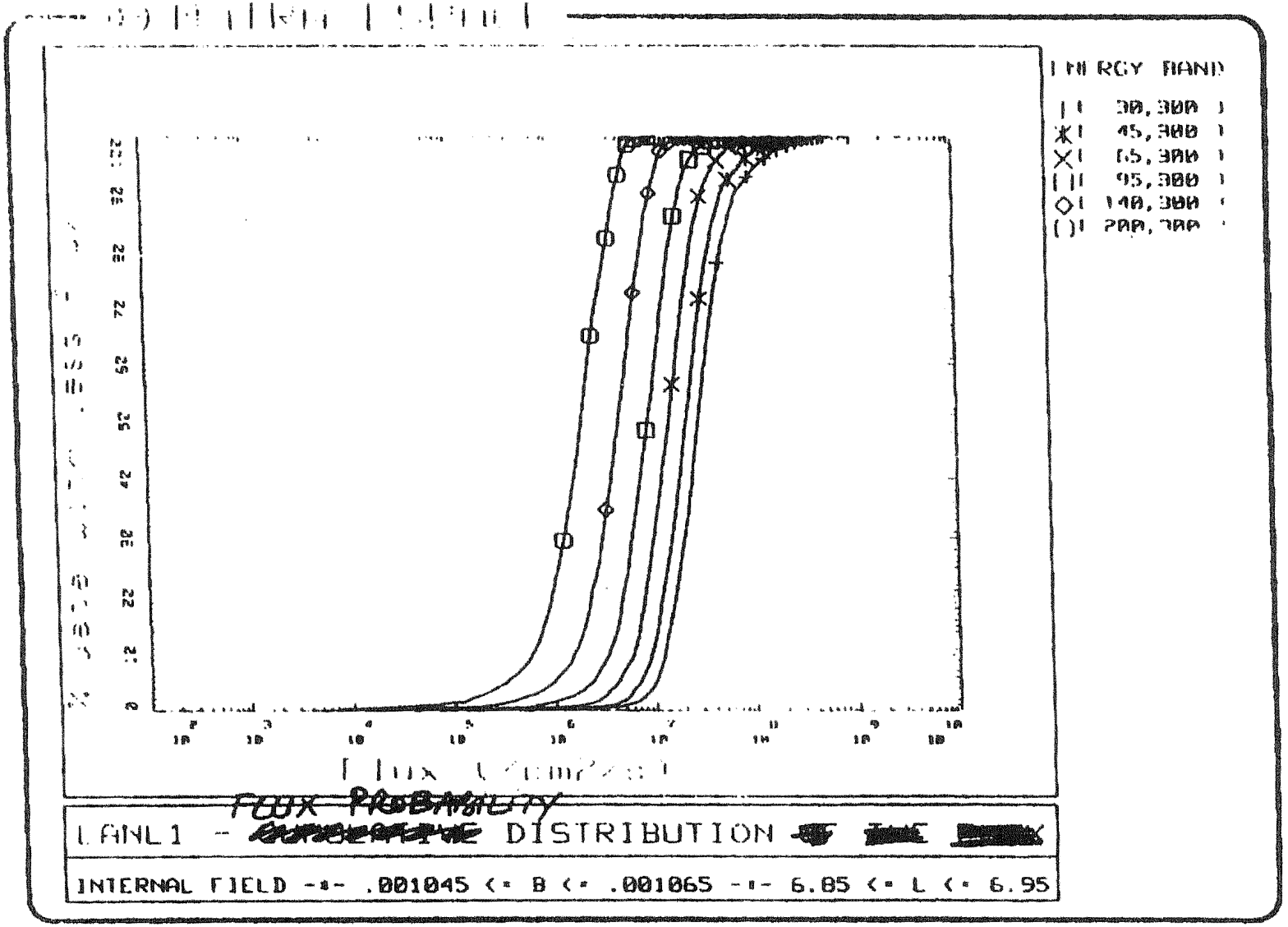

Fig.4-9. Cumulative distribution of LANL1 data with flux values (in selected energy bands) smaller than the numbers given in abscissa.

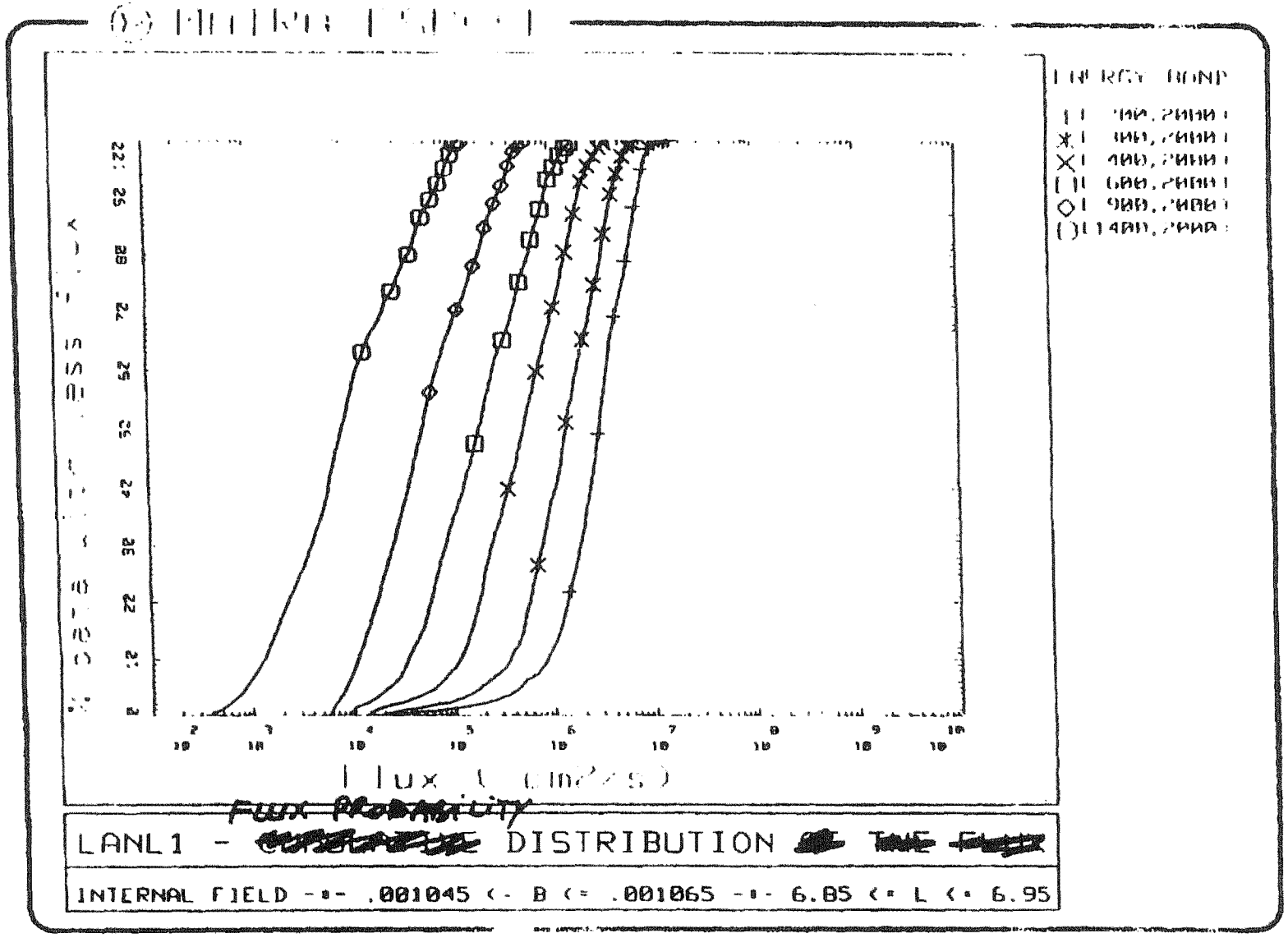

Fig.4-10. Same as fig.4-9, but for higher energy bands.

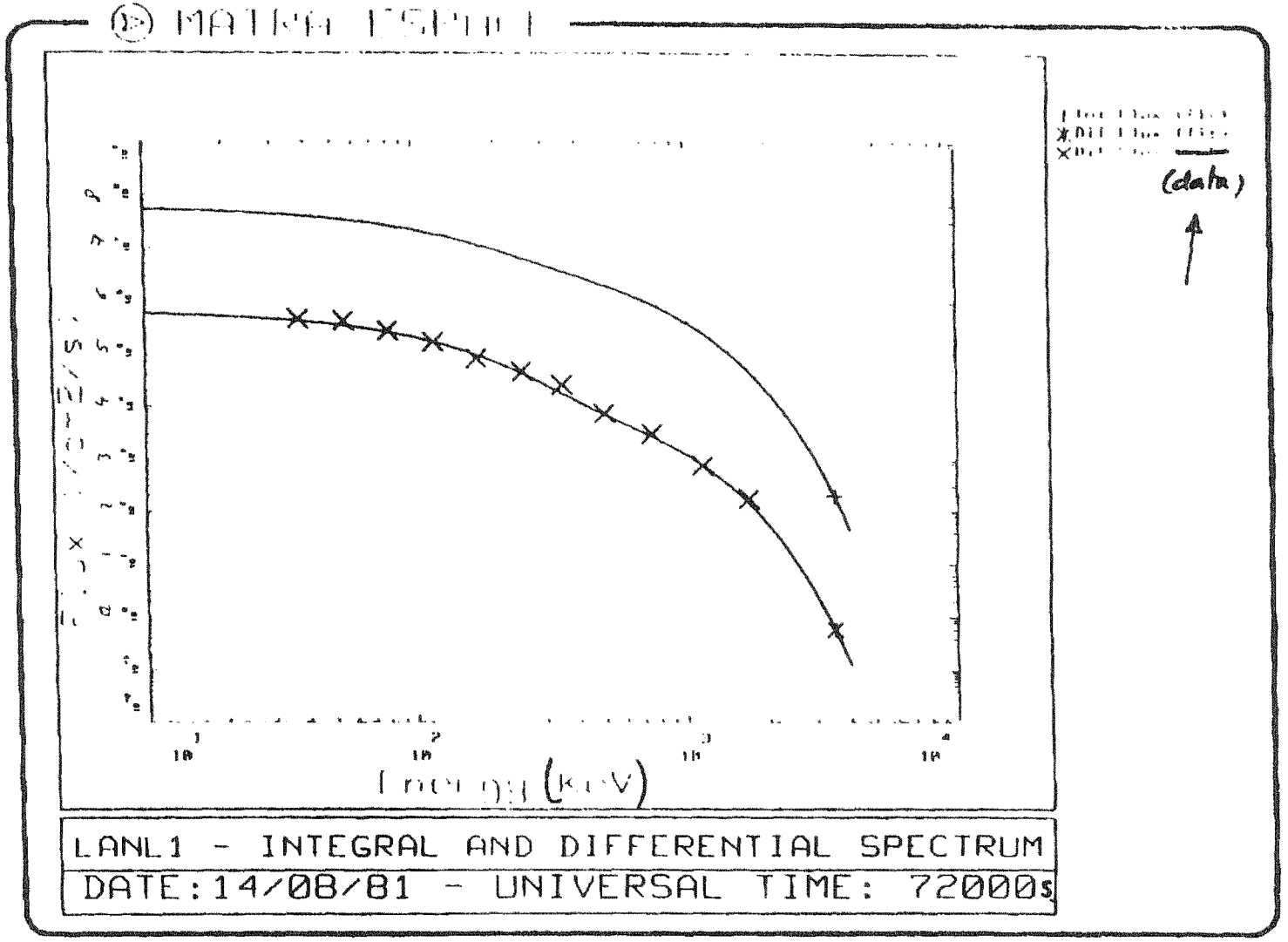

Fig.4-11. Average differential energy spectrum for all LANL1 data set (X). The solid line (lower curve) corresponds to a best fit obtained with a double exponential function.
Units for the differential spectrum are $cm^{-2}\ s^{-1}keV^{-1}$. The upper curve corresponds to the integral flux spectrum J(>E) in units of $cm^{-2}\ s^{-1}$.

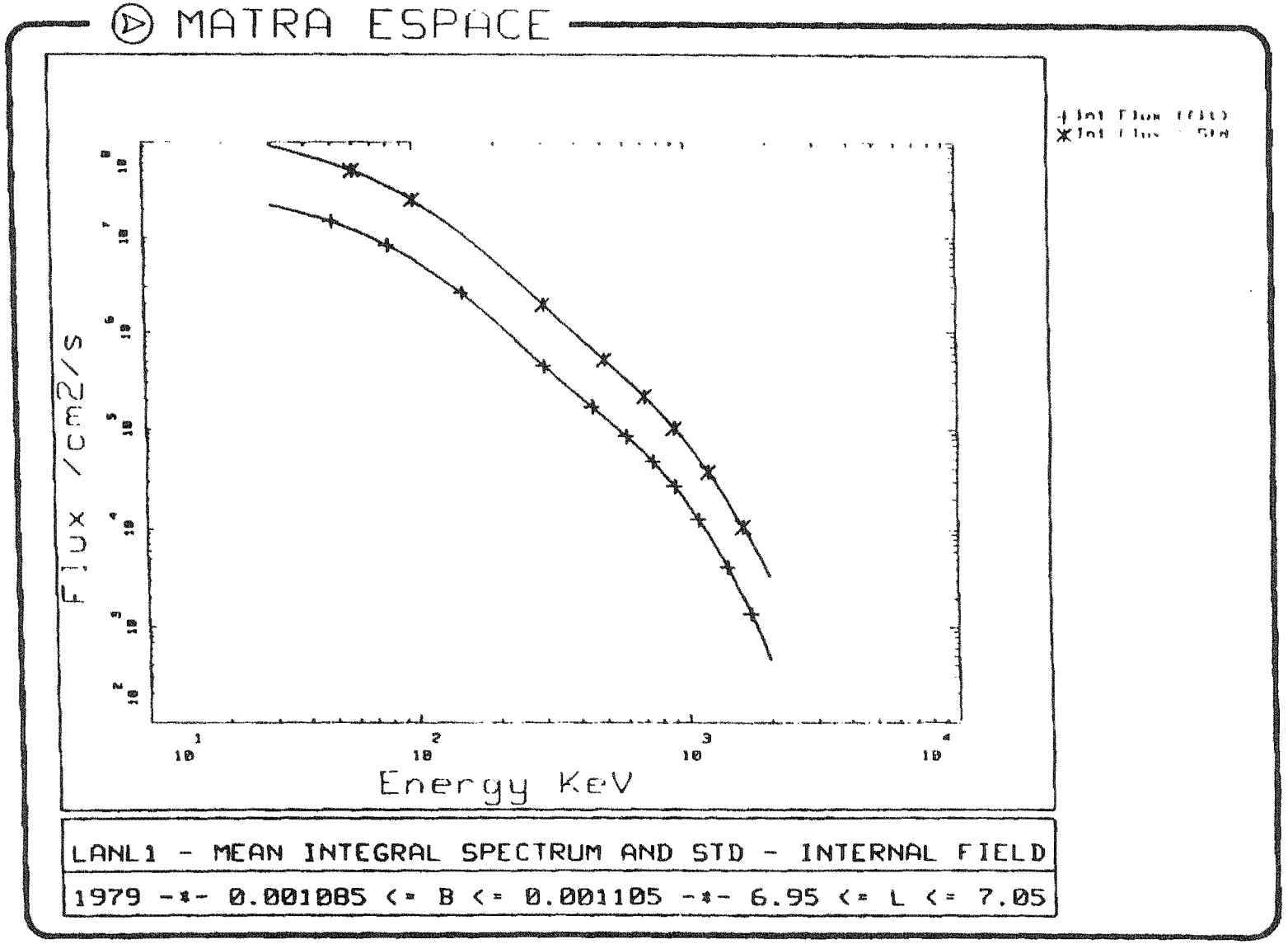

Fig.4-12.Average integral spectrum (data +; and double exponential fit) of LANL1 data. The upper curve and data points (*) correspond to the standard deviation of the log J(>E) for the same data set.

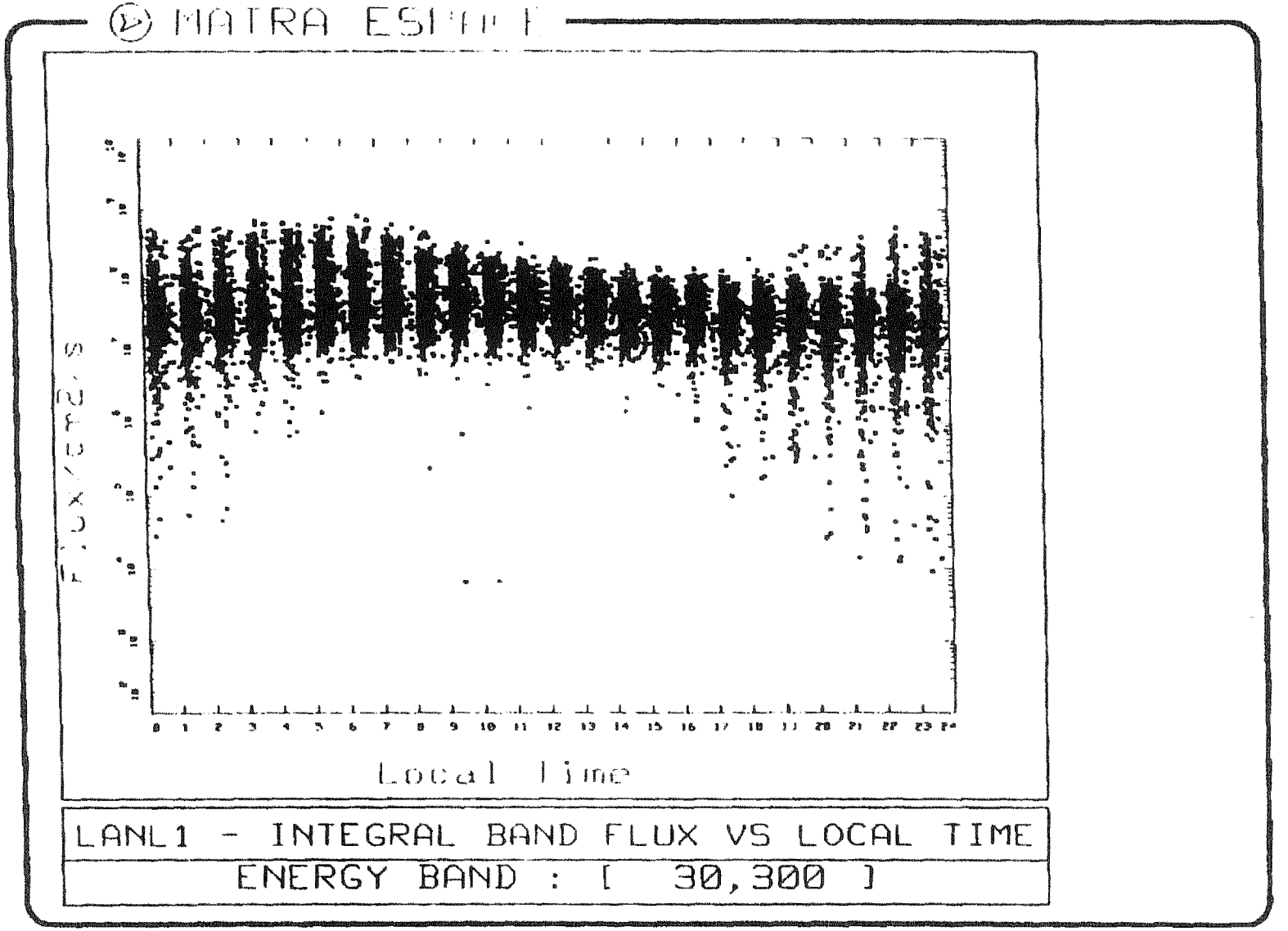

Fig.4-13.Scatter plot showing the local time distribution of all LANL1 flux measurements in the energy interval 30-300 keV.

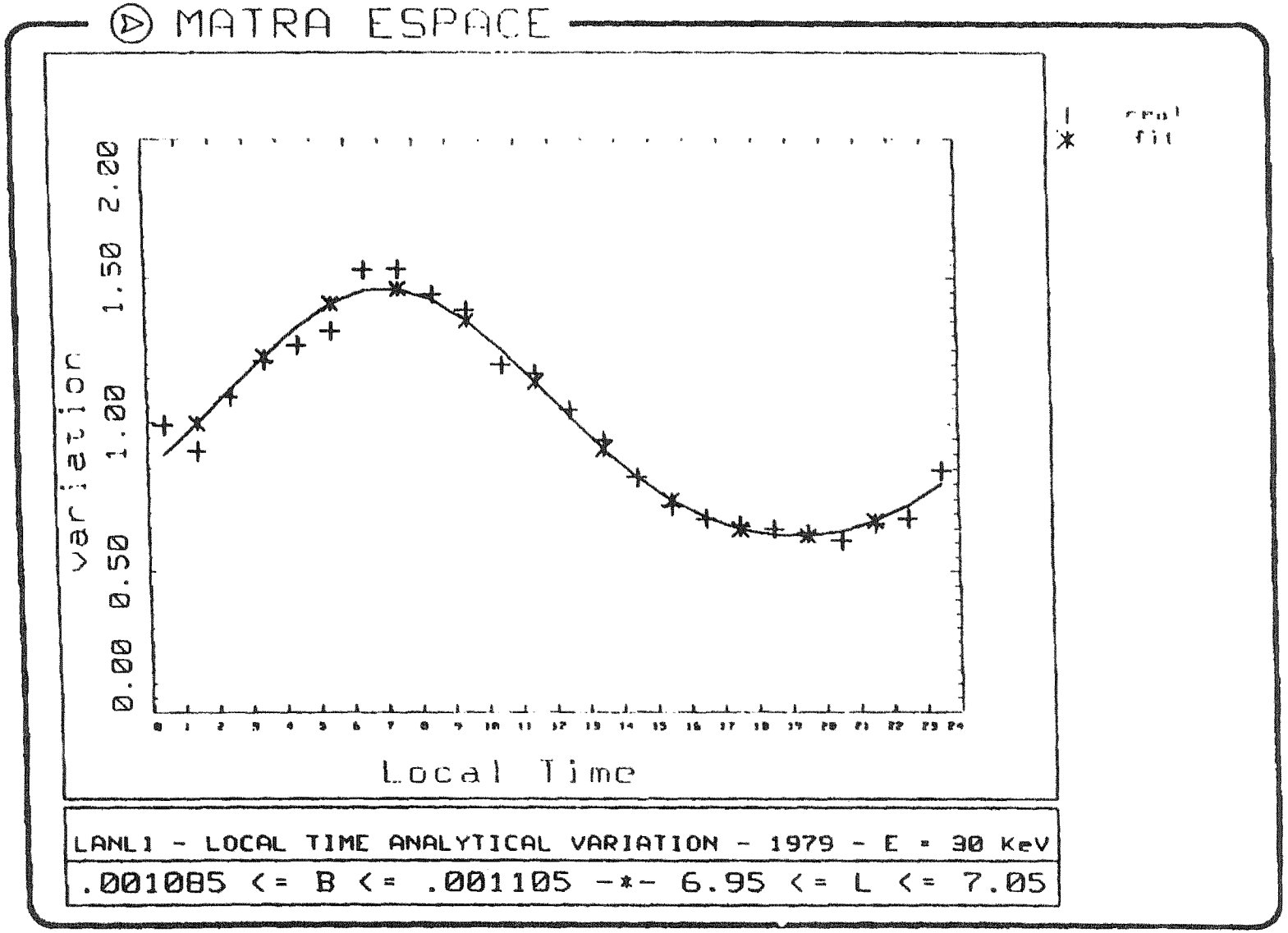

Fig.4-14.Average local time variation for LANL1 integral fluxes values for energies above 30 keV. The solid line and * symbols correspond to a best fit of the average flux measurements (marked by +).

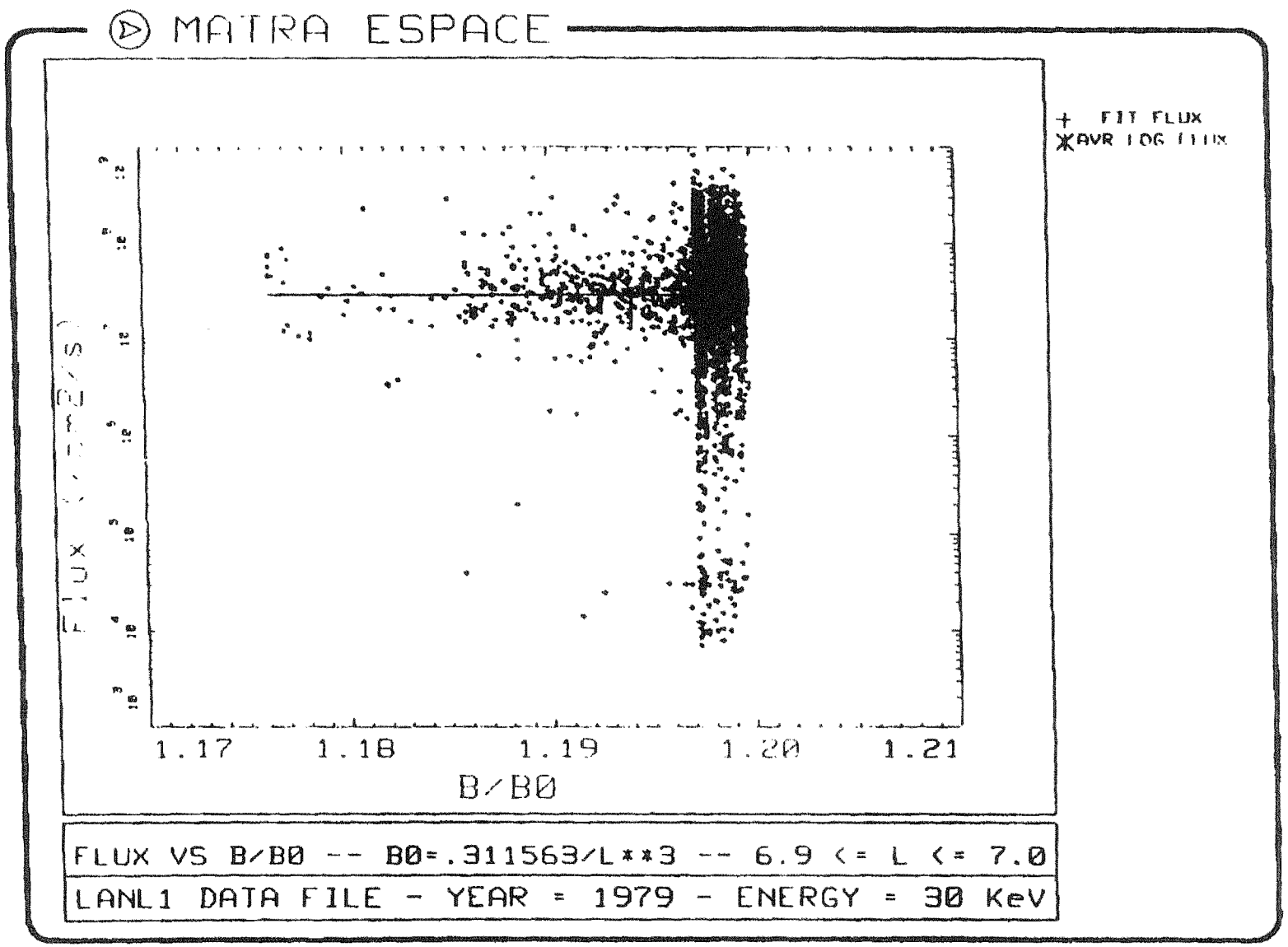

Fig.4-15.Scatter plot of LANL1 integral flux values, J(E>30keV) as a function of B/Bo for a constant L-value (:6.9≤L>7.0). The solid line corresponds to an average value which can be extrapolated for B/Bo=1 corresponding to the magnetic equatorial plane.

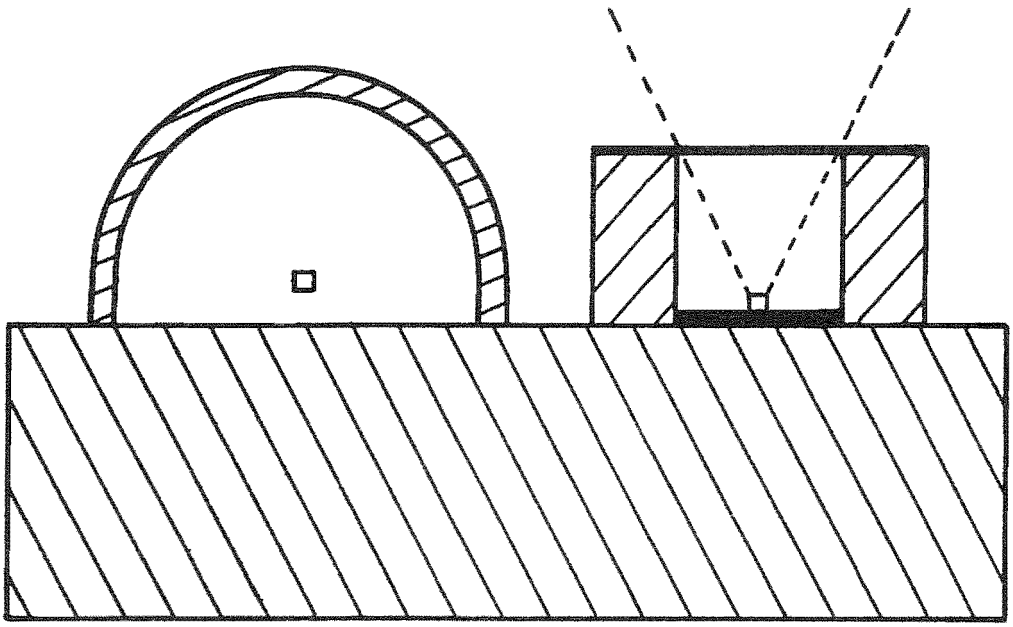

Fig. 5-1 Geometry of bafles for an omnidirectional detector (hemispherical bafle, on the left) and directional detector (cylindrical bafle, on the right hand side)

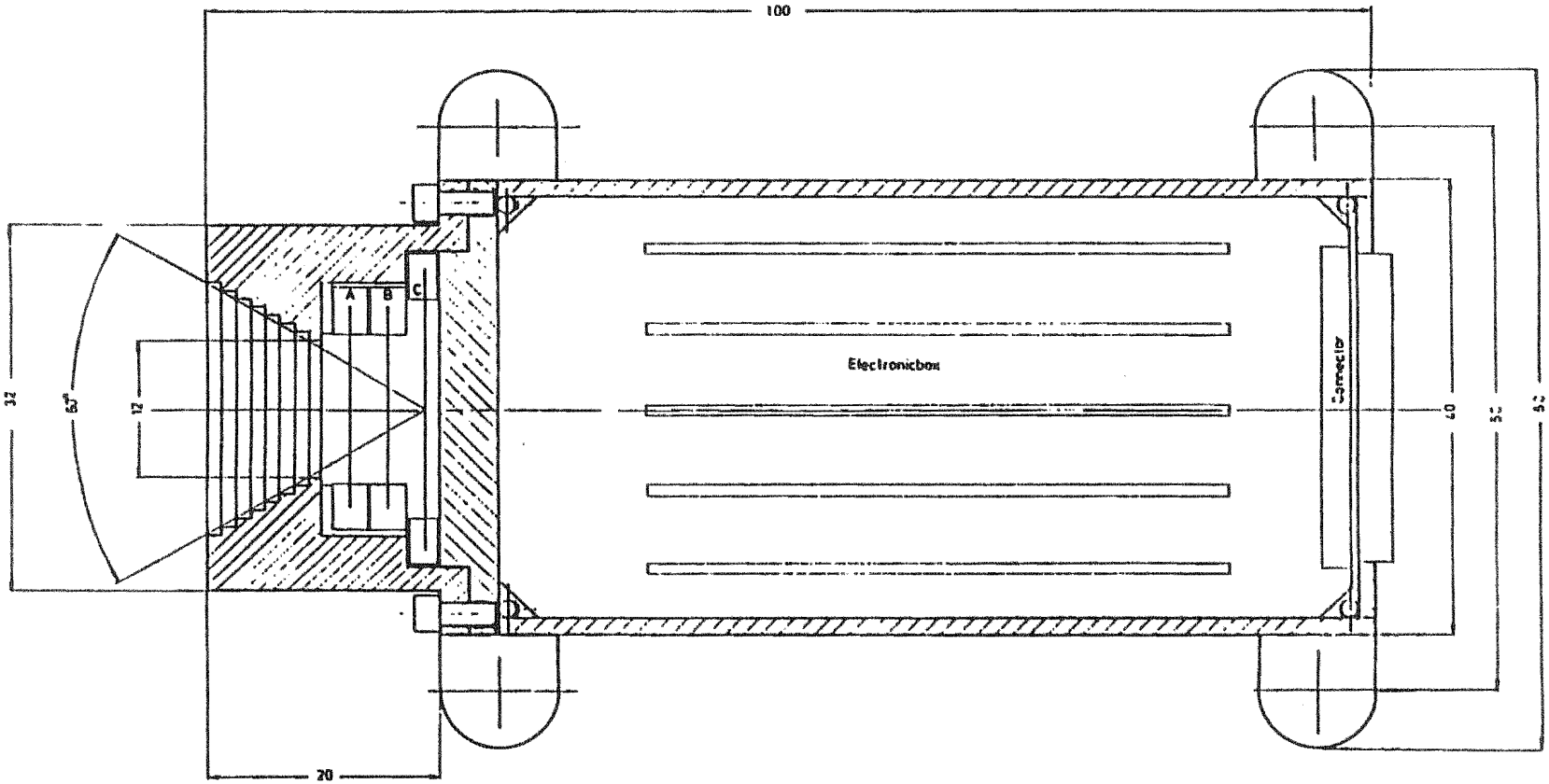

Fig.5-2. Cross-section of a directional particle telescope built by Space Technology Ireland Ltd. (McKenna-Lawlor et al. 1981, 1987, 1990).